THE 7TH INTERNATIONAL WORKSHOP ON INNOVATIVE SIMULATION FOR HEALTH CARE

SEPTEMBER 17 – 19, 2018
BUDAPEST, HUNGARY

EDITED BY
AGOSTINO G. BRUZZONE
MARCO FRASCIO
FRANCESCO LONGO
VERA NOVAK

PRINTED IN RENDE (CS), ITALY, SEPTEMBER 2018

ISBN 978-88-85741-15-7 (Paperback)
ISBN 978-88-85741-14-0 (PDF)

ISBN 978-88-85741-15-7 (Paperback)
ISBN 978-88-85741-14-0 (PDF)

THE 7TH INTERNATIONAL WORKSHOP ON INNOVATIVE SIMULATION FOR HEALTH CARE, IWISH 2018

SEPTEMBER 17-19, 2018

BUDAPEST, HUNGARY

ORGANIZED BY

DIME – UNIVERSITY OF GENOA

LIOPHANT SIMULATION

SIMULATION TEAM

IMCS – INTERNATIONAL MEDITERRANEAN & LATIN AMERICAN COUNCIL OF SIMULATION

DIMEG, UNIVERSITY OF CALABRIA

MSC-LES, MODELING & SIMULATION CENTER, LABORATORY OF ENTERPRISE SOLUTIONS

HUNGARIAN ACADEMY OF SCIENCES CENTRE FOR ENERGY RESEARCH

AUTONOMOUS UNIVERSITY OF BARCELONA

MODELING AND SIMULATION CENTER OF EXCELLENCE (MSCOE)

LATVIAN SIMULATION CENTER – RIGA TECHNICAL UNIVERSITY

LOGISIM

LSIS – LABORATOIRE DES SCIENCES DE L'INFORMATION ET DES SYSTEMES

MIMOS – MOVIMENTO ITALIANO MODELLAZIONE E SIMULAZIONE

MITIM PERUGIA CENTER – UNIVERSITY OF PERUGIA

BRASILIAN SIMULATION CENTER, LAMCE-COPPE-UFRJ

ISBN 978-88-85741-14-0; Bruzzone, Frascio, Longo and Novak Eds.

MITIM - McLeod Institute of Technology and Interoperable Modeling and Simulation – Genoa Center

M&SNet - McLeod Modeling and Simulation Network

Latvian Simulation Society

Ecole Superieure d'Ingenierie en Sciences Appliquees

Facultad de Ciencias Exactas. Ingegneria y Agrimensura

University of La Laguna

CIFASIS: CONICET-UNR-UPCAM

INSTICC - Institute for Systems and Technologies of Information, Control and Communication

National Russian Simulation Society

CEA - IFAC

University of Bordeaux

University of Cyprus

Dutch Benelux Simulation Society

I3M 2018 Industrial Sponsors

CAL-TEK SRL

LIOTECH LTD

MAST SRL

SIM-4-FUTURE

ISBN 978-88-85741-14-0; Bruzzone, Frascio, Longo and Novak Eds.

I3M 2018 MEDIA PARTNERS

INDERSCIENCE PUBLISHERS – INTERNATIONAL JOURNAL OF SIMULATION AND PROCESS MODELING

INDERSCIENCE PUBLISHERS – INTERNATIONAL JOURNAL OF SERVICE AND COMPUTING ORIENTED MANUFACTURING

IGI GLOBAL – INTERNATIONAL JOURNAL OF PRIVACY AND HEALTH INFORMATION MANAGEMENT (IJPHIM)

HALLDALE MEDIA GROUP: THE MILITARY SIMULATION AND TRAINING MAGAZINE

HALLDALE MEDIA GROUP: THE JOURNAL FOR HEALTHCARE EDUCATION, SIMULATION AND TRAINING

SAGE
SIMULATION TRANSACTION OF SCS

DE GRUYTER
INTERNATIONAL JOURNAL OF FOOD ENGINEERING

MDPI - SUSTAINABILITY

EUROMERCI: THE ITALIAN MONTHLY LOGISTICS JOURNAL

ISBN 978-88-85741-14-0; Bruzzone, Frascio, Longo and Novak Eds.

EDITORS

AGOSTINO G. BRUZZONE
MITIM-DIME, UNIVERSITY OF GENOA, ITALY
agostino@itim.unige.it

MARCO FRASCIO
UNIVERSITY OF GENOA, ITALY
mfrascio@unige.it

FRANCESCO LONGO
DIMEG, UNIVERSITY OF CALABRIA, ITALY
f.longo@unical.it

VERA NOVAK
BETH ISRAEL DEACONESS MEDICAL CENTER, HARVARD MEDICAL SCHOOL, USA
vnovak@bidmc.harvard.edu

THE INTERNATIONAL MULTIDISCIPLINARY MODELING AND SIMULATION MULTICONFERENCE, I3M 2018

GENERAL CO-CHAIRS

AGOSTINO G. BRUZZONE, *MITIM DIME, UNIVERSITY OF GENOA, ITALY*
MIQUEL ANGEL PIERA, *AUTONOMOUS UNIVERSITY OF BARCELONA, SPAIN*

PROGRAM CO-CHAIRS

FRANCESCO LONGO, *DIMEG, UNIVERSITY OF CALABRIA, ITALY*
YURY MERKURYEV, *RIGA TECHNICAL UNIVERSITY, LATVIA*

THE 7TH INTERNATIONAL WORKSHOP ON INNOVATIVE SIMULATION FOR HEALTH CARE, IWISH 2018

GENERAL CO-CHAIRS

MARCO FRASCIO, *UNIVERSITY OF GENOA, ITALY*
VERA NOVAK, *HARVARD MEDICAL SCHOOL, USA*

ISBN 978-88-85741-14-0; Bruzzone, Frascio, Longo and Novak Eds.

IWISH 2018 INTERNATIONAL PROGRAM COMMITTEE

MATTEO AGRESTA, *UNIVERSITY OF GENOA, ITALY*
MAJA ATANASIJEVIC-KUNC, *UNIVERSITY OF LJUBLJANA, SLOVENIA*
WERNER BACKFRIEDER, *UNIVERSITY OF APPLIED SCIENCES, UPPER AUSTRIA*
JERRY BATZEL, *UNIVERSITY OF GRAZ, AUSTRIA*
FELIX BREITENECKER, *TU VIENNA, AUSTRIA*
AGOSTINO G. BRUZZONE, *UNIVERSITY OF GENOA, ITALY*
EDUARDO CABRERA, *UNIVERSIDAD AUTONOMA DE BARCELONA, SPAIN*
RICCARDO DI MATTEO, *UNIVERSITY OF GENOA, ITALY*
RAFAEL DIAZ, VMASC VIRGINIA MODELING, ANALYSIS AND SIMULATION CENTER, VIRGINIA, *USA*
ANDREA DE GAETANO, *CNR IASI LABORATORIO DI BIOMATEMATICA, ITALY*
GOTTFRIED ENDEL, *ASSOCIATION OF AUSTRIAN SOCIAL SECURITY, AUSTRIA*
GIONATA FRAGOMENI, *UNIVERSITY MAGNA GRAECIA, ITALY*
CATERINA FUSTO, UNIVERSITY OF CALABRIA, ITALY
MARCO FRASCIO, *UNIVERSITY OF GENOA, ITALY*
NANDU GOSWAMI, *MEDICAL UNIVERSITY OF GRAZ, AUSTRIA*
AMIR HUSSAIN, *UNIVERSITY OF STIRLING, SCOTLAND, UK*
WITOLD JACAK, UNIVERSITY OF APPLIED SCIENCES, UPPER AUSTRIA
KORINA KATSALIAKI, *INTERNATIONAL HELLENIC UNIVERSITY, GREECE*
WERNER CHRISTIAN KURSCHL, *UNIVERSITY OF APPLIED SCIENCES, AUSTRIA*
FRANCESCO LONGO, *UNIVERSITY OF CALABRIA, ITALY*
GIANLUCA MAGLIONE, *UNIVERSITY OF GENOA, ITALY*
MARINA MASSEI, *UNIVERSITY OF GENOA, ITALY*
NAVAIL MUSTAFEE, *UNIVERSITY OF EXETER, UK*
MUAZ NIAZI, BAHRIA *UNIVERSITY OF ISLAMABAD, PAKISTAN*
LETIZIA NICOLETTI, *CAL-TEK, ITALY*
VERA NOVAK, *HARVARD MEDICAL SCHOOL, USA*
METTE OLUFSEN, *NORTH CAROLINA STATE UNIVERSITY, USA*
ANTONIO PADOVANO, *UNIVERSITY OF CALABRIA, ITALY*
NIKI POPPER, *DWH SIMULATION SERVICES VIENNA, AUSTRIA*

TRACKS AND WORKSHOP CHAIRS

APPLICATION OF SIMULATION FOR HEALTHCARE SUPPLY CHAINS
CHAIRS: NAVONIL MUSTAFEE, UNIVERSITY OF EXETER, UK; KORINA KATSALIAKI, INTERNATIONAL HELLENIC UNIVERSITY, GREECE

HEALTHCARE AND PUBLIC HEALTH M&S
CHAIRS: RAFAEL DIAZ, VMASC VIRGINIA MODELING, ANALYSIS AND SIMULATION CENTER, USA; EDUARDO CABRERA, UNIVERSIDAD AUTONOMA DE BARCELONA, SPAIN

MODELING AND SIMULATION FOR COGNITIVE COMPUTATION
CHAIRS: MUAZ NIAZI, BAHRIA UNIVERSITY, PAKISTAN; AMIR HUSSAIN UNIVERSITY OF STIRLING, UK

STUDYING BIOMECHANICAL PROBLEMS FOR CARDIOTHORACIC AND CARDIOVASCULAR CLINICAL PROBLEMS: MODELS, DESIGNING TOOLS, SIMULATION ENVIRONMENTS AND CRITICAL CONDITION PREDICTION FOR SURGICAL INTERVENTIONS.
CHAIR: GIONATA FRAGOMENI, UNIVERSITY MAGNA GRAECIA, ITALY

PATIENT SPECIFIC MODELING OF THE CARDIOVASCULAR-RESPIRATORY SYSTEM: INTERDISCIPLINARY APPROACHES TO THEORY AND PRACTICE
CHAIRS: JERRY BATZEL, UNIVERSITY OF GRAZ, AUSTRIA; NANDU GOSWAMI, MEDICAL UNIVERSITY OF GRAZ, AUSTRIA; METTE OLUFSEN, NORTH CAROLINA STATE UNIVERSITY, USA

MATHEMATICAL MODELING AND HEALTH TECHNOLOGY ASSESSMENT
CHAIRS: NIKI POPPER, DWH SIMULATION SERVICES VIENNA; FELIX BREITENECKER, VIENNA UNIV. OF TECHNOLOGY, AUSTRIA; GOTTFRIED ENDEL, MAIN ASSOCIATION OF AUSTRIAN SOCIAL SECURITY INSTITUTIONS, AUSTRIA

MODELLING AND SIMULATION IN PHYSIOLOGY AND MEDICINE (COMMON TRACK IWISH-EMSS)
CHAIRS: MAJA ATANASIJEVIC-KUNC, UNIV. LJUBLJANA, SLOVENIA; FELIX BREITENECKER, VIENNA UIV. OF TECHNOLOGY, AUSTRIA

SIMULATION AND MODELING IN COMPUTER AIDED THERAPY
CHAIRS: WERNER BACKFRIEDER, UNIVERSITY OF APPLIED SCIENCES, UPPER AUSTRIA; WITOLD JACAK, UNIVERSITY OF APPLIED SCIENCES, UPPER AUSTRIA

DATA DRIVEN SYSTEM SIMULATION - MODELLING & SIMULATION OF COMPLEX SYSTEMS
CHAIR: NIKI POPPER, DEXHELPP (AUSTRIA)

MATHEMATICAL PATHOPHYSIOLOGY
CHAIR: ANDREA DE GAETANO, CNR IASI LABORATORIO DI BIOMATEMATICA (ITALY);

WELCOME MESSAGE 2018

Here we are as every year!
The IWISH aims is to bring together scientists from engineering, natural and life sciences to stimulate discussion on new methods and topics in the emerging field of health care and also this edition will cover the main aspects of health care.
Just a glance to the speakers permit to realize that they are coming from Germany,Usa, Spain, France, Malaysia, Austria, Thailand, Italy. Few congresses could claim a so wide and skilled "parterre".
Simulation in Health Care is the mainstream, managed by engineers and medical doctors who discuss and present each over project and research, that often represent start point for international cooperation.
Subjects of the 2018 edition cover cardiology, neurology, telemedicine, in-hospital transport, emergency call center, radiology, risk management: a so wide container is a warranty of creative difference and positive contamination.

Marco Frascio
University of Genoa
Department of surgical sciences and integrated diagnostic
Italy

Vera Novak
Harvard Medical School
USA

ISBN 978-88-85741-14-0; Bruzzone, Frascio, Longo and Novak Eds.

ACKNOWLEDGEMENTS

The IWISH 2018 International Program Committee (IPC) has selected the papers for the Conference among many submissions; therefore, based on this effort, a very successful event is expected. The IWISH 2017 IPC would like to thank all the authors as well as the reviewers for their invaluable work.
A special thank goes to all the organizations, institutions and societies that have supported and technically sponsored the event.

I3M 2018 INTERNAL STAFF

MATTEO AGRESTA, *SIMULATION TEAM, ITALY*
AGOSTINO G. BRUZZONE, *DIME, UNIVERSITY OF GENOA, ITALY*
ALESSANDRO CHIURCO, *DIMEG, UNIVERSITY OF CALABRIA, ITALY*
RICCARDO DI MATTEO, *SIMULATION TEAM, ITALY*
JESSICA FRANGELLA, *CAL-TEK SRL, ITALY*
CATERINA FUSTO, *DIMEG, UNIVERSITY OF CALABRIA, ITALY*
LUCIA GAZZANEO, *DIMEG, UNIVERSITY OF CALABRIA, ITALY*
FRANCESCO LONGO, *DIMEG, UNIVERSITY OF CALABRIA, ITALY*
MARINA MASSEI, *DIME, UNIVERSITY OF GENOA, ITALY*
LETIZIA NICOLETTI, *CAL-TEK SRL, ITALY*
ANTONIO PADOVANO, *DIMEG, UNIVERSITY OF CALABRIA, ITALY*
ANTONIO REDA, *CAL-TEK SRL, ITALY*
CATALDO RUSSO, *CAL-TEK SRL, ITALY*
KIRILL SINELSHCHIKOV, *SIMULATION TEAM, ITALY*
CARMINE TOTERA, *CAL-TEK SRL, ITALY*
MARCO VETRANO, *CAL-TEK SRL, ITALY*
BEATRICE ZACCARO, *SIMULATION TEAM, ITALY*

This International Workshop is part of the I3M Multiconference: the Congress leading **Simulation around the World and Along the Years**

ISBN 978-88-85741-14-0; Bruzzone, Frascio, Longo and Novak Eds.

Index

ISBN 978-88-85741-14-0; Bruzzone, Frascio, Longo and Novak Eds.

SIMULATION FRAMEWORK FOR MOBILE PATIENT MONITORING SYSTEMS

Michael Aleithe[(a)], Philipp Skowron[(b)], Angela Carell[(c)], Daniel Böttger[(d)], Tobias Goblirsch[(e)] , Bogdan Franczyk[(f)]

[(a),(b),(e),(f)] Leipzig University, Grimmaische Straße 12, 04109 Leipzig, Germany
[(c)] adesso AG, Stockholmer Allee 20, 44269 Dortmund, Germany
[(d)] Stiftung Deutsche Depressionshilfe, Semmelweisstraße 10, 04103 Leipzig, Germany

[(a)]aleithe@wifa.uni-leipzig.de, [(b)] skowron@wifa.uni-leipzig.de, [(c)] angela.carell@adesso.de,
[(d)] daniel.boettger@medizin.uni-leipzig.de, [(e)] goblirsch@wifa.uni-leipzig.de, [(f)] franczyk@wifa.uni-leipzig.de

ABSTRACT
There is a large variety of data-centered therapy support systems involving self-management for medical purposes, usually referred to as Mobile Patient Monitoring Systems (MPMS). The considerable growth of MPMS and the variety of options afforded by the mobile sensors of smart instruments lead to enormous development cost. The range of options is commonly explored in trial and error, incurring significant expenditures of time and funds. This paper presents a simulation framework that offers a capability to run these trials in a simulation-based fashion and thereby achieve quicker and more cost-effective results than was previously possible.

Keywords: *Mobile Patient Monitoring Systems, Cyber Physical Systems, Failure Mode and Effects Analysis*

1. INTRODUCTION

The development of data-based therapy support system is driven by the rise of the Internet of Things (IoT). Accordingly, it suffers from the same range of difficulties that is commonly encountered in this area. In (Baig et al. 2015) the main kinds of issues are summarized. They include in particular the reliability and effectiveness of data transfer from utilized smart devices via Bluetooth. Additionally, the energy management of the mobile devices is a determinant of correct function of data-based therapy support systems. In addition to the typical issues of IoT systems, development of therapy support systems in particular is defined by additional criteria. These involve validation of the results of development. Unlike usual tests and validations, those of data-based therapy support systems need to be run in practical use by actual patients. For example, the energy management of devices used needs to adapt to the daily schedule of therapy support. So in this instance, validation includes the recruitment and instruction of patients. Depending on the particulars of the situation, ethics approval as well as compliance with elaborate regulatory frameworks concerning personal medical data and medical devices may be necessary. The combination of these factors makes the development of data-based therapy support systems considerably more difficult and costly than development of more common IoT devices. However, the use of a simulation presents an alternative that makes it possible to speed up the lengthy validation process and thereby reduce costs. The following chapter looks at existing simulation frameworks. These turn out to be inadequate for the requirements in question. A detailed introduction of the simulation framework developed in this work follows.

2. STATE OF THE ART

Simulations have been used in the health domain in various ways in recent years. This chapter is intended to provide a brief outline of these different types of simulations in health as well as to name some significant works in concrete terms.
One type of simulation is manual testing under laboratory conditions in order to analyze the effects of certain parameters in a model-like manner. (Geis et al. 2011) used laboratory simulations to define roles and scopes of healthcare practice. In their conclusion can simulation help to determine provider workload, refine team responsibilities and identify latent safety threats. A pilot project is demonstrated which provides as a template for evaluation of new teams and clinical settings before patient exposure. (Lammers et al. 2014) systematically observed many types of errors and identified some of the underlying causes during simulated, prehospital, pediatric cardiopulmonary arrest. Numerous, multifactorial, and sometimes, synergistic causes of medication dosing errors were identified which can used by emergency medical services to prevent future errors. A pilot study by (Gittinger et al. 2017) used a simulation-based platform to evaluate the effect of an automated mechanical chest compression device on team communication and patient management. In result simulation-based assessments offer important insights into the effect of technology on healthcare teams. (Fernandez et al. 2017) survey the relationship between team cognition and team performance in healthcare and suggests a role for simulation in the development of this team-level

construct. They synthesize foundational knowledge regarding team cognition and highlight best practices for using simulation to target team cognition.

Other types of simulations are summarized by (Almagooshi 2015). He presents different simulation approaches with the underlying models in the area of health. There is a fundamental distinction between *discrete event simulation* (DES) and an *agent based simulation* (ABS). The DES models the operation of a system as a discrete sequence of events in time whereby each event occurs at a particular instant in time and marks a change of state in the system. The ABS models the actions and interactions of the system as autonomous agents. Some of the approaches cited in (Almagooshi 2015) are listed below. (Ahmed and Amagoh 2008) utilizes a simulation model for DES to investigate patients flow in a hospital to investigate how the resources are utilized to respond to health care systems. A DES model to evaluate the clinical benefit from reducing delays in the emergency stroke pathway is presented by (Monks et al. 2012). Another novel DES model of sudden cardiac death is described by (Andreev et al. 2013). This model quantifies the chains of events associated with the formation, growth, and rupture of atheroma plaques, and the subsequent formation of clots, thrombosis and on-set of arrhythmias within a population. (Shi et al. 2014) developed a simulation model to study the performance of clinic operations. The appropriate DES model captures the patient flow characteristics of the studied clinic, and it is validated by comparing the simulation results with the real key performance measures obtained from in the clinic. The system performance is mainly measured by two metrics: one is how the clinic makes efficient use of its resources, and the other is how long the patients need to wait for services. (Lee et al. 2010) demonstrate an agent-based computer simulation model (ABM) of the greater Washington, DC, metropolitan region to assist the Office of the Assistant Secretary of Public Preparedness and Response, Department of Health and Human Services, to address several key questions regarding vaccine allocation during the 2009 H1N1 influenza pandemic, including comparing a vaccinating children (i.e., highest transmitters)-first policy versus the Advisory Committee on Immunization Practices (ACIP)-recommended vaccinating at-risk individuals-first policy. Also an agent-based modeling and simulation is presented by (Cabrera et al. 2011). They use it to design a decision support system for healthcare emergency department to aid in setting up management guidelines to improve it.

After an overview of the general approaches of the general approaches of simulations in the field of health has now been presented, we will now specifically deal with simulations concerning MPMS, since these represent the focus of this work. Therefore (Panigrahi et al. 2001) and (Rakhmatov et al. 2003) simulated the battery life of embedded systems using stochastic models. These simulations are highly mathematically focused and therefore very sensitive to changed parameters, limiting the flexibility of this approach. (Yun et al. 2007) simulated the speed of sensor data processing in body area networks. The focus of his work is on securing critical processing time bounds in order to perform realtime processing. More simulations of runtime and energy consumption aspects of wireless body area networks have been studied by (Nguyen et al. 2008). This type of simulation is limited to a prototypical implementation of the sensor network under study. This precludes adaptability to other practical applications. There was also a simulation of hypertension monitoring in rural Africa performed by (Bolaji 2014). The relevant sensor data was generated by implanted sensors and transmitted to the nearest medical center using GPRS. This simulation focuses on data transmission and its reliability.

Since existing approaches are not adequate to the requirements of developing data-based therapy support systems, a new simulation approach is required and will be described in detail in the following chapters.

3. SIMULATION APPROACH

The following simulation approach is based on the idea in (Lunze 1995) of distinguishing between qualitative and quantitative simulation models. Qualitative models are characterized by an arbitrary degree of abstraction, permitting great flexibility. But this flexibility is achieved at a cost of precision. In many practical scenarios, however, the degree of precision possible with qualitative models is sufficient. A high degree of precision is achieved in numeric models, at a cost of flexibility in the simulation and involving more time-consuming work than a qualitative approach. These models can only be created in later design phases, after the specifications of components and parameters are complete. There is currently no way to transform qualitative to quantitative models and vice versa. Due to these characteristics of the two types of simulation models, our work uses a hybrid approach in an attempt to catch the positive qualities of both. We begin with a general overview using a qualitative strategy. We then focus on areas of particular interest using numeric simulation in order to achieve the required degree of precision in these.

3.1. Qualitative Approach

The qualitative simulation model for the general overview of the entire system is created using an analytical method of reliability engineering called *Failure Modes Effects Analysis* (FMEA) and used for preventative quality assurance. This method was originally developed in the United States military (MIL-P-1629 1949) and was later introduced to industrial production (Carlson 2012). Both (Carlson 2012) and (Tietjen et al. 2011) cover the practical application of this analytical method. The basic setup of the individual parts of FMEA is visualized in Figure 1. It begins with a separation of the various items both from a design perspective and from a process perspective. Then each of these items is assigned one or several functions that

they perform within the system as a whole. From each of these functions potential failure modes can be derived. Additional failure modes may be added over the course of development as more experience is gained. Each of these failure modes is then analyzed and assigned various causes that have been found to lead to the failure mode. The main goal of FMEA is to use the causes to define actions that can be taken to prevent potential causes and thereby prevent potential failures and achieve quality assurance. Of particular note is the identification of single points of failure, weaknesses where a single failure can lead to a failure of the entire system.

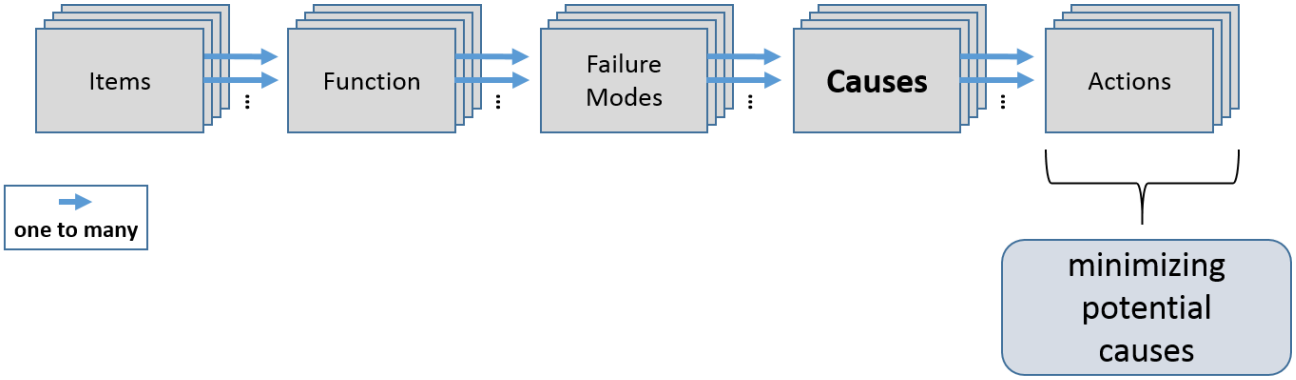

Figure 1: the individual phases of Failure Modes Effects Analysis (FMEA)

3.2. Numeric Approach

After the general overview analysis using FMEA has been performed and single points of failure have been identified, these are studied in detail using numeric simulation models. In these models, the systems under analysis are separated into various aggregation layers. Each system can be divided into subsystems, with the arbitrary depth of the mapping of interlocking subsystems dependent on the requirements of the application. The behavior of each subsystem is defined mathematically with respect to the variables that the simulation focuses on.

4. FMEA OF THE THERAPY SYSTEM

The application on which the present paper is based is a data-based therapy support system for self-management of clinical depression. Here psycho-physiological signal data of patients with depression is collected using the prevalent sensors of smartphones and smart watches. From this dataset, critical patterns are extracted in order to predict future relapses. The design of the overall system, understood as FMEA items, is visualized in Figure 2. The sensors of the smart watch are accompanied by preprocessing and data transmission to the smartphone via Bluetooth. In addition to this data, the smartphone contains additional sensors generating more sensor data. The data preprocessed by the smart watch as well as the data generated by the smartphone are then preprocessed by the smartphone. The algorithms for pattern recognition are then run both on the smartphone itself and on a separate server systems due to high demand for processing capacity. Besides the use of sensor data, the depression patients also enter self-reported rating data into the smartphone. Both the smartphone and the smart watch depend on an energy supply, which is required for all function. Both the self-reported rating data and the sensor data are dependent on patient compliance, i.e. the subjective component of whether the patient uses the sensors and the self-reported rating correctly and regularly. The entire system is framed by an overarching component of data security requiring its own explicit considerations. Compliance and data security are not the subject of the present paper. With all items of the therapy support system listed in Figure 2 in a structured fashion, each item is assigned functions and each function is assigned failure modes. The assignment of failure modes to each item is visualized schematically in Figure 3, using a visualization that demonstrates dependencies of individual failure modes on each other and sorts them hierarchically. This form of visualization is also called a fault tree (Carlson 2012). This form of presentation makes it quite obvious that energy supply, especially of the smartphone is a single point of failure, where failure of the item leads to failure of the entire system. This makes the weak point of energy supply a high priority for more detailed study (Chapter 5) in order to produce better assessments of the behavior of the entire system. These can be fed into the process of designing the system and help create a better system design.

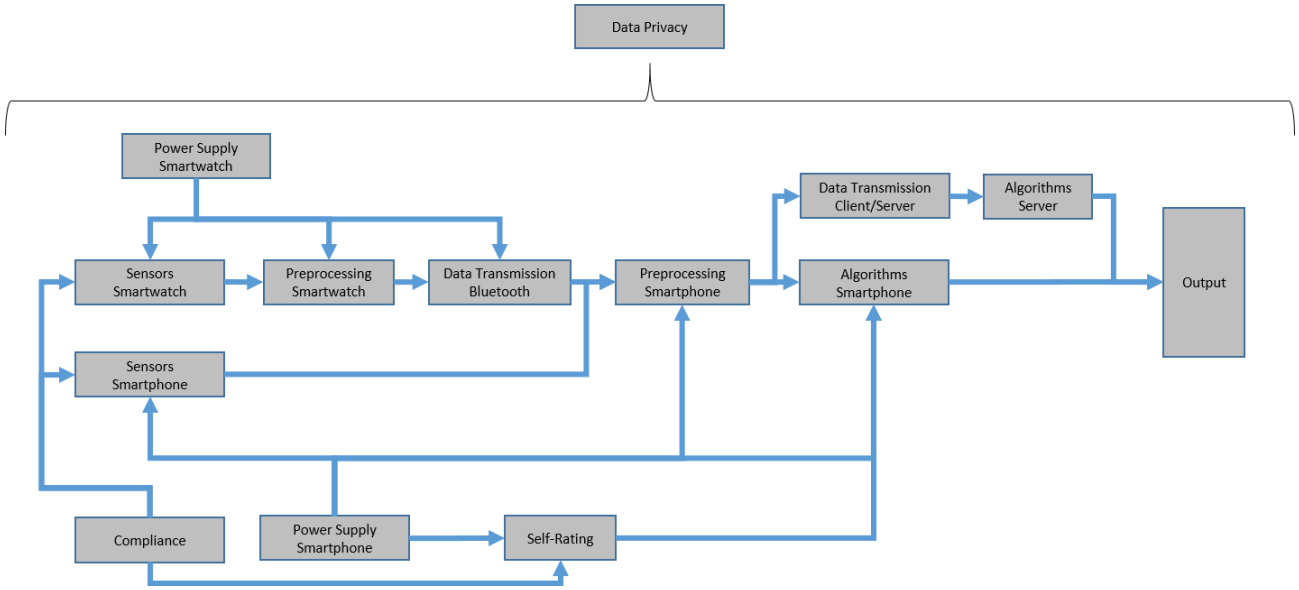

Figure 2: structural elements overview of the whole self-management system for therapy assistance as the first step of FMEA-analysis (items and their dependencies)

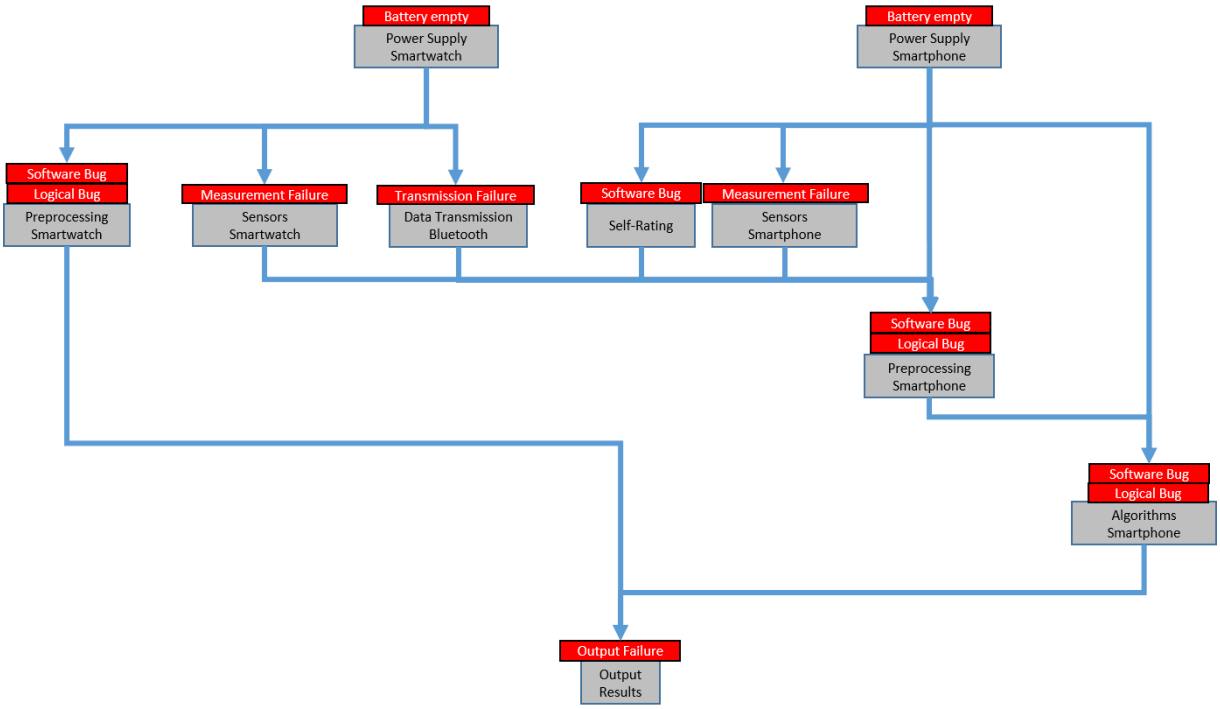

Figure 3: overview of fault-tree analysis

5. SIMULATION OF ENERGY USAGE

This work‘s numeric simulation is implemented in the simulation tool MATLAB/Simulink. This tool has native support for the division into subsystems described in chapter 3.2, allowing a structured implementation of the individual parts of the system In order to simulate the energy supply of the therapy support system, the system is first divided into the subsystem smartphone and the subsystem smart watch. Further subdivision of the subsystem smartphone is visualized in Figure 5. The subdivision of the smart watch is done analogously, with different values of some parameters as the only difference between the behavior of the two subsystems. All values used here are notional for presentation purposes and would have to be changed in practice. Basically, the energy consumption of the smartphone is described by a basic

consumption representing consumption without any influence from the therapy support system. In the example of the simulation in Figure 5, basic consumption is characterized as a linear decline of energy over 24 hours. This linear decline can be accelerated by the additional subsystems WLAN, Bluetooth, GPS and CPU. The influence of these subsystems on basic consumption is parametrized by an amplification and by a time interval over which it occurs. In the example in Figure 5, a random interval for each subsystem is used. The parametrization of this amplification and the time interval can be adapted in accordance with the application scenario. For a more detailed look at the influence of individual subsystems on energy consumption, the enablers (see Figure 5) are implemented to enable turning each subsystem on or off. The combined effect of all the subsystems included in Figure 5 (WLAN, Bluetooth, GPS and CPU) on the energy supply of the smartphone are compared to basic consumption in Figure 4.

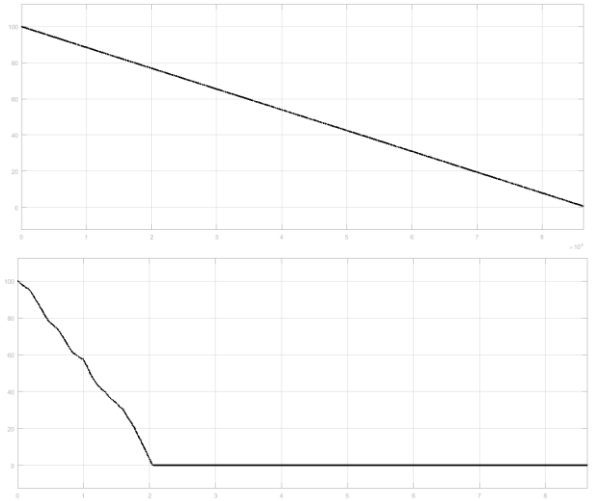

Figure 4: basic consumption of smartphone energy usage without (upper plot) and with (lower plot) enabled influence of subsystems WLAN, Bluetooth, GPS and CPU

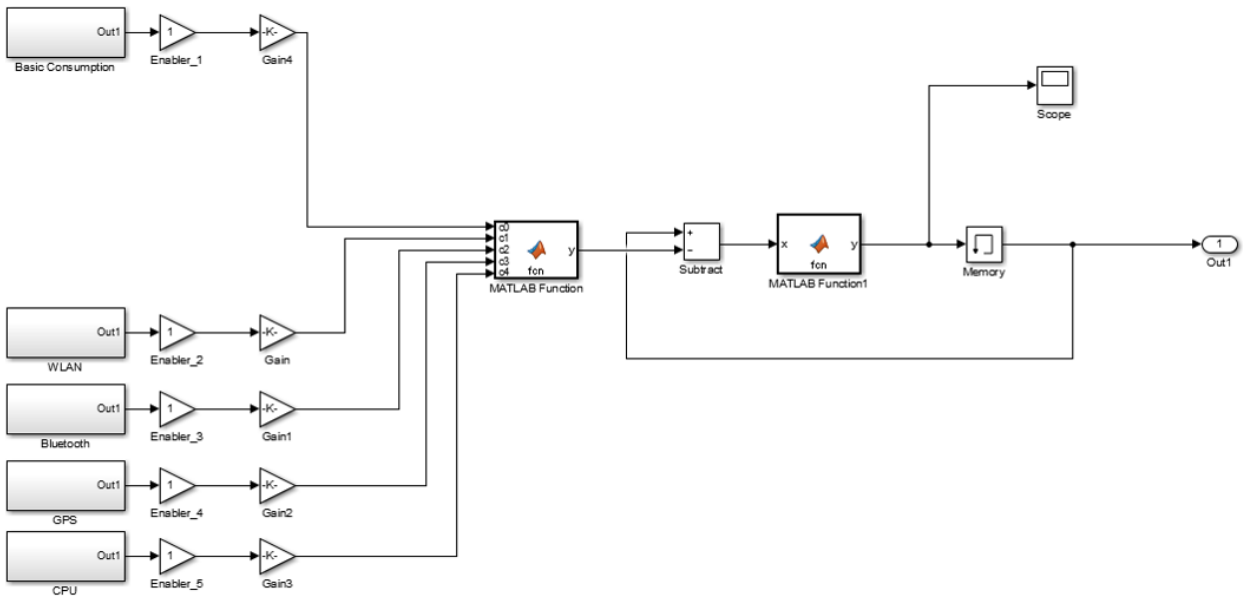

Figure 5: implementation of Numeric Simulation of Power Consumption in the Subsystem Smartphone in MATLAB/Simulink

6. RESULTS

The hybrid framework consists of a structured and analytical FMEA method to initially describe the overall system and look for potential weak points. After identifying such weak points, these are simulated numerically using the tool implemented in MATLAB/Simulink. Advantages of this implemented tool include easy and clear structuring of the individually separated subsystems, improving applicability in practice. In addition, the effect of individual subsystems on overall energy consumption can be viewed individually using the enablers, increasing the value of the framework for practical use. This framework turns out to save a lot of time and resources in comparison to series of experimental trials. In contrast to manual execution of tests, the following simulation case is used to demonstrate the time savings with the support of this simulation framework. The remaining time of the power supply of the smartphone is required if the GPS module is used differently. On the one hand, the GPS module can provide high-resolution

local information, thus consuming more energy or, on the other hand, it provides less local information in low resolution and consumes less energy. With the help of the numerical simulation of the power consumption, this issue of the GPS module was investigated, whereby the results are demonstrated in Figure 6. Due to a lower resolution of the sample rate 10000, the energy discharge takes place in 9.4 hours, whereas the high-resolution version with a sample rate of 1000 requires 7.2 hours. Consequently, the higher resolution of the GPS module accelerates the energy discharge of the power supply of the smartphone by 2.2 hours.

7. CONCLUSION AND FUTURE WORK

In summary, the present paper has introduced a simulation framework for medical applications, which responds to the challenge of interoperability between a highly diverse set of possible configurations of mHealth Devices through simulation. The generalizability of this simulation approach and the use of structured methods are essential elements of its usability as a reference. This ensures adaptability to other system, making this simulation framework capable of flexible use in other systems. Another unique feature is the inclusion of data privacy into the simulation workflow, which shall be developed further in ongoing work. Another priority will be to include usability of the mHealth systems on the patient side and its effects on the system as a whole.

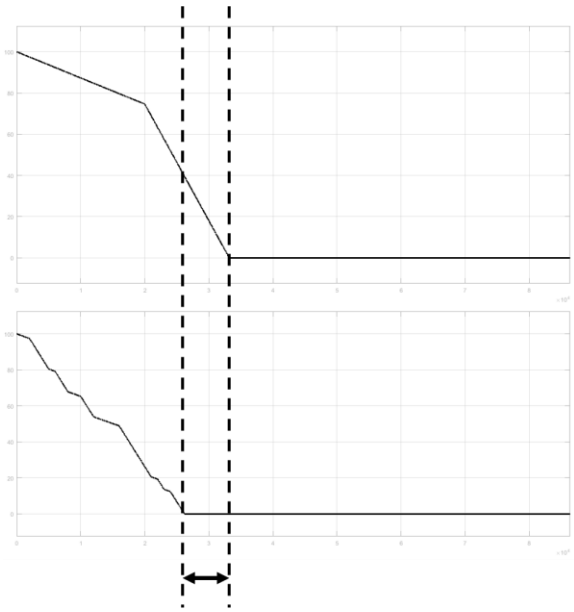

Figure 6: time difference of the available energy consumption with different use of the GPS module; in the upper part of the picture the GPS module is sampled at low rate of 10000 and leads to a total energy consumption of the system within 34000s (9.4 h); in the picture below the GPS module is sampled at high rate of 1000 and causes a total energy consumption within 26000s (7.2 h)

ACKNOWLEDGMENTS

This work was fully conducted in the scope of the research project STEADY (13GW0162D), funded by the German Federal Ministry of Education and Research.

REFERENCES

Ahmed S., Amagoh F., 2008. Modeling Hospital Resources with Process Oriented Simulation. Central Asia Business 2008 . pp. 5–20.

Almagooshi S., 2015. Simulation Modelling in Healthcare: Challenges and Trends. Procedia Manufacturing 3 . pp. 301–307.

Andreev V. P., Head T., Johnson N., Deo S. K., Daunert S., Goldschmidt-Clermont, P. J., 2013. Discrete event simulation model of sudden cardiac death predicts high impact of preventive interventions. Scientific reports 3 . pp. 1771.

Baig M. M., Gholamhosseini H., Connolly M. J., 2015. Mobile Healthcare Applications: System Design Review: Critical Issues and Challenges. Australasian Physical & Engineering Sciences in Medicine 38(1): pp. 23–38.

Bolaji A., 2014. Simulation of a Real-time Mobile Health Monitoring System Model for Hypertensive Patient in Rural Nigeria. African Journal of Computing & ICT.

Cabrera E., Luque E., Taboada M., Epelde F., Iglesias M. L., 2012. Optimization of emergency departments by agent-based modeling and simulation. 13th International Conference on Information Reuse & Integration (IRI) . pp. 423–430. Las Vegas, NV, USA.

Carlson C. S., 2012. Effective FMEAs. Hoboken, NJ, USA: John Wiley & Sons, Inc.

Fernandez R., Shah S., Rosenman E. D., Kozlowski S. W. J., Parker S. H., Grand J. A., 2017. Developing Team Cognition: A Role for Simulation. Simulation in healthcare. journal of the Society for Simulation in Healthcare 12(2): pp. 96–103.

Geis G. L., Pio B., Pendergrass T. L., Moyer M. R., Patterson M. D., 2011. Simulation to assess the safety of new healthcare teams and new facilities. Simulation in healthcare. journal of the Society for Simulation in Healthcare 6(3): pp. 125–133.

Gittinger M., Brolliar S. M., Grand J. A., Nichol G., Fernandez R., 2017. Using Simulation as an Investigational Methodology to Explore the Impact of Technology on Team Communication and Patient Management: A Pilot Evaluation of the Effect of an Automated Compression Device. Simulation in healthcare. journal of the Society for Simulation in Healthcare 12(3): pp. 139–147.

Lammers R. L., Willoughby-Byrwa M., Fales W. D., 2014. Errors and error-producing conditions during a simulated, prehospital, pediatric cardiopulmonary arrest. Simulation in healthcare. journal of the Society for Simulation in Healthcare 9(3): pp. 174–183.

Lee B. Y., Brown S. T., Korch G. W., Cooley P. C., Zimmerman R. K., Wheaton W. D. et al., 2010. A computer simulation of vaccine prioritization.

allocation, and rationing during the 2009 H1N1 influenza pandemic. Vaccine 28(31): pp. 4875–4879.
Lunze J., 1995. Künstliche Intelligenz für Ingenieure. München, Wien: Oldenbourg. pp. 182-192.
MIL-P-1629. 1949. Procedures for Performing a Failure Mode, Effects and Criticality Analysis.
Monks T., Pitt M., Stein K., James M., 2012. Maximizing the population benefit from thrombolysis in acute ischemic stroke: a modeling study of in-hospital delays. Stroke 43(10): pp. 2706–2711.
Nguyen K. D., Cutcutache I., Sinnadurai S., Liu S., Basol C., Sim E., 2008. Fast and accurate simulation of biomonitoring applications on a wireless body area network. 5th International Summer School and Symposium on Medical Devices and Biosensors . pp. 145–148. Hong Kong, China.
Panigrahi D., Chiasserini C., Dey S., Rao R., Raghunathan A., Lahiri K., 2001. Battery life estimation of mobile embedded systems. Proceedings of 14th International Conference on VLSI Design . pp. 57–63. Bangalore, India.
Rakhmatov D., Vrudhula S., Wallach D. A., 2003. A model for battery lifetime analysis for organizing applications on a pocket computer. IEEE Trans. VLSI Syst. 11(6): pp. 1019–1030.
Shi J., Peng Y., Erdem E., 2014. Simulation analysis on patient visit efficiency of a typical VA primary care clinic with complex characteristics. Simulation Modelling Practice and Theory 47: pp. 165–181.
Tietjen T., Decker A., Müller D. H., 2011. FMEA Praxis: Das Komplettpaket für Training und Anwendung. 3. überarb. Aufl. München. Hanser.
Yun L., Roychoudhury A., Mitra T., Herbstritt M., 2007. Timing Analysis of Body Area Network Applications. Schloss Dagstuhl - Leibniz-Zentrum fuer Informatik GmbH, Wadern/Saarbruecken, Germany.

AUTHORS BIOGRAPHY

Michael Aleithe studied Systemdesign at Ernst-Abbe University for Applied Sciences and specialized at Modeling and Simulating of Complex Technical Systems. In the past he was employee at Xceptance Software Technologies GmbH and works on agent-based simulations. His research-interest include interconnected data, simulation and mHealth. He is currently working on a PhD thesis in the area of designing mHealth systems at Leipzig University, Germany supervised by Prof. Dr.-Ing. Bogdan Franczyk.

Philipp Skowron studied Business Information Systems at Harz University of Applied Sciences and afterwards he continued his studies at University of Leipzig in the same area of study. Currently, he is writing on his PHD about the simulation of cyber physical systems using artificial intelligence in the mHealth area, which is also his specialization and research interest. Supervisor is Prof. Dr.-Ing. Bogdan Franczyk.

Angela Carell studied educational science at University of Dortmund. She made her PhD at the Universities of Bochum and Dortmund about computer supported collaborative learning. Currently she is head of research at the adesso AG.

Daniel Böttger studied IT at the University of Applied Sciences Mittweida. He has been working at the University of Leipzig developing medical software for psychiatry and currently does the same at the German Depression Foundation. His research interests include EEG analysis and eHealth for clinical depression.

Tobias Goblirsch received the M.S. degree in electronic engineering at the Leipzig University of Applied Science. He is currently a PhD student in the Information Systems Institute at University of Leipzig. His main research interests include data acquisition, data integration and data modelling in the context of environmental monitoring. Parallel to his scientific activities, he works for the Kompass GmbH.

Bogdan Franczyk is professor at Leipzig University since 2002. In the past he was the research director of Intershop AG as well as professor in Swinburne, Australia and Wroclaw, Poland. His research-area includes especially information management systems.

BENEFITS OF AUTOMATED WHEELCHAIRS IN A HOSPITAL: A SIMULATION APPROACH

Iván Castilla-Rodríguez[(a)], Rafael Arnay[(b)], Jonel Rodríguez[(c)], Raquel Rodríguez[(d)]

[(a),(b),(c)(d)] Departamento de Ingeniería Informática y de Sistemas. Universidad de La Laguna. Spain

[(a)]icasrod@ull.edu.es, [(b)]rarnayde@ull.edu.es, [(c)]jonelr93@gmail.com
[(d)]rodriguezdiazraquel51@gmail.com

ABSTRACT
Autonomous vehicles are increasingly becoming a solution to improve the functioning of the processes of many organizations and, even, society. In a hospital, there are multiple opportunities to use this type of vehicle, especially for the transport of heavy loads, but its use to take patients has not yet been sufficiently studied. In this paper, the organizational impact of replacing manual wheelchairs from the reception of a small hospital by autonomous wheelchairs is analyzed using a discrete event simulation model. The results show that automated wheelchairs benefit the hospital, both economically and in the quality of the assistance.

Keywords: autonomous wheelchair, discrete-event simulation, economic assessment

1. INTRODUCTION

Technological advances mean that autonomous vehicles are appearing more and more frequently in our society. The use of these vehicles is well established in controlled and closed environments, such as production plants or logistics distribution centers. However, the use of these same vehicles in open environments, where they have to interact with other vehicles or with people, has only been possible with the enormous advance in techniques of detection and avoidance of obstacles. We can see the last state-of-the-art example in Tesla's and Google's vehicles circulating in the streets.
The corridors of a hospital are a closed environment, where it makes sense to apply a global planning of a route but, at the same time, they are dynamic environments, where the vehicle requires local planning techniques to avoid unexpected obstacles (LaValle 2006). In this environment, there are former examples of autonomous vehicles tested in this environment, such as the Hospital Transport Robot FIRST (Aldon and Benoit 1995), intended to transport heavy loads, but the viability of using vehicles that can transport patients with reduced mobility remains unexplored. When transporting people, these vehicles must include even more security measures and be more careful with the management of their maneuvers, which cannot be so abrupt so as not to embarrass or frighten the passenger.
Hospitals receive a very high volume of patients who require assistance to travel through their facilities. Leaving aside the emergencies, where this problem is aggravated by the pression and dynamism of the situations that occur, many elective patients also require this assistance upon arrival at the hospital. Although some of these patients arrive at the hospital with their own wheelchair, many of them are helped by hospital staff (usually a janitor) to be accommodated in a wheelchair that the hospital itself makes available. Afterwards, this same janitor pushes the wheelchair to the consultation room, where a doctor will take care of the patient, or to the facility where some test will be done.
The Robotics group from the Universidad de La Laguna (ULL) has been working for several years with a prototype of an autonomous wheelchair (Arnay et al. 2018). This prototype follows the ideas of former developments such as those described in (Faria, Reis, and Lau 2014). Before testing this prototype in a real environment, we need to study the performance of the control software. To carry out these experiments, we start with a computerized recreation of the plane of a test environment, and simulate the operation of the wheelchair in that environment by means of simulation. Hence, we can observe the response of the wheelchair to static and dynamic obstacles in that environment. ROS libraries (Quigley et al. 2009) allow these studies to be carried out, by incorporating a reliable reproduction of the sensors and actuators of the vehicle, and their relationship with the physics of the environment. It is through this type of libraries that it is possible to collect data on the possible behavior of the wheelchair in the environment where it is desired to be implemented. Moreover, we can test different contexts, such as hours of greater and lesser number of patients, areas reserved for the passage of the chair or shared routes... We can raise technical and, at most, operational analyses of the performance of the wheelchair with these tools but, what about the impact on the organization? Do these wheelchairs improve the quality of patient care? Do they reduce their waiting times? Do

they save costs or, on the contrary, do they suppose an extra cost to afford? Is it equally beneficial to replace the entire fleet of manual chairs with autonomous chairs that replace only one part? To answer these questions there are other tools, oriented to the modeling and simulation of organizations, that can facilitate the study of the impact of this technology in the use of resources and the definition of hospital processes.

2. METHODS

In this work, we have used a discrete-event simulation library to model and simulate the impact of the implementation of autonomous wheelchairs in an environment based on the provision of an actual hospital in the south of the island of Tenerife.

2.1. PSIGHOS

PSIGHOS is a discrete-event-simulation library implemented in Java, and developed by the ULL Simulation group (Castilla, García, and Aguilar 2009). There are different approaches or worldviews that can be posed to model a system by using discrete-event simulation (Balci 1988). Among them, PSIGHOS adheres to the process-oriented worldview, which focuses on the entities that interact within the system, and the ordering and characteristics of the different steps (activities) that these entities carry out to achieve their objectives, as well as the resources required to perform these steps.

There is no standard approach to carry out the modelling of the processes that describe a system; however, van der Aalst et al. (2003) proposed a set of workflow patterns that can be used to model business processes. PSIGHOS starts from the definitions of control workflow patterns, and applies them to describe any system, such as help desks (Castilla et al. 2007) or the transshipment operations in a container port (Castilla-Rodríguez et al. 2017).

2.2. Conceptual model

We have posed a scenario in which patients with reduced mobility arrive at the hospital for a general consultation. Upon arrival, they request a wheelchair and are brought to the consultation room. After being seen by the general practitioner (GP), the patients return to the hospital reception and leave the chair. From a conceptual point of view, the model treats patients with reduced mobility as the entities of the system.

The process that these patients follow within the hospital requires interaction with several resources: first, wheelchairs, either autonomous or manual, in which the patient seat; second, the janitors, which accommodate the patients in the wheelchairs (manual or autonomous), push them to the consultation room (only in the case of manual wheelchairs), and finally help them get out of the wheelchair when leaving the hospital; and, finally, the GPs who, in a simplified way, are used only as a control to adequately size the hospital's patient care capacity.

The route that the patients follow to arrive at the consultation room is divided into several stretches. We use ROS to compute the estimated time to traverse each one of these stretches under several occupancy conditions, by setting a varied number of obstacles. The workflow required to model this system treats each stretch as a single activity where the patient “stays” as long as estimated by ROS. At the higher abstraction level proposed by PSIGHOS, we do not consider possible conflicts among wheelchairs trying to traverse the same stretch, since we assume that the interferences among them are already captured by the time estimations simulated with ROS. Figure 1 shows a simplified view of the flow described.

1.1. Parameterization and case study

We started from the floorplan of a hospital in the South of Tenerife (Figure 2). In this floor, there are several consultation rooms for GPs. The South of Tenerife is a mass tourism area where there are not only local population with reduced mobility, but many elder tourists that may require this kind of service during their visit to the island. Therefore, a noticeable number of outpatients that attend to an appointment at the hospital have reduced mobility and require a wheelchair to move from the reception room to the consultation room. For the sake of simplicity, we only focused on these patients with reduced mobility and ignored the rest of patients. Therefore, we modeled a subset of the GPs actually available, and assumed that they were completely devoted to this kind of patients.

Currently, all the wheelchairs are manual. We tested the economic and quality-of-service impact of replacing all or several of the manual wheelchairs by automated wheelchairs. We did not consider unexpected arrivals, but just the elective outpatients. We limited the time horizon of the simulation to an 8-hour shift, and fixed the last arrival of patients one hour before the end of the shift. The simulation was configured to stop when the last patient was seen, even when it could mean extending the simulation time beyond the initial time horizon.

Table 1 summarizes the parameters utilized to define the different scenarios to test. We focused on a busy day and obtained times to traverse the stretches by setting high density of obstacles in ROS. Based on the characteristics of the real system, we defined a base case, with 2 GPs, 2 janitors, 5 wheelchairs, and 5 patients per appointment slot. Afterwards, we performed a full-factorial experimental design, by using the number of janitors available, the patients per appointment and the total number of wheelchairs available as factors. Within each number of wheelchairs, we used the case where all the wheelchairs were manual as a reference, and then we tested all the possible combinations of automated and manual wheelchairs.

We run 100 replications per experiment, and applied the common random numbers technique to reduce the variance of the results among the experiments.

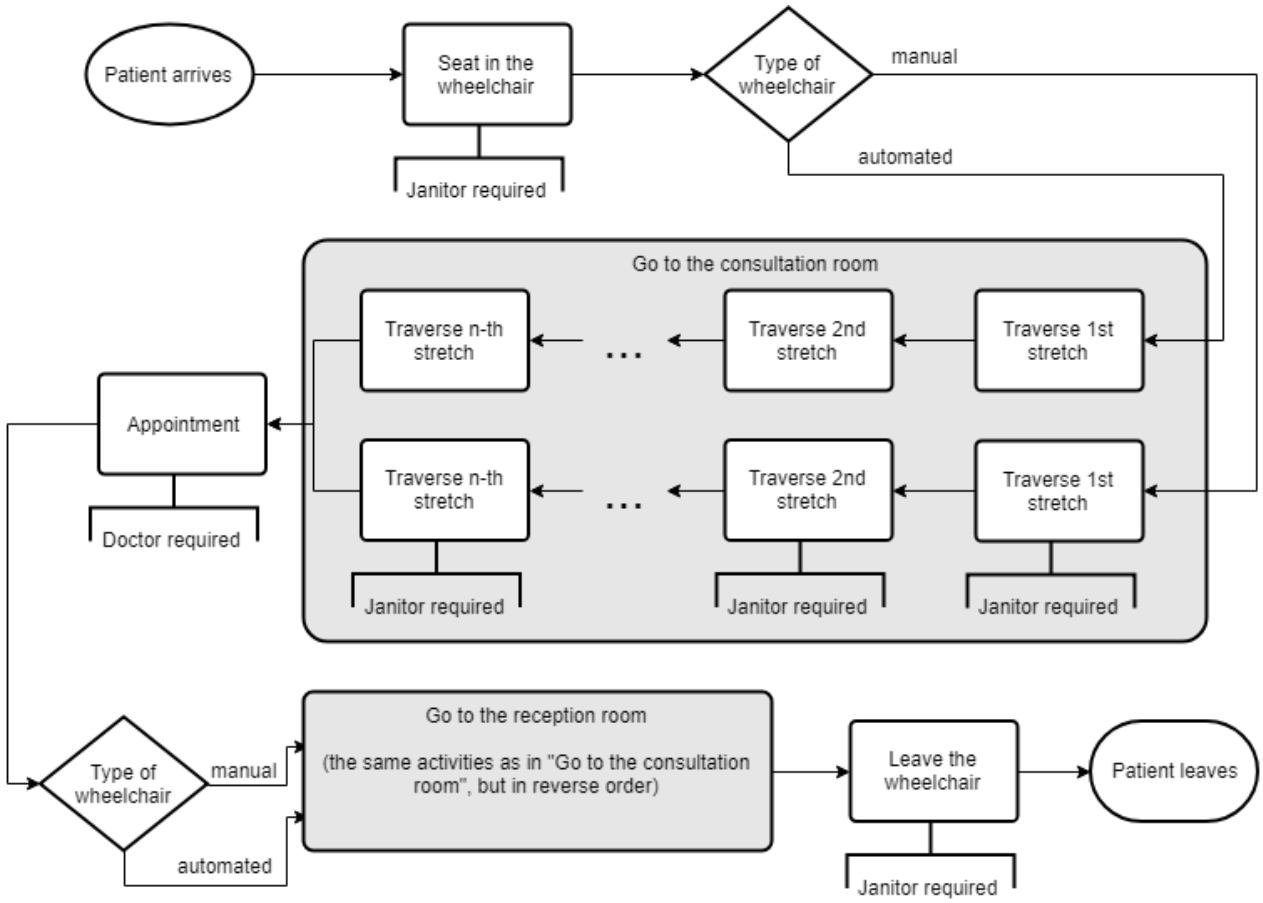

Figure 1: Conceptual model

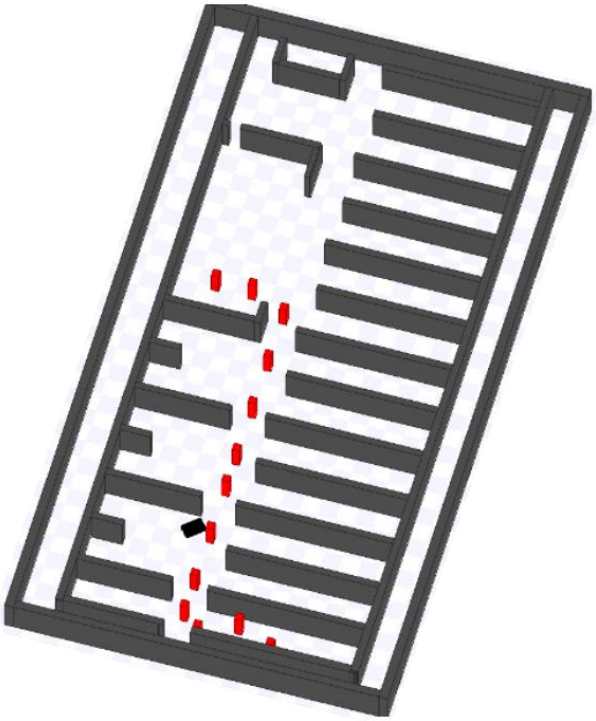

Figure 2: Simplified floorplan of the hospital

Table 1: Parameters of the case study

Parameter	Value	Varied in scenarios
GPs	2	
Janitors	2	1 – 2
Duration of consultation activity	10-15 minutes (uniform)	
Duration of seating	1-3 minutes (uniform)	
Duration of standing up	1-3 minutes (uniform)	
Time between appointments	30 minutes	
Patients per appointment slot	5	4 – 6
Wheelchairs available	5	5 – 8

With respect to the economic parameters, we estimated the acquisition cost of the automated wheelchairs, based on our prototype, in around 5,000 €, whereas we assume 1,000 €/year as their maintenance cost. We conservatively assumed no maintenance cost for manual wheelchairs. Based on data from the hospital, we also assumed the annual contracting cost of a janitor to be 21,600 €.

3. RESULTS

Table 2 summarizes the results of the base case. Although not statistically significant, there is a consistent improvement in the total waiting time of patients as the proportion of automated wheelchairs increase. The total waiting time includes both the time waiting for being accommodated on a wheelchair and the time waiting to be attended by the GP. Each automated wheelchair that replaces a manual one saves around 100 minutes of work from the janitors per shift. When considering a larger time horizon (5 years) and a completely automated wheelchair park, it would be possible to save up to 70,000 €.

If we fix the number of wheelchairs available to 5, we can analyze the impact of varying other conditions of the system (Figures 3 and 4). As seen in Figure 3, scenarios with 2 janitors are well balanced, independently on the number of automated wheelchairs. However, critical scenarios with only 1 janitor available may lead to extreme waiting times, even at the lowest rates of arrival of patients. These critical scenarios clearly benefit from the automated wheelchairs, achieving almost equal waiting times as the corresponding 2-janitor experiments when every wheelchair is automated.

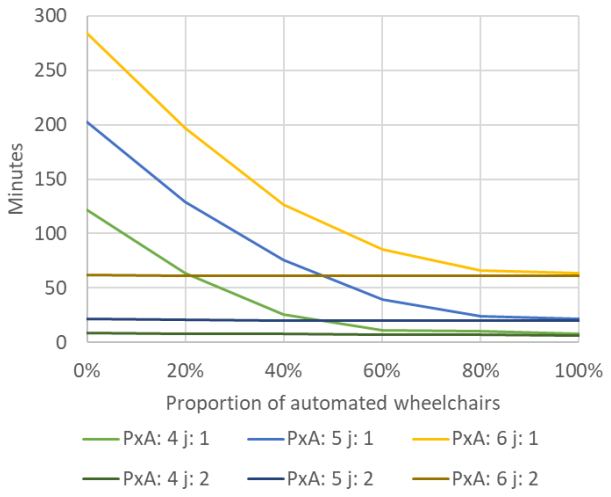

Figure 3: Total waiting time of patients with respect to the proportion of automated wheelchairs in different scenarios (5 wheelchairs available). PxA: patients per appointment slot; j: janitors available.

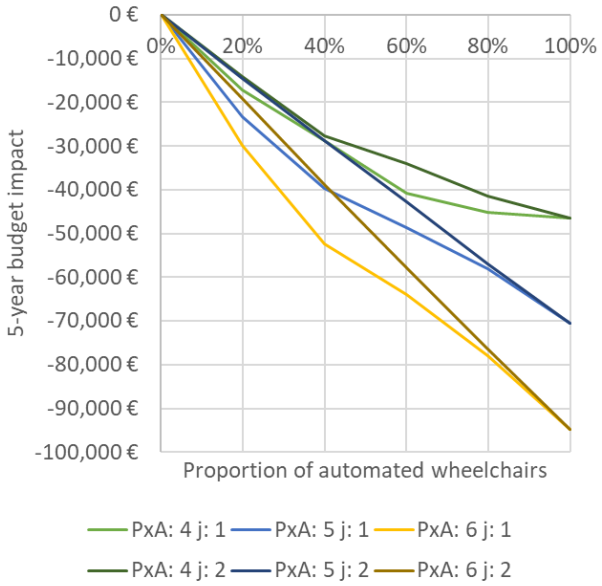

Figure 4: 5-year budget impact with respect to the proportion of automated wheelchairs in different scenarios (5 wheelchairs available). PxA: patients per appointment slot; j: janitors available.

With respect to the economic impact, switching to automated wheelchairs is cost-saving in all cases (Figure 4), with a benefit that increases as the proportion of automated wheelchairs does. Those scenarios with a higher flood of patients with reduced mobility are more prone to benefit from the use of automated wheelchairs, up to around 95,000 € in a 5-year time horizon.

Having more than 5 wheelchairs at the janitor's disposal does not modify the performance of the hospital, because they are the janitors and not the wheelchairs, who create a bottleneck in the system. Figure 5 shows the waiting time when there are 8 wheelchairs. The results are very similar to those in Figure 3, even in absolute numbers of wheelchairs, i.e. there is no extra benefit in having more than 5 automated wheelchairs (62,5% out of 8, 100% out of 5).

In terms of economic benefit, adding more than 5 automated wheelchairs has a negative impact when the attendance is low or average (4-5 patients per appointment slot). This situation reverses when all the 8 wheelchairs are automated and the hospital receives 6 patients per appointment slot (Figure 6).

Table 2: Results of testing a 2-janitor, 8-wheelchair, 5 patient-per-arrival scenario

Wheelchairs		Time (Average [95% CI])		Economic impact (Average [95% CI])
#automated	#manual	Waiting time (minutes)	Time saved from janitors (minutes)	5-years budget impact
0	5	21.48 [17.11, 26.15]	-	-
1	4	20.56 [15.57, 25.48]	108.78 [82.57, 135.04]	-14,476 € [-20,384 €, -8,578 €]
2	3	20.31 [14.93, 25.50]	217.10 [192.71, 245.80]	-28,847 € [-35,304 €, -23,360 €]
3	2	19.89 [14.52, 24.65]	323.82 [294.19, 353.85]	-42,860 € [-49,617 €, -36,192 €]
4	1	19.82 [14.29, 24.57]	430.79 [404.53, 458.99]	-56,927 € [-63,274 €, -51,019 €]
5	0	19.81 [14.28, 24.47]	536.08 [511.67, 559.51]	-70,619 € [-75,890 €, -65,126 €]

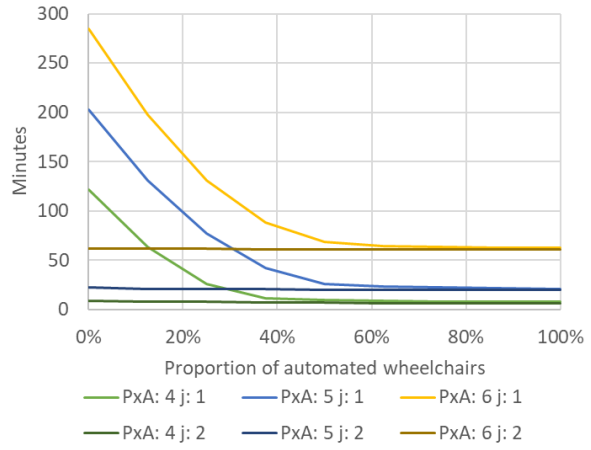

Figure 5: Total waiting time of patients with respect to the proportion of automated wheelchairs in different scenarios (8 wheelchairs available). PxA: patients per appointment slot; j: janitors available.

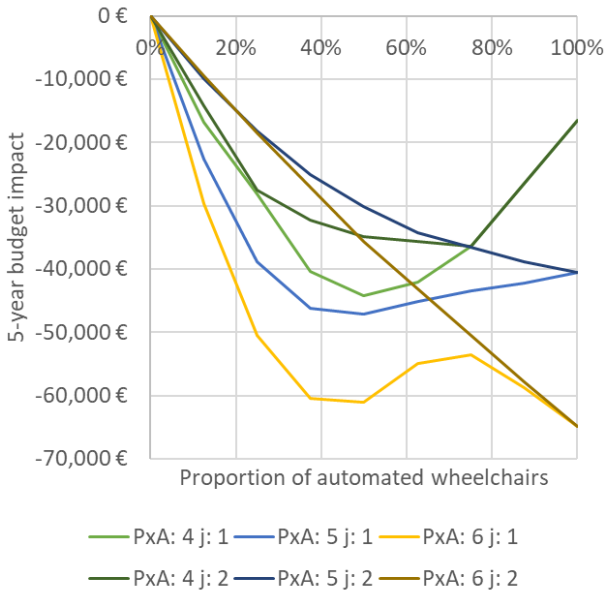

Figure 6: 5-year budget impact with respect to the proportion of automated wheelchairs in different scenarios (8 wheelchairs available). PxA: patients per appointment slot; j: janitors available.

4. DISCUSSION

Although previously published papers have dealt with the technical assessment of autonomous vehicles in different environments, they have not analyzed the actual impact on the organization where these vehicles will be used. We have studied the impact of replacing manual wheelchairs by automated ones in a small hospital in the South of Tenerife. Automated wheelchairs involve a considerable initial expenditure and higher maintenance cost than manual wheelchairs. However, the base case results show that, from the first automated wheelchair, the hospital may save budget due to the opportunity cost of using janitors for alternative tasks. These savings remarkably increase as the proportion of automated wheelchairs does.

Automated wheelchairs are especially useful in critical situations where the number of available janitors is downsized or the number of patients with reduced mobility increases. In the real hospital, other staff (GPs, nurses, nursing assistants…) may help to solve these situations, but at the expense of a higher cost.

The use of automated wheelchairs also offers a modest improvement in the quality of service for patients, as regards of their total waiting time. From the perspective of the hospital that we are analyzing, which depends on the public health system, this is not a critical aspect to consider. However, private clinics may offer premium services based on this technology. Apart from the quality of service, they could provide their clients with additional features in the wheelchairs, such as a tablet with entertainment or information contents.

The approach presented in this paper can be easily adapted to biggest hospitals. The major difficulties are on the side of collecting the data from the actual performance of the automated wheelchairs in the hospital. Currently, we are working in a tool to facilitate the communication between the technical-operational simulations performed with ROS (that we would use to collect the required data) and the higher level simulations presented in this paper. Airports, nursing homes, governmental buildings, malls… are also areas of interest for this research.

ACKNOWLEDGMENTS

The authors want to thank Catalina Raquel Mari Sánchez, María Teresa Martín González, Ángel Vázquez López and the rest of staff from Hospital Nª Sra. de Candelaria for the floor plans and the assistance during this research.

This work was supported by the Spanish Ministry of Science and Technology [grant number: DPI2017-90002-R].

REFERENCES

Aldon M.J., Benoit M., 1995. Localization system of the hospital transport robot FIRST. IFAC Proceedings Volumes, 28 (11), pp. 229-234. 12-14 June 1995, Espoo, Finland.

Arnay R., Hernández-Aceituno J., Toledo J., Acosta L., 2018. Laser and optical fusion for a non-intrusive obstacle detection system on an intelligent wheelchair. IEEE Sensors Journal, 18 (9), pp. 3799 – 3805.

Balci O., 1998. The implementation of four conceptual frameworks for simulation modeling in high-level languages. In: Proceedings of the 20th conference on Winter simulation - WSC '88. pp. 287–95. 12-14 December 1988, San Diego, California, USA.

Castilla I., García F.C., and Aguilar R.M. 2009. Exploiting concurrency in the implementation of a discrete event simulator. Simulation Modelling Practice and Theory, 17(5), pp. 850-870.

Castilla-Rodríguez I., Expósito-Izquierdo C., Aguilar-Chinea R.M., Melián-Batista B., Moreno-Vega J.M. 2017. A simulation approach for the transshipment operations at maritime container terminals. In: Proceedings of The 14th International Multidisciplinary Modelling & Simulation Multiconference (I3M). 18-20 September 2017, Barcelona, Spain.

Castilla I., Muñoz R., Baquero P. J., Aguilar R.M. 2007. Helpdesk Modeling and Simulation with Discrete Event Systems and Fuzzy Logic. In: Proceedings of the European Modeling and Simulation Symposium EMSS. 4-6 October 2007, Bergeggi, Italy.

Faria B.M., Reis L.P., and Lau N., 2014. A Survey on Intelligent Wheelchair Prototypes and Simulators. In: Rocha Á., Correia A., Tan F., Stroetmann K., eds. New Perspectives in Information Systems and Technologies, Volume 1. Advances in Intelligent Systems and Computing, vol 275: Springer, Cham, pp. 545-557.

LaValle S.M., 2006. Planning Algorithms. Cambridge University Press

Quigley M., Conley K., Gerkey B.P.., Faust J., Foote T., Leibs J., Wheeler R., and Ng A.Y. 2009. ROS: An open-source robot operating system. ICRA Workshop on Open Source Software.

van der Aalst W., ter Hofstede A., Kiepuszewski B., Barros A.P. 2003. Workflow patterns. Distributed and Parallel Databases, 14(1), pp. 5-51.

AUTHORS BIOGRAPHY

Iván Castilla-Rodríguez received his B. Sc. and M. Sc. in Computer Engineering from Universidad de La Laguna, Spain, in 2004. He obtained his PhD on Modeling and Simulation from the same university in 2010. He worked as Health Economic Modeler until 2015, when he returned to Universidad de La Laguna as Assistant Professor. His research fields include applying modeling, simulation and soft computing techniques to solve problems in any area.

Rafael Arnay was born in 1982. He received the M.Sc. and Ph.D. degrees in Computer Science from the University of La Laguna (Spain), in 2007 and 2014, respectively. He joined the Department of Computer Science and Systems, University of La Laguna in 2007, where he is currently an Assistant Professor. His current research interests include object segmentation and recognition, feature extraction and deep learning, applied both to robotics and medical images.

Raquel Rodríguez was born in 1995. In the year 2017, she graduated from Universidad de La Laguna obtaining a college degree in Industrial Electronic and Automatic Engineering. Currently, she is a Master's Program student in Disaster Management in Universidad Complutense de Madrid. Her research field includes autonomous systems, risk management, sensorial robotic systems, and modeling and data analysis.

Jonel Rodríguez was born in 1993. He received his college degree in Industrial Engineering from Universidad de La Laguna, Spain, in 2017. His current research interest include autonomous vehicles and simulation of different environments.

EVALUATION OF HARDWARE-BASED EVOLUTIONARY ALGORITHMS FOR THE IDENTIFICATION OF MOTION-BASED ACTION POTENTIALS IN NEURAL BUNDLES

Volkhard Klinger

Department of Embedded Systems

University of Applied Science Hannover (FHDW)

D.30173 Hannover, LS, Germany

volkhard.klinger@fhdw.de

ABSTRACT

The recording and interpretation of nerve signals for controlling exoprosthesis is a current challenge in medical technology. The aim of the higher-level project is both the measurement and identification of bio-signals. Based on evolutionary algorithms, using deep learning strategies, a model is created in a learning phase that describes the correlation between electroneurogram (ENG)-signals and motion sequences. In the following operation phase, this model will be used in daily life to control the prosthesis. In order to make the model adaptive in operation mode depending on various parameters, such as physiological parameters, body condition, change in position of the implanted cuff electrode and changes and further additions to the relationship between movement and ENG-signals, the objective is to provide continuous optimization of the model even in operation mode. This article presents an evaluation of a hardware implementation of an evolutionary algorithm with regard to speed and hardware-resources and compares it with a corresponding software solution. The results are evaluated both for use of a hardware solution as a local model optimizer and for use as a speed-up device within the learning mode.

Keywords: system identification, deep learning, hardware-based evolutionary algorithm, electroneurogram, configurable logic

1. INTRODUCTION

The intelligent control of prostheses or handicapped limbs based on peripheral nerve signals is a key challenge in medical technology. The use of peripheral nerve signals has some advantages compared to the use of electroencephalogram (EEG)- or electromyogram (EMG)-signals. The EEG-signal is buried within other brain activity (general background brain activity), as well as within electrical and muscle activity from different sources outside, like movement of the jaw or neck. The EMG-signals of complex structures, responsible for the movement of e.g. the forearm and the hand, are distributed over lots of muscles. And, in case of an amputation, these muscles are not available.

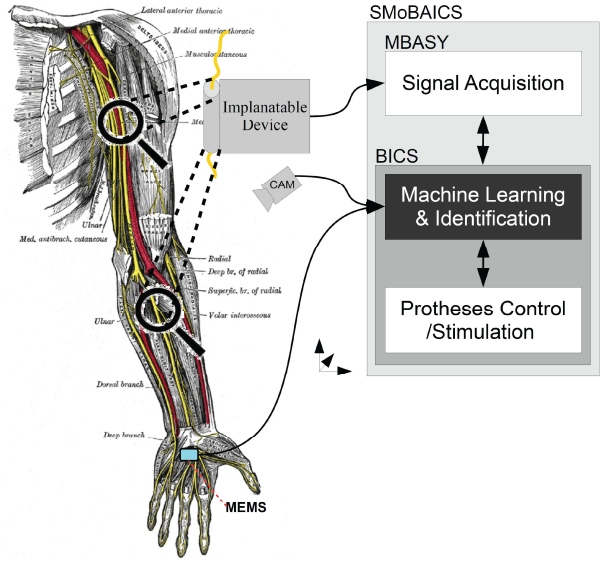

Figure 1: System Overview

Our approach is the direct use of the action potentials of peripheral neural bundles via an ENG (Gold, Henze, and Koch 2007), (Navarro, Krueger, Lago, Micera, Stieglitz, and Dario 2005), (Neymotin, Lytton, Olypher, and Fenton 2011). The ENG-signals are recorded via a cuff-electrode, using a minimal invasive technique, preprocessed by an specific designed analog frontend electronic (AFE), improving signal to noise ratio (SNR) for the demanding ENG-signals and identified based on machine learning algorithms (Klinger 2015), (Klinger and Klauke 2013), (Klinger and Klauke 2015). This proposal of a smart modular biosignal acquisition, identification and control system (SMoBAICS) (Klinger 2015), (Klinger 2017) integrates all necessary tasks in one framework (Hazan, Zugaro, and Buzsaki 2006), shown in Figure 1. The biosignal acquisition is done by the modular biosignal acquisition system (MBASY)-subsystem, the next generation of our own frontend-hardware/software-system (Klinger 2015).
The central part of the identification process is integrated in the biosignal identification and control system (BICS). It consists of two parts: the machine learning &

identification and the prostheses control/stimulation. While the second part is designed by state-of-the-art technology, the machine learning & identification is composed of multi-agent-based optimization algorithm and an evolutionary correlation of different types of nerve signals and of additional information, like camera tracking data or data from microelectromechanical systems (MEMS) (Klinger, 2018), realizing a deep learning environment. The verification of the identification method is realized based on the symbiotic cycle, combining a physical system, a simulation system and an agent based machine learning system, interacting in a symbiotic way (Klinger and Bohlmann 2017).

1.1. Machine Learning: Operation Modes

The machine learning and identification, implemented using deep learning algorithms, is the most complex module within SMoBAICS. The machine learning is based on evolutionary algorithms – a generic population-based meta-heuristic optimization algorithm inspired by biological evolution (De Jong 2006), (Schmidt and Lipson 2009) – embedded in a multi-stage and multi-agent implementation – using a symbiotic approach. Identification is the essential approach for implementing an ENG-based motion control. This identification method provides a model, describing the fundamental relation between ENG-signals and motion. The identification process is subdivided into two different phases, a learning phase and an operation phase.

1.2. Identification & Machine Learning

The identification is based on a two-stage design. The subdivision in two phases is necessary to allow a learning mode and an operation mode, described in the following itemized breakdown and shown in Figure 2:

- Learning Mode
  Based on a symbiotic learning algorithm, based on evolutionary algorithm and introduced in (Klinger and Bohlmann 2017), the model is generated from scratch, the base model. A sensor fusion with the trajectory information of a camera improves the model further. The required computing power is very high, provided by an external server farm.
- Operating Mode
  After the learning mode the generated model is transferred and used during the operating mode. This mode enables a mobile operation based on body-mounted computing power and a body-mounted system for trajectory information, a MEMS. For the local optimization of the model, which must be adapted by changing various parameters in the course of use, it is necessary to assess whether a body-mounted component can implement this task. Changes that require

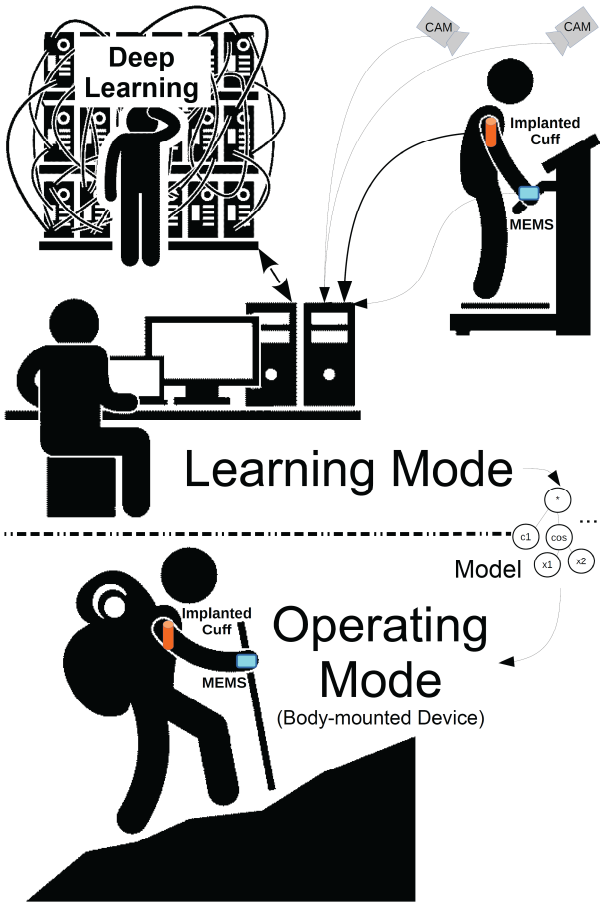

Figure 2: Learning and Operating Mode

adaptation of the model includes e.g. changes in physiological parameters (stress, physical exertion, etc.), changing the position of the cuff electrode, etc..

During the operation mode the base model from the learning mode is used by a mobile device, which supports a fitting of the model to changing parameters and a continuous learning for model improvements. One future objective is to integrate the necessary components for this mode, implanting it using a system in package (SIP). New technologies, like energy harvesting, have to be used to operate this device implant. In this paper we focus on hardware-based evolutionary algorithms (Kok, Gonzalez, Walker, Gurnett, and Kelson 2010), evaluating the scope of application within SMoBAICS (Klinger 2017). There are two main criteria for evaluation, speed and power consumption, described in the following paragraph.

- Speed
  The identification algorithm used is heuristic, so the run-time is not deterministic. However, complex problems, which clearly include this one, require a lot of computing power, which is provided by the use of a server farm. To allow a direct comparison between a software solution running on a processor and the hardware

solution, standardization is important. Here the focus is on individual operations of the selected evolutionary algorithm, for example described on the evolutionary steps: evolutionary operations per second (EOPS).

- Power Consumption
  After analyzing the speed or performance per operation, in the next step it is very important to consider the power consumption, as the system is in mobile operation during the operation mode.

2. HARDWARE-IMPLEMENTATION OF AN EVOLUTIONARY ALGORITHM

The evolutionary algorithm, chosen for hardware evaluation, is the genetic algorithm (GA), a meta-heuristic, because of its fast convergence and also as it does not require intermediate derivation. The design is based on a hardware description language (HDL) (very high speed circuit HDL (VHDL)) to realize a technology independent hardware design and to provide a fast prototyping on a field programmable gate array (FPGA) (Rashid 2017). The GA is the most popular type of evolutionary algorithm (EA), originally proposed by J.H. Holland (Holland 1975). They have been successfully applied by D.E. Goldberg (Goldberg 1989) and J.R. Koza (Koza 1992) to a wide range of real-world NP (non-deterministic polynomial) problems of significant complexity. The meta-heuristic of the GA repeatedly modifies a population of individual numerical solutions. Over successive generations, the solution evolves toward an optimal solution. The genetic algorithm can also address problems of mixed integer programming, where some components are restricted to be integer-valued. Inspired by natural evolution, GA provides fast convergence to a solution, in contrast to other evolutionary algorithms. The reason of GA being so fast is the collaboration of many individual sub-processes that lead to a fast convergence. Additionally there is no need for any further derivations which would slow down the process as more statements will take longer time to execute. The performance of the GA is influenced mainly by the crossover and mutation operators as they are responsible for generating the new variations as well as taking GA to better solutions related to the cost function. There are different ways to perform crossover and mutation. Depending on the problem, one had to be selected according to the results. The GA uses three major types of rules at each step to create the next generation from the current population:

- Selection
  It selects the fittest individuals, called elite parents, that contribute to the population at the next generation.
- Crossover
  It combines random individual entries from two parents to form new entries for the next generation.
- Mutation
  It applies random changes to individual entries in parents to form next generation.

The GA performs the following base steps according the idea of the meta-heuristic:

1) The algorithm begins by creating an initial population using random number generators. For a continuous model optimization, a base model can be used to start (operation mode).
2) The algorithm then creates a sequence of new populations. At each step, the algorithm uses the individuals in the current population (parent) to create the next population (offspring).
   a. Fitness value of each member of the current population is computed. These values are called the fitness scores or hits.
   b. Selects individuals based on their fitness score. These individuals are called parents.
   c. Some individuals in the current population that have higher number of hits are chosen as “elite”. These elite individuals are passed to the next population.
   d. Produces next population from the selected parents either by making random changes to a single parent (mutation) or by combining parent’s entries as pair (crossover).
   e. Replaces the current population with these solutions to form the next generation.
3) The algorithm stops when one of the stopping criteria is met.

When solving problems using GA, the iterations are repeating to reach the solution that fits the criteria. It may take tens to millions of iterations to find a suitable result and here the parallel processing nature of FPGA can be utilized. GA was implemented on Altera Cyclone V FPGA by using VHDL as HDL. Some basic differences in a HDL and software programming language (SPL):

- HDL code is compiled to construct the logic and storage elements and implement them onto targeted logic device on which software is run.
- SPL have sequential execution of instructions whereas in HDL it can be sequential as well as parallel.
- The length of data blocks in HDL is not as flexible as in SPL and there are no dynamic implementations in HDL on FPGA. However, reconfiguration is also possible in operations mode, for this reconfiguration times are in the ms range.

The hardware implementation was done for maximum of 32 numerical values per data-set. The abstraction level of individual modules is register transfer level (RTL) but the control unit has behavioral level of abstraction. The implementation of the GA on FPGA in HDL is done using a finite state machine (FSM).

Following each module is explained in more detail.

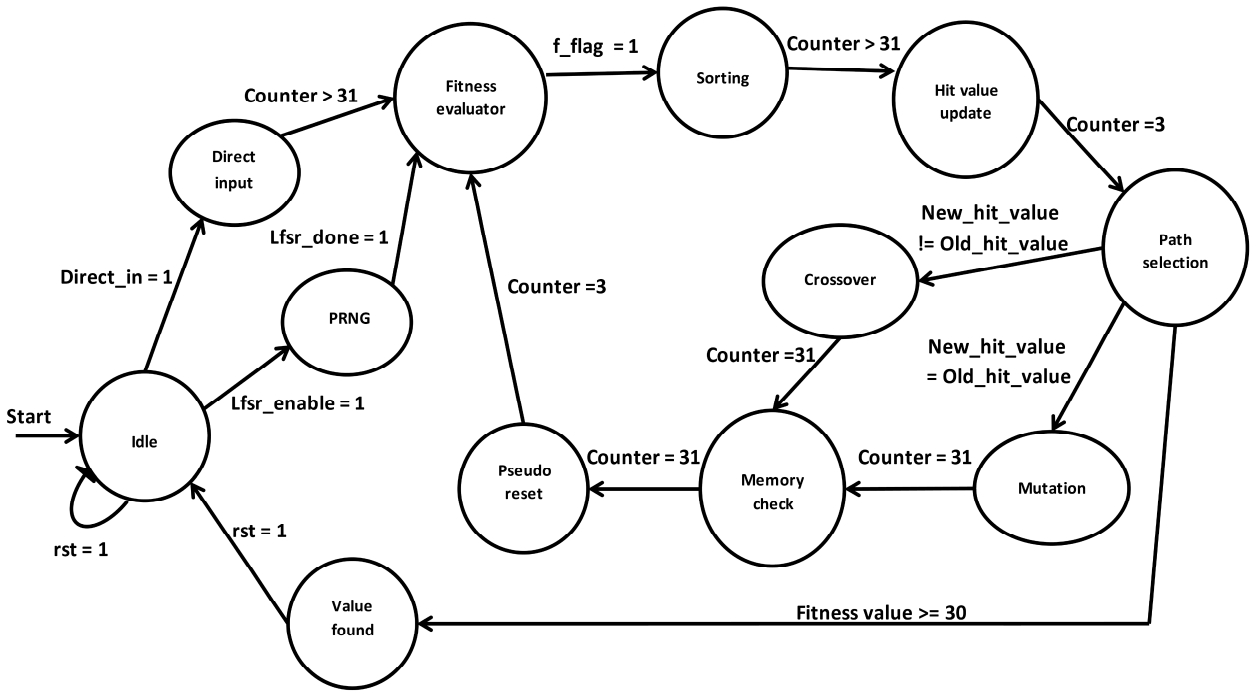

Figure 3: FSM of the Control Unit

2.1. Control Unit

This block controls the data flow in GA. As shown in Figure 3, the algorithm starts in the state "Idle", in this state all signals are initialized and remain in idle state until any state transition signal (Direct in or Lfsr enable) is detected or if "rst = 1". If "Direct in = 1", the values of coefficients are taken directly from the external memory and stored in the internal random access memory (RAM), here a device-specific block RAM (BRAM). The write address counter of the internal RAM counts till it reaches 31 then it moves to the "Fitness evaluator" state. If "Lfsr enable = 1", the coefficient values are generated by a pseudo random number generator (implemented with a LFSR block) and then stored in the internal RAM till it receives "Lfsr done = 1" from "PRNG" sub-module, then it move to "Fitness evaluator" state. Each single numerical value consists of 36 bits. The first 8 bits represent the fitness value; the next 8 bits represent the a-coefficient value followed by the b-coefficient in the next 8 bits. The remaining 12 bits are divided in 4 sets with 3 bits per set representing indexes (0 to 7) either for crossover or for mutation operator. The "Fitness evaluator" module reads coefficients values from the internal RAM as well as data-set values (stored via .mif file) from the other RAM and computes fitness till "f flag = 1", meaning all data values are computed. Next state is "Sorting". In it the data values are sorted in a descending order and written back into RAM. Transition to next state occurs when write address counter reaches 31. In "Hit value update" state the old value is replaced by a new 0th address value. It takes only 3 clock cycles so after counter reaches count of 3, the algorithm moves to "Path selection". In "Path selection" if the fitness value of the new hit value is greater than or equal to 30 (which is the set criterion), the algorithm terminates; moving to the state "Value found". In "Value found" the value of a- and b-coefficients is displayed as output and this state continues till the algorithm is restarted (rst = 1). But if the set criterion is not reached, the algorithm checks if the old hit value is equal to the new hit value. In case they are same mutation operation is performed otherwise crossover operation is done. In "Crossover" or "Mutation" states the values are rewritten in RAM after being operated by "Crossover" or "Mutation" modules. Transition to another state occurs after write address counter reaches 31. Further in an extra state "Memory check"; the contents of the internal RAM are read and can be compared with the results from software implementation to confirm if both implementations result in same values on same number of iteration. Finally, using "Pseudo reset" all signals except iteration number counter and internal RAM contents are reset to their initial values so that every module is active only on its turn. Then the process continues further with "Fitness evaluator" until the criterion is fulfilled. Some interim states are also included in between the major states discussed above for the proper functioning of the Control Unit FSM.

2.2. Initial Population (PRNG)

To generate the initial population using HDL the concept of linear feedback shift register (LFSR) was used as they are a common practice in generating pseudo random numbers where the input bit of a shift register is a linear function of its previous state (Meyer-Baese 2013). Implementation of this linear function is

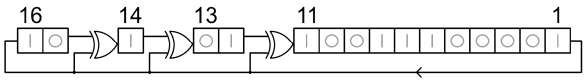

Figure 4: LFSR

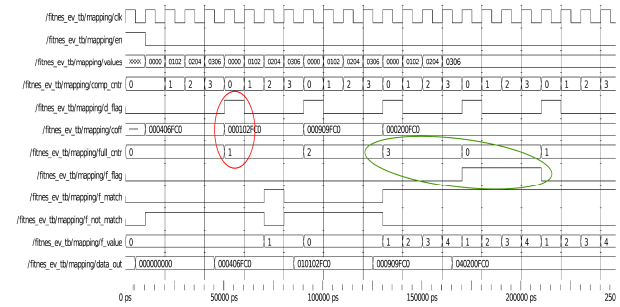

Figure 5: Timing Diagram of the Fitness Evaluator

normally done by exclusive-OR gates (XOR) where specific bits (taps) are XORed with the input or previous state to generate a new sequence of bits. But its output is deterministic and same sequence of numbers is generated every time the LFSR is restarted. The type of LFSR implemented was Galois LFSR as they do not concatenate every tap to produce the new input rather the XORing or the linear function is implemented inside the LFSR. The remaining bits are run in serial, see Figure 4. Therefore, the propagation times are reduced to that of one XOR rather than a whole chain and it is possible for each tap to be computed in parallel increasing the speed of execution. The sequence of taps was chosen from the XILINX data sheet for LFSR (Alfke 1996). There were two different LFSRs implemented; one is 16-bit for generation of a-coefficient and b-coefficient (each being 8-bit in size) and other is 12-bit LFSR for generation of index points for crossover and mutation operators. The initial value (seed) for both LFSRs is same i.e. 0x01 but the difference is in the position of the taps. These taps generated the longest possible sequence without repeating itself with Exclusive- NOR gates (XNOR). The only sequence of numbers this LFSR cannot achieve is all '1's. The whole hardware is synchronous and all signals transition to new state on the rising edge of the clock (clk) to avoid implementation of any latch. The reset signal (rst) is used to initialize all signals to '0'. The outputs from 16- bit LFSR (temp out) and 12-bit LFSR (temp out crs) are concatenated to give the final output of the whole module i.e. rdm out. To make it clear enough to be included in report, the LFSR is run only to get 4 required outputs then the signal (lfsr Done) becomes '1'. This is marked as "stop condition" and the module is stopped with further outputs neglected.

2.3. Fitness Evaluator

This module is the most complex and consumes a lot of the device resources as it includes multipliers which are themselves composed of adders. Here counters were used in replacement for "for-loops" and pipelining was done to use same hardware for the each computation instead for creating individual hardware for each computation making it hardware efficient. Figure 5 gives insight in implementation details. The enable signal (en) here works as a reset to initialize all signals , when the signal changes to '0' the module becomes active. The two main inputs are:

1) Numerical values that need to be evaluated and are provided by the user (signal name: values)
2) Numerical values generated by the PRNG module that are prospective solutions to the user provided values (signal name: coff).

The address (comp cntr) for values(values) changes every clock cycle whereas the address (full cntr) for coefficients (coff) changes every 4 clock cycles or after all values are computed for single value of coefficients. Individually every single computation results in coefficients either satisfying (f match) or not satisfying (f not match) that cumulative gives fitness value (f value). It is further concatenated with the input coefficients values on the falling edge of clock so that fitness values are attached to the right coefficients. As shown in the red colored ellipse (see Figure 5) only after all values are computed for a single a- and b-coefficient, there is transition to a new coefficient value; a flag (d flag) is raised for one clock pulse to show that a new output (data out) has been computed, that is further processed in the control unit. As shown by green colored ellipse after all values are evaluated with all coefficients; final flag (f flag) is raised that means that job of fitness evaluator module is done and data flows to next module.

2.4. Sorting

Unlike normal GA where selection operator is used to select for the best current solutions and using them further in generating new generations which is known as "Elitism", for this project, which deals with purely numerical values, elitism is not required. Rather the greater the numbers of entries, greater are the chances of convergence to a particular numerical solution. So this module has just to order the entries in descending order. The module is synchronous and implemented as a state machine with 4 states:

- s0: Idle state.
- s1: Fill internal memory.
- s2: Sorting out contents of internal memory.
- s3: Output the contents of internal memory to output.

In state s0 every signal is reset to its initial value until the reset signal is '0', next state is state s1. Here a memory submodule was created where all the inputs (data in) are stored at address (cntr in). After counter achieves its maximum value, transition is made to the state s2. Here, two nested forloops were implemented providing the bubble sort algorithm. The comparator checks the fitness values and orders the memory contents in ascending order. Here a counter runs to provide the memory enough clock cycles so that its contents are

settled. Then state transition is done. In state s3 these values are given to output (data out) in descending order and flag is raised marking that data is reading to be picked up from sorting module.

2.5. Crossover

This module is also synchronous to the positive edge of the clock (clk). Pipeline was used in order to optimize the use of resources. When reset (en) is '1', all signals are initialized to '0s'. When reset is '0', the module is active and input data (coff) is read from internal RAM, where last 12-bits are decoded into the indexes for bits of a- and b-coefficient which are to be swapped. These bits are named as: a crs, a crs1, b crs and b crs1. Finally, new values of coefficients were generated which are ready to be processed further in control unit.

2.6. Mutation

This module is similar to crossover module, the only difference is the basic operation i.e. instead of swapping the bits; they are toggled (from '1' $\rightarrow$ '0' or '0' $\rightarrow$ '1'). As shown in Figure 6, when the reset (en) is '1', all signals are initialized to '0s'. When reset is '0', the module is active and the red ellipse marks the first input read from the internal RAM. The last 12-bits of input are decoded into the indexes for bits of a- and b-coefficient which are to be toggled. These bits are marked with green ellipse. After applying the mutation function the new mutated values of a- and b-coefficient are concatenated with the non-mutated values of fitness values (signal f) and mutation bits. The output (coff out) of the mutation module is marked by blue ellipse. These values are the new generation that will again be processed by control unit.

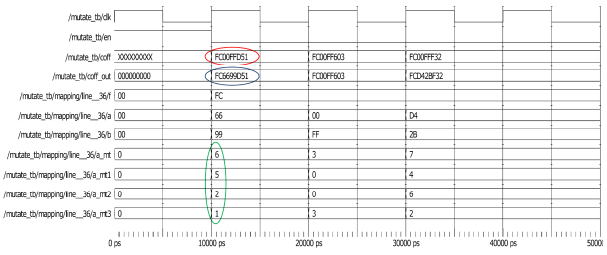

Figure 6: Mutation: Timing Diagram

3. RESULTS

The hardware implementation has been tested with a corresponding software implementation to ensure that the same operations are performed. Using this software implementation, the equivalence between hardware and software instance can be realized by the same use of the random number seed. The software implementation is realized in C++ on a Pentium 2.1 GHz processor; the hardware implementation in VHDL is based on an Altera Cyclone V FPGA, a reconfigurable hardware device.

The comparisons of the individual operations are shown in Table I in Figure 7. The acceleration factor is considerable. The partitioning of the body-mounted design into a control unit and a dedicated unit for model

Table I
SPEEDUP

Module Name	Run Time		SpeedUp
	software Implementation $[\mu s]$	hardware Implementation $[\mu s]$	
PRNG	$0.8 \cdot 10^4$	0.35	$> 2.2 \cdot 10^4$
Fitness Evaluator	$1.8 \cdot 10^4$	10.58	$> 1.7 \cdot 10^3$
Sorting	$1.7 \cdot 10^4$	0.99	$> 1.7 \cdot 10^4$
Crossover	$2.0 \cdot 10^4$	0.35	$> 5.7 \cdot 10^4$
Mutation	$2.1 \cdot 10^4$	0.36	$> 5.8 \cdot 10^4$

Table II
FPGA RESOURCES

FPGA Family	Altera Cyclone V			
Device	5CEBA9F23C7			
No. of values per data-set	4	8	16	32
Logic utilization (in ALMs)	1,410/ 113,560 (1%)	3,060/ 113,560 (3%)	12,981/ 113,560 (11%)	52,153/ 113,560 (46%)
Total registers	820	913	1345	2069
Total pins	84 / 224 (38%)	84 / 224 (38%)	84 / 224 (38%)	84 / 224 (38%)
Total RAM Blocks	2 / 1,220 (< 1%)	2 / 1,220 (< 1%)	2 / 1,220 (< 1%)	2 / 1,220 (< 1%)
Total DSP Blocks	1 / 342 (< 1%)	1 / 342 (< 1%)	1 / 342 (< 1%)	1 / 342 (< 1%)

Figure 7: Results Tables

optimization based on an application-specific hardware solution shows many advantages. If the error of the basic model or the already optimized model increases, the evolutionary model processor (EMP) can be switched on to realize a continuous model improvement.

Table II in Figure 7 shows the resources required for various implementations in the selected FPGA. The correct integration of all modules, forming the hardware implementation of GA, is shown in Figure 8. All modules, described in section II, are connected in the detailed schematic diagram that supplies a good overview of the hardware implementation of GA.

Based on the reconfigurable platform in an FPGA, the essential parameters of the algorithm can be adapted. This adaption is even possible to reconfigure the FPGA during the operation mode, if there are different algorithms necessary. The resource requirements for different hardware configurations are given in Table II. The power consumption of the hardware- and software approach is not yet finished and an ongoing process. To overcome the drawbacks observed in hardware implementation and to extend the area of operation of the algorithm for diverse problems following can be considered as future objectives.

- Realization of an inter-operation with a host system (micro controller (uC)) to provide an application dependent partitioning of hardware and software tasks and to use the FPGA as a EMP.
- Using multiple modules at the same time to find solution for multiple data-sets of numerical values from user instead of just one data-set

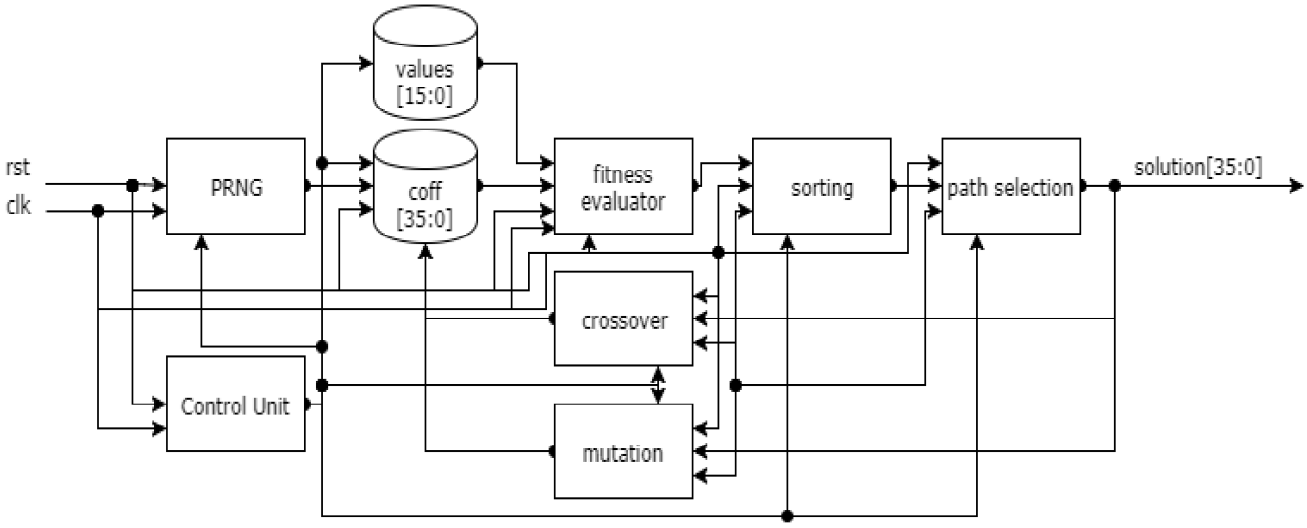

Figure 8: Block Diagram of GA-Algorihm

by implementing pipelining to increase resource efficiency and to increase parallelism.

- Implementation of multiple modules in one FPGA that collaborate and share their results to solve not only algebraic equations but also trigonometric and exponential equations.

4. SUMMARY AND FURTHER WORK

To compare hardware and software implementations, both were coded to have same behavior and results for verification. The hardware implementation of the genetic algorithm has demonstrated the great potential of application-specific hardware realization. The speed up for basic operations of the selected evolutionary algorithm is remarkable and ranges in order of magnitude between 10^3 and 10^4, see Table I. The use of reconfigurable modules and of the technology independent HDL for design also shows sufficient flexibility to be able to implement application-specific changes efficiently. Furthermore there is still potential for improvement in the implementation (e.g. pipelining) and in the cooperation with the micro controller (uC) (uC ↔ EMP).

The realization of an EMP, acting as a co-processor, seems to be a meaningful solution for the body-mounted device used in the operation mode. But also for the learning mode such a hardware accelerator, based on a FPGA, has the power to speed up the model generation significantly. While the learning process shows significant potential to speed-up the model generation, the power consumption in this mode is negligible. For operation mode, the power consumption is a key interest, but it is still under evaluation. Using the

EMP as a coprocessor in operation mode, it can be activated and deactivated very fast on demand, which is of interest particularly. The further work has the following key aspects:

- The used FPGA supports a dual core Advanced RISC Machines (ARM)-Cortex A9, so two different architectures have to be designed taking several constraints for learning and for operation mode into consideration. Here a partitioning between hardware and software is necessary to optimize speedup and efficiency. In particular power consumption is a key factor for the operation mode architecture, providing mobile operation.
- The hardware implementation has to be evaluated with regard to an agent-based design of the evolutionary algorithm in hardware. Here the resource requirements for a single agent is important with regard to the overall available resources of the chosen FPGA (see Table II in Figure 7).
- The reconfiguration capability of the FPGA has to be evaluated according the sequential execution of different evolutionary algorithm, like deepest descent, to provide a use of the EMP for application-specific optimization algorithms, depending on the error metric.

REFERENCES

Alfke, P. (1996). Efficient shift registers, lfsr counters, and long pseudo-random sequence generators. Technical report, XILINX. Version 1.1.

De Jong, K. A. (2006). Evolutionary Computation: A Unified Approach. MIT press.

Gold, C., Henze, D. A., and Koch, C. (2007). Using extracellular action potential recordings to constrain compartmental models. Journal of Computational Neuroscience, 23(1):39–58.

Goldberg, D. (1989). Genetic Algorithms in Search, Optimization and Machine Learning. Addison Wesley, MA.

Hazan, L., Zugaro, M., and Buzs´aki, G. (2006). Klusters, NeuroScope, NDManager: A free soft-

ware suite for neurophysiological data processing and visualization. J Neurosci Methods, 155(2):207–216.

Holland, J. (1975). Adaptation in natural and artificial systems. University of Michigan Press, Ann Arbor.

Klinger, V. (2015). Biosignal acquisition system for prosthesis control and rehabilitation monitoring. In Bruzzone, A., Frascio, M., Novak, V., Longo, F., Merkuryev, Y., and Novak, V., editors, 4nd International Workshop on Innovative Simulation for Health Care (IWISH 2015).

Klinger, V. (2017). SMoBAICS: The Smart Modular Biosignal Acquisition and Identification System for Prosthesis Control and Rehabilitation Monitoring. International Journal of Privacy and Health Information Management (IJPHIM), 5(2).

Klinger, V. (2018). An IoT-Based Platform for Rehabilitation Monitoring and Biosignal Identification. International Journal of Privacy and Health Information Management (IJPHIM), 6(1).

Klinger, V. and Bohlmann, S. (2017). Closed-Loop Verification Approach for the Identification of Motion-Based Action Potentials in Neural Bundles using a Continuous Symbiotic System. In Bruzzone, A., Frascio, M., Novak, V., Longo, F., Merkuryev, Y., and Novak, V., editors, 6nd International Workshop on Innovative Simulation for Health Care (IWISH 2017).

Klinger, V. and Klauke, A. (2013). Identification of motion-based action potentials in neural bundles using an algorithm with multiagent technology. In Backfrieder, W., Frascio, M., Novak, V., Bruzzone, A., and Longo, F., editors, 2nd International Workshop on Innovative Simulation for Health Care (IWISH 2013).

Klinger, V. and Klauke, A. (2015). Identification of motion-based action potentials in neural bundles. International Journal of Privacy and Health Information Management (IJPHIM), 3(1).

Kok, J., Gonzalez, L. F., Walker, R. A., Gurnett, T., and Kelson, N. A. (2010). A synthesizable hardware evolutionary algorithm design for unmanned aerial system realtime path planning. In Wyeth, G. and Upcroft, B., editors, Australasian Conference on Robotics and Automation 2010 (ACRA 2010), Brisbane, QLD.

Koza, J. R. (1992). Genetic programming: On the programming of computers by means of natural selection. MIT Press, Cambridge, MA.

Meyer-Baese, U. (2013). Digital Signal Processing with Field Programmable Gate Arrays. Signals and Communication Technology. Springer Berlin Heidelberg.

Navarro, X., Krueger, T. B., Lago, N., Micera, S., Stieglitz, T., and Dario, P. (2005). A critical review of interfaces with the peripheral nervous system for the control of neuroprostheses and hybrid bionic systems. Journal of the Peripheral Nervous System, 10(3):229–258.

Neymotin, S., Lytton, W., Olypher, A., and Fenton, A. (2011). Measuring the quality of neuronal identification in ensemble recordings. J Neurosci, 31(45):16398–409.

Rashid, H. (2017). Evaluation of hardware implementation of evolutionary algorithm. Project work, Technical University Hamburg-Harburg, Institute for Nano and Medical Electronics.

Schmidt, M. and Lipson, H. (2009). Distilling free-form natural laws from experimental data. Science, 324(5923):81–85.

AUTHORS BIOGRAPHY

VOLKHARD KLINGER is a professor for embedded systems and computer science at the university of applied science FHDW in Hannover and Celle since 2002. After his academic studies at the RWTH Aachen he received his Ph.D. in Electrical Engineering from Technische Universität Hamburg-Harburg. During his 8-year research activity at the Technische Universität Hamburg-Harburg and research laboratories he did research in asic design and automation. He teaches courses in computer science, embedded systems, electrical engineering and ASIC/system design. His email address is <Volkhard.Klinger@fhdw.de>.

SIMULATION STUDY ON THE INFLUENCE OF LEAFLET SHAPE ON BLOOD FLOW THROUGH MECHANICAL ARTIFICIAL HEART VALVE

Chatpon Sukta[(a)], Pichitra Uangpairoj[(b)]

[(a)]School of Mechanical Engineering, Institute of Engineering, Suranaree University of Technology, Nakhon Ratchasima, Thailand.

[(a)]Champchatpon@gmail.com, [(b)]Pichitrau@sut.ac.th

ABSTRACT

This study mainly focuses on the influence of leaflet shape of mechanical heart valve on the characteristics of blood flow through the valve. A three dimensional study was undertaken to investigate the velocity profile and characteristics of blood flow through fully opened flat bi-leaflet, flat tri-leaflet, downward concave tri-leaflet, and upward concave tri-leaflet heart valves. The k-ω turbulent model in FLUENT was applied to analyze unsteady incompressible blood flow. As the results of computational simulation, the maximum velocity is found at the central orifice between the leaflets of bi-leaflet valve and at the orifice between the leaflets and housing of tri-leaflet valves. The concave leaflet valve generates larger circulation and higher maximum velocity than the flat leaflet valves. Meanwhile, the maximum velocity of the flow through the flat tri-leaflet valve is lower than that through the flat bi-leaflet valve. Therefore, the flat tri-leaflet is promising to reduce blood flow circulation and minimize the thrombus formation.

Keywords: mechanical heart valve, leaflet shape, tri-leaflet, concave leaflet

1. INTRODUCTION

The heart has four valves: the tricuspid, pulmonary, mitral and aortic valves. When one of native heart valves does not work normally, it is one cause of heart valve diseases. Heart valve diseases can be caused by rheumatic fever, degeneration related age changes, and infection. This causes has change the flexibility and shape of a native heart valves. Dysfunctional heart valve disease cannot open or close completely, resulting in backward blood flow through the valve. This makes heart to work harder to supply blood to other organs sufficiently. The remedy of heart valves disease can be treated by taking medicines, repairing or replacing heart valves. Doctor may prescribe medicines to prevent arrhythmias, lower blood pressure which can reduce workload of the heart and relieve a symptoms. For the treatment with a repairing and replacing heart valves, the treatments depend on many factors, including severity of heart valve disease, and age of patients.

Repairing heart valves can preserve the function of heart muscle, it results in lower risk of endocarditis and it does not need to take anticoagulants. However, patients who have severe symptoms, they need to be treated by replacing heart valves with prosthesis heart valves.

Currently there are two major types of prosthesis heart valves: biological prostheses and mechanical heart valves. Biological prostheses are tissue heart valves grown from pig, cow, or human tissue. Patients who implants with biological prostheses do not need to take anticoagulants. However, the biological prostheses has a low lifespan, they are suitable for being implanted into elderly.

A mechanical heart valve is a medical device used to replace dysfunctional heart valve in patients with heart valve diseases. Several types of mechanical heart valves have been developing, e.g. caged ball valves, mono-leaflet, bi-leaflet, and tri-leaflet valves (Pibarot and Dumesnil 2009; Gallegos et. al. 2006). They are durable to implant in young patients who need long lifetime of the valve to sustain their life.

Replacing heart valve treatment has many complicated after surgery obstacles, including hemolysis that damages red blood cells and platelet destruction. This destruction of red blood cell and platelet can induce thrombus formation around the leaflet and housing of mechanical heart valve prostheses (Hong and Kim 2011). This thrombosis shortens the lifetime of the valve after the implantation in patients. The patients with implanted mechanical heart valves need to take anticoagulants, e.g. vitamin-K antagonists (VKA), to prevent thrombus formation near the leaflet and housing of the valves. Consequently, bleeding becomes a major concern in the patients with implanted mechanical heart valves, they need intensive monitoring of the anticoagulation status for their entire life (Verheugt 2015). Several recent studies suggest that the hemodynamics of blood flow through the mechanical heart valves plays dominant role in the thrombus formation (Cheng, Lai, and Chandran 2004; Krishnan et. al. 2006). Types of mechanical heart valve influence jet flow, elevated shear stresses, areas of flow separation and recirculation, shed vortices, and

turbulent flow that may induce platelet activation and lead to formation of blood clots. Thus, the mechanical heart valves have been designing based on hemodynamic improvement that minimize the thrombus deposition.

Tri-leaflet mechanical heart valves imitated from actual tri-leaflet tissue heart valves are promising to use and perform to safety levels comparable with bi-leaflet mechanical heart valves (Gallegos et. al. 2006; Kiang-ia and Chatpun 2013). However, the effects of design parameters of tri-leaflet mechanical heart valves on blood flow have been restrictively investigated. This study primarily investigates the influence of the leaflet shape of mechanical heart valves, including the number of leaflet and the leaflet curvature, on the characteristics of blood flow through the valves. The results of this study is expected to use for fine modification of the leaflet of mechanical heart valve.

2. MATERIALS AND METHODS

In this study, the mechanical heart valves with a diameter of 27 mm (Figure. 1) were modeled with different types of leaflet: flat bi-leaflet, flat tri-leaflet, downward concave tri-leaflet, and upward concave tri-leaflet. The valves replaced the aortic valve and located closed to the aortic sinus. The model of the valve connected with the aortic sinus is shown in Figure 2. The geometrical model blood flow through the valves were created with SOLIDWORKS 2016. The computational simulations were based on the finite volume method conducting with ANSYS Fluent 18.0. In the discretization, the optimum element size of 0.6 mm was applied to all geometrical models, resulting in the number of elements about 2.4 million elements for all models. In this study, models were set in aortic position with fully open angle of 85°.

Boundary conditions were set based on Shahriari et al. (2012). The inlet velocity inlet was applied at the left ventricle side of the model as presented in Figure 3. The blood flow was modeled as unsteady incompressible turbulent flow using k-omega turbulent model with the time step size of 5 ms, and the number of calculation of 50 iterations per step. The blood properties are considered to be constant along the flow channel: ρ = 1056 kg/m3, and $\mu = 3.5 \times 10^{-3}$ Pa.s.

The two-dimensional (2D) blood flow through bi-leaflet valve model was simulated to validate the computational model with the study of Bluestein, Rambod et al. (1999). Next, the three-dimensional (3D) blood flow through bi-leaflet valve was modeled and was compared with the flow through the 2D bi-leaflet valve. The 3D blood flow through flat bi-leaflet, flat tri-leaflet, and concave tri-leaflet valves were also simulated to compare the velocity profiles and flow characteristics of the blood flow.

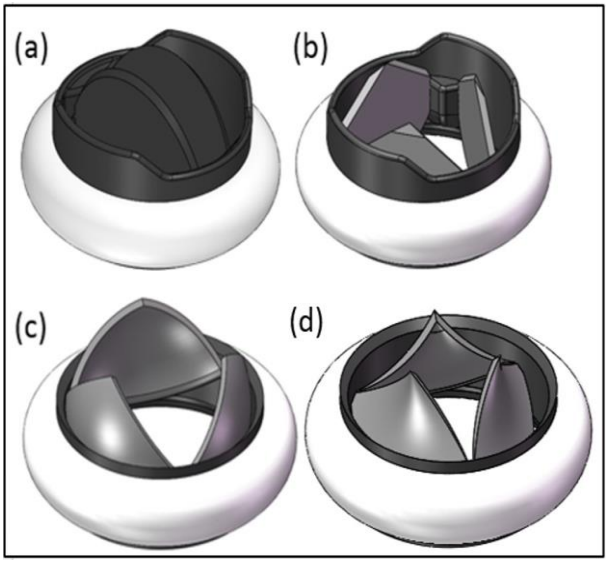

Figure 1: (a) Flat Bi-leaflet Valve, (b) Flat Tri-leaflet Valve, (c) Downward Concave Tri-leaflet Valve, (d) Upward Concave Tri-leaflet Valve.

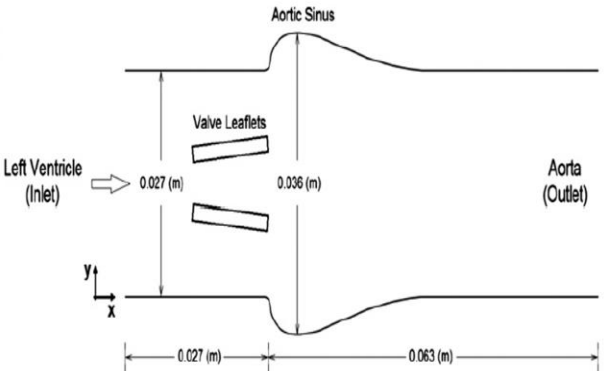

Figure 2: A Schematic Diagram and Dimensions of Mechanical Heart Valve and Aortic Sinus (Shahriari et al. 2012).

2.1. Theories and Principles

The physical phenomena of blood flow in the study system based on the conservation of mass and conservation of momentum. The blood flow is considered to be incompressible turbulent flow. Mathematical model of the blood flow is governed by Reynolds-averaged Navier-Stokes (RANS) equations.

$$\frac{\partial\left(\rho u_i u_j\right)}{\partial x_i} = -\frac{\partial P}{\partial x_i} + \frac{\partial}{\partial x_i}\left(\mu\left(\frac{\partial u_i}{\partial x_j} + \frac{\partial u_j}{\partial x_i}\right)\right) + \frac{\partial}{\partial x_i}\left(-\rho\overline{u_i' u_j'}\right) \tag{2.1}$$

where ρ is flow density, u is flow velocity, P is pressure, and μ is viscosity.

The effect of turbulent fluctuations, $-\rho\overline{u_i' u_j'}$ is called the reynolds stresses. The Reynolds stresses can be

related to the mean velocity gradients by using Boussinesq hypothesis as in equation:

$$-\rho\overline{u_i'u_j'} = \mu\left(\frac{\partial u_i}{\partial x_j}+\frac{\partial u_j}{\partial x_i}\right)-\frac{2}{3}\left(\rho k+\mu_t\frac{\partial u_k}{\partial x_k}\right)\delta_{ij} \quad (2.2)$$

Where k is turbulent dissipation rate. In this study, the Standard k- ω model was used as the turbulent model. The RANS equations was solved using Finite volume method with ANSYS Fluent 18.0.

3. RESULTS

Figure 4 shows the correspondence among the velocity profile obtained from the study of Bluestein, Rambod et al. (1999) and the velocity profile obtained from 2D and 3D blood flow simulation through the flat bi-leaflet. As the results of the study, the maximum axial velocity locates near the central orifice between the leaflets of the bi-leaflet valve. The lowest velocity locates near leading edges and housing area. While the small difference in the velocity gradient can be observed near the housing area.

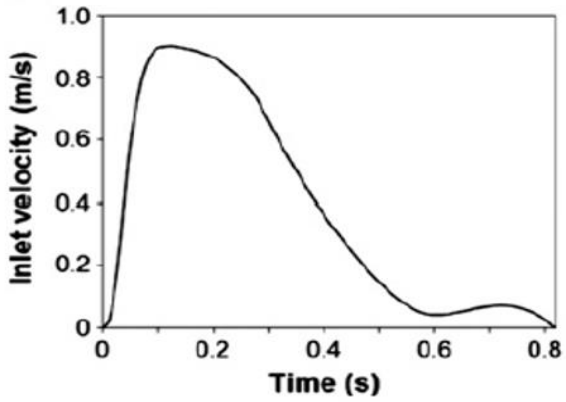

Figure 3: Inlet Velocity Wave Form (Shahriari et al. 2012).

The velocity profiles in Figure 4 also correspond to velocity contour in Figure 5 (a) that shows the corresponding area of maximum velocity. From the velocity contours in Figure 5 and the velocity profiles in Figure 6, the maximum velocity locates at the central orifice between the leaflets of the bi-leaflet valve, and at the orifice between the leaflets and the housing of the tri-leaflet valves. At t = 105ms, the maximum velocity of the blood flow through the flat bi-leaflet, flat tri-leaflet, downward concave tri-leaflet, and upward tri-leaflet valves are 1.27 m/s, 1.156 m/s, 1.313 m/s, and 1.80 m/s respectively. The maximum velocity varies with the inlet velocity that can be seen in the variation of the flow maximum velocity with time. At t = 300ms when the inlet velocity decelerates, the maximum velocity of the blood flow through the flat bi-leaflet, flat tri-leaflet, downward concave tri-leaflet, and upward tri-leaflet valves are 0.927 m/s, 0.8498 m/s, 0.9761 m/s, and 1.377 m/s respectively (Figure 7). At t = 500ms, the maximum velocity of the blood flow through the flat bi-leaflet, flat tri-leaflet, downward concave tri-leaflet, and upward tri-leaflet valves are 0.3119 m/s, 0.3182 m/s, 0.386 m/s, and 0.4689 m/s, respectively (Figure 8).

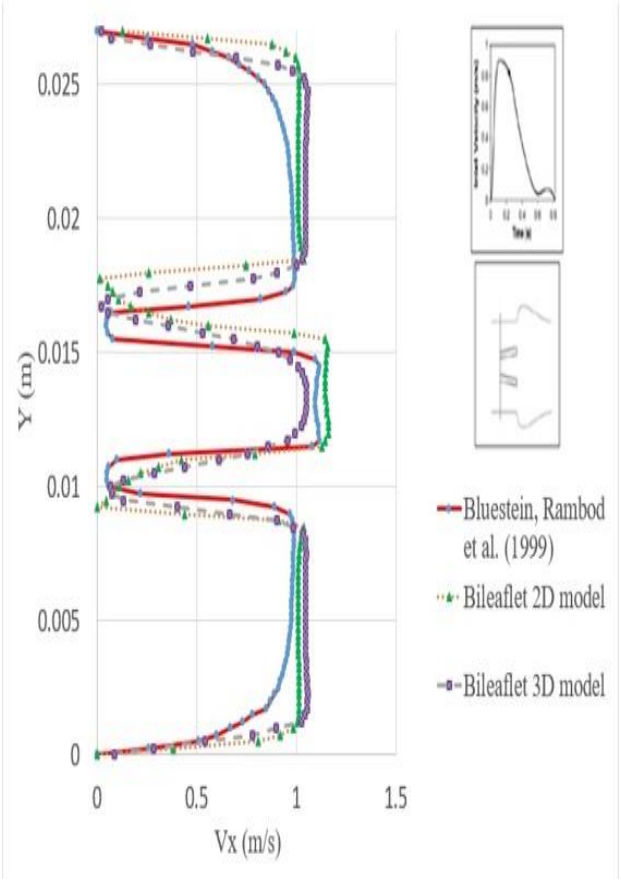

Figure 4: Comparison of Velocity Profile at the Leading Edge (at 105 ms after Peak Systole) Obtained from the Study of Bluestein, Rambod et al. (1999), 2D and 3D Simulation Results of the Flow through Bi-leaflet Valve.

The blood flow through the upward concave tri-leaflet has the highest maximum velocity compared to the flow through the other valves while the flat tri-leaflet induces the lowest maximum velocity. The flow separation region and circulation region can observed near the aortic sinus for the blood flow through all types of mechanical heart valve. They are enlarged with time, especially during the deceleration of the velocity inlet (Figure 5, 7, 8). Moreover, the flow separation and circulation can also be seen on the curvature surfaces of the concave tri-leaflet valves. The upward concave tri-leaflet induces the largest flow circulation and fluctuation compared to the other valves. This large circulation can induce greater shear stress and the development of thrombus near the leaflet tips of the concave tri-leaflets and aortic sinus. Meanwhile, the large flow channel at the central of fully opened flat tri-leaflet provides the lowest maximum velocity as well as small flow circulation near the leaflet tips and the aortic

sinus. Therefore, the flat tri-leaflet is promising to reduce blood flow circulation and minimize the thrombus formation (Kiang-ia and Chatpun 2013).

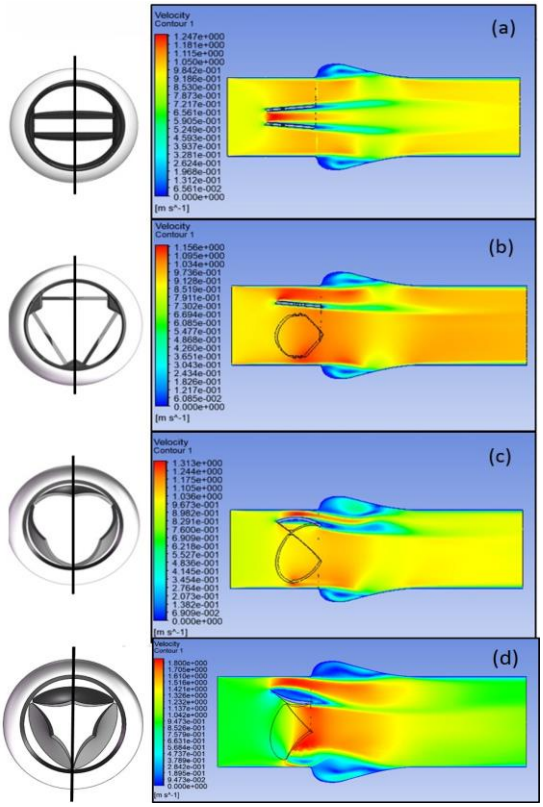

Figure 5: Velocity Contour of (a) Flat Bi-leaflet Valve, (b) Flat Tri-leaflet Valve, (c) Downward Concave Tri-leaflet Valve, (d) Upward Concave Tri-leaflet Valve (at t = 105 ms)

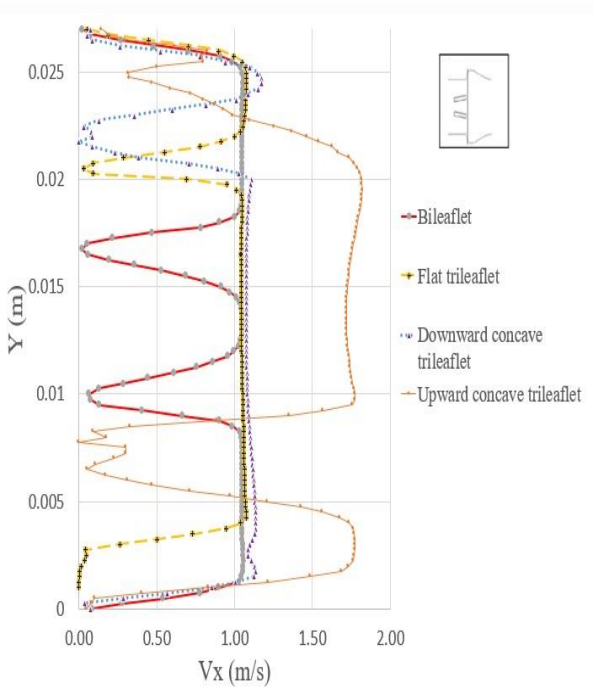

Figure 6: Comparison of Velocity Profile at the Leaflet Tips (at 105 ms after Peak Systole)

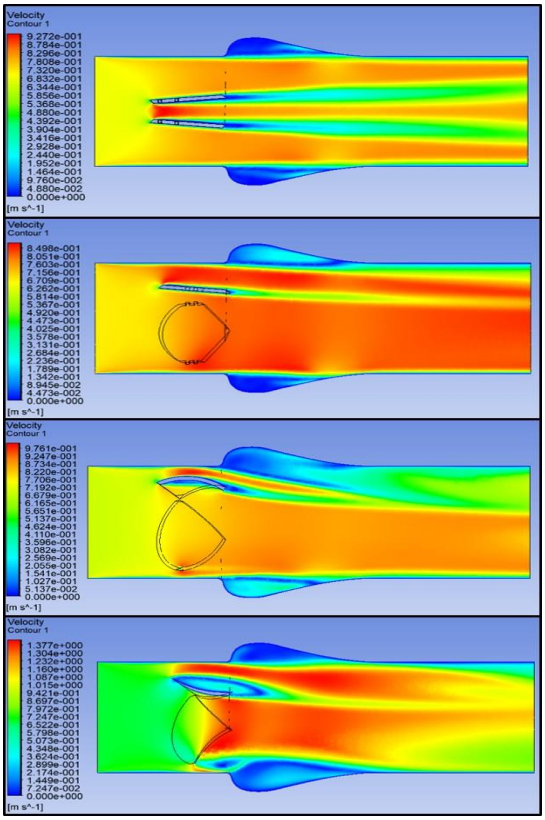

Figure 7: Velocity Contour of (a) Flat Bi-leaflet Valve, (b) Flat Tri-leaflet Valve, (c) Downward Concave Tri-leaflet Valve, (d) Upward Concave Tri-leaflet Valve (at t = 300 ms)

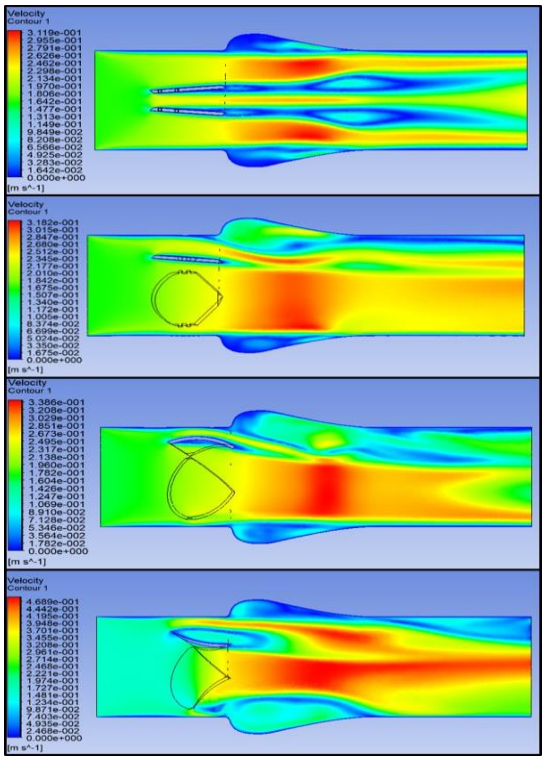

Figure 8: Velocity Contour of (a) Flat Bi-leaflet Valve, (b) Flat Tri-leaflet Valve, (c) Downward Concave Tri-leaflet Valve, (d) Upward Concave Tri-leaflet Valve (at 500 ms)

4. CONCLUSION

The purpose of this research is to demonstrate the effects of the leaflet shape on the flow characteristics of the blood flow through the mechanical heart valves. The blood flow simulations through different types of the valves were based on the finite volume method conducting with commercial software. As the results of the study, the flat tri-leaflet is promising to reduce flow velocity, flow separation, and flow circulation of the blood flow. While the number of leaflet and the leaflet curvature affect the maximum velocity and flow circulation of blood flow through fully opened valve. Therefore, these factors should be considered when we design the mechanical heart valve prostheses. However, the simulation study needs to be improves by applying fluid structure interaction to the blood flow simulation.

REFERENCES

Bluestein D., Rambod E., Gharib M., 1999. Vortex Shedding as a Mechanism for Free Emboli Formation in Mechanical Heart Valves, Journal of Biomechanical Engineering 122(2), 125-134.

Pibarot P., Dumesnil J. G., 2009. Prosthetic Heart Valves: Selection of the Optimal Prosthesis and Long-Term Management, Circulation, 119, 1034-1048.

Gallegos R.P., Rivard A.L., Suwan P.T., Black S., Bertog S., Steinseifer U., Armien A., Lahti M., Bianco R.W., 2006. In-vivo experience with the Triflo trileaflet mechanical heart valve, J Heart Valve Dis, 15(6), 791-799.

Hong T., Kim C.N., 2011. A numerical analysis of the blood flow around the Bileaflet Mechanical Heart Valves with different rotational implantation angles, Journal of Hydrodynamics, Ser. B, 23(5), 607-614

Verheugt F. W.A., 2015. Anticoagulation in patients with mechanical heart valves: follow the guidelines!, Neth Heart J, 23(2), 109–110.

Cheng R., Lai Y.G., Chandran K.B., 2004. Three-dimensional fluid-structure interaction simulation of bileaflet mechanical heart valve flow dynamics, Annals of Biomedical Engineering, 32,1469–1481.

Krishnan S., Udaykumar H.S., Marshall J.S., Chandran K.B., 2006. Two-dimensional dynamic simulation of platelet activation during mechanical heart valve closure, Ann Biomed Eng, 34, 1519–1534.

Kiang-ia A., Chatpun S., 2013. Mechanical analysis of mechanical aortic heart valve: Trileaflet versus bileaflet, Proceeding of Biomedical Engineering International Conference. October 23-25, Krabi, Thailand.

Shahriari S., Maleki H., Hassan I., Kadem L., 2012. Evaluation of shear stress accumulation on blood components in normal and dysfunctional bileaflet mechanical heart valves using smoothed particle hydrodynamics, J Biomech, 45(15),2637-2644.

AUTHORS BIOGRAPHY

Chatpon Sukta received the B.Eng. (2016) in Mechanical Engineering from Suranaree University of Technology, Thailand. He is a Master student in Mechanical and Process System Engineering Program at Suranaree University of Technology, Thailand. His current interests include the applications of numerical simulation in artificial heart valves

Pichitra Uangpairoj received the B.Sc. (2007) in Food Technology, M.E. (2010) in Mechanical Engineering from Suranaree University of Technology, Thailand. She also received her PhD in Functional Control Systems from Shibaura Institute of Technology, Japan. Her current interests include the applications of numerical simulation in artificial heart valves, and automation systems for medicine.

THE SPREAD OF AI, COMING CHANGES IN HEALTHCARE DELIVERY AND THE IMPLICATIONS FOR SIMULATION IN HEALTHCARE

C. Donald Combs, PhD
Vice-President and Dean, School of Health Professions
Eastern Virginia Medical School
Norfolk, Virginia
combscd@evms.edu

ABSTRACT
The changing practice of healthcare, particularly the increasing use of applications of artificial intelligence (AI), requires significant reforms in educating healthcare professionals. Without reform, practitioners will underperform and fail to realize the potential of personalized care. There have been many reports about needed reforms that have common themes: including expanded emphasis on communication, teamwork, risk-management, and patient safety. These reforms are essential, but insufficient. Most of the proposals do not address the most fundamental challenge—the fact that the practice of medicine is rapidly transitioning from one based on information to one based on artificial intelligence. What most employers need are healthcare professionals who are able to work at the top of their license, possess knowledge spanning the various health professions and the care continuum, effectively leverage data platforms, focus on analyzing outcomes and improving performance, and communicate the meaning of the probabilities generated by big data to patients.

Keywords: artificial intelligence, knowledge capture, healthcare practice, medical education, simulation

Introduction
The practice of medicine in the 21st century is being transformed largely through the convergence of science and technology. Each day brings more news of the impact of these changes on the practice of medicine. While policy proposals, changes to laws and regulations, and new diagnostic and therapeutic regimens reflect the traditional sources of change, healthcare is entering an era of rapidly evolving digital technologies that will fundamentally change what it means to be part of the medical profession. Among those technologies are: portable and direct-to-consumer diagnostics and therapeutics; artificial intelligence in medical decision-making; precision medicine enhanced by digital biology; augmented reality; and affective computing.

New reports are frequently published on the changing state of the medical profession and the required reforms in medical curricula that will enable more effective entry into contemporary practice. Common themes include renewed emphasis on communication, teamwork, risk-management and patient safety. These are important reforms, but they are insufficient given what is coming.
Increased and focused attention needs to be given to addressing the most fundamental change of all: *the practice of medicine is rapidly transitioning from the information age to the age of artificial intelligence*. The consequences of this transition are profound, and demand the reformulation of current educational programs most often attended by students, residents, and practitioners. A guiding principle in this reformulation is that students and practitioners understand the implications of the difference between "information" and "artificial intelligence" in clinical practice.

Information and Artificial Intelligence
The information age (roughly from the 1970's to the emergence of Watson, AlphaGo and other machine learning tools during the 2010's) featured the utilization of data that: is accurate and timely, specific and organized for a purpose, presented within a context that gives it meaning and relevance, and leads to an increase in understanding and decrease in uncertainty (Oxford online dictionary 2017). As enormous amounts of data are organized and converted into information for human users, the primary challenges for physicians thus far have been determining its validity and learning how to process and effectively use the available information.

Artificial intelligence—the mimicking of human cognition by computers—was once a science fiction fable. The ability of a computer or computer-controlled robot to perform tasks commonly associated with intelligent beings is now commonly accepted. But more importantly, the term applies to the development of systems endowed with the intellectual processes characteristic of humans, such as the ability to reason, discover meaning, generalize, and/or learn from

experience (Copeland 2017). Also known as "deep learning," these systems represent a growing branch of machine learning technology that is most often used synonymously with artificial intelligence. For example, the combination of big data and artificial intelligence is already changing radiology and pathology, and will gradually change other medical specialties (Saurabh and Topol 2016,). Although reports of various specialists being imminently replaced by computers are exaggerated, many specialties, especially those that are pattern-recognition based, must plan for a future in which rapid, accurate and sophisticated visual comparisons and diagnoses completed by machines are a major part of practice. It is clear that the emerging artificial intelligence tools are disruptive and will require fundamental changes in medical practice and standards and is rapidly becoming a reality in medicine (Wartman and Combs 2017).

Google, Amazon, Facebook, Apple and many other technology companies have been using deep learning for big data analysis for years to predict how individuals search the internet, where they like to travel, what they like to purchase, what their favorite food is, and who their potential friends are. Deep learning will revolutionize health care by facilitating the identification of patients who are likely to develop a disease and, among those with a particular condition, identifying patients who need to be seen more frequently and treated more aggressively while also determining the specific treatments that are most appropriate for those patients (i.e., "precision medicine") (Wong and Bressler 2016).

As Susskind and Susskind note, "machines and systems will work alongside tomorrow's professionals as partners. The challenge here is to allocate tasks, as between human beings and machines, according to their relative strengths." (Susskind and Susskind 2015)
Because humans are unable to process the exploding volume of medical knowledge and data, machines eventually will come to know more and be able to perform more assignments than caregivers as they gradually out-perform human capacity in many cognitive and physical tasks. How practicing professionals will interpret and act upon this machine learning is unclear, but no less than the future effectiveness of medical practice is at stake.

Implications for Clinical Practice
Medical practice of the future will have four overriding characteristics that fundamentally change the ground rules for physicians. First, care can and will be provided anywhere. Technology will move with and inside the patient's body and provide a continuous flow of data. As large data holding and processing infrastructures become more readily accessible in real time, patients, insurers, and regulators will insist on convenience (one-stop shopping) and demonstrable results in relatively short time frames. Second, care will be provided by newly constituted healthcare teams. The sacrosanct one-to-one doctor-patient relationship will be replaced by relationships with multiple health professionals. Physician team leaders will need to learn how to gain the most value from team care. The teams will promote the careful re-design of the scopes of practice of their members to align with new medical practice modalities and infrastructures. Third, care will increasingly be delivered based on large data sets and artificial intelligence. Incorporation of machine-based analysis of huge meta-data sets will become standard for patient care, eventually leading to continuous monitoring of each patient in the creation of a real-time learning healthcare system. As a result, a new interpretive and functional practice infrastructure will need to be developed both to manage the data and assess the expanding reams of information. Physicians will practice in an environment where decision-making takes place at the interface of machines, an expanding variety of health professionals, patients and their families. Fourth, and finally, the interface between medicine and machines will need to be skillfully managed. Because machines will know more and be able to perform more tasks than traditionally performed by physicians, caregivers will need to come to terms with the observation that devices will, on an increasing scale, out-perform humans both cognitively and physically.

Professional practice will embrace data analytic platforms such as Watson and robots that can not only dispense medications, but also assist in surgery, monitor the elderly and others who need episodic surveillance. As the authors previously cited state: "Human professionals will have to come to terms with the need to defer to the superior capabilities of machines" (Susskind and Susskind). The new tools for tailoring treatment will demand a greater tolerance of uncertainty and greater facility for calculating and interpreting probabilities than we have been used to as physicians and patients. Assessing and acting on these probabilities will require approaches to data presentation, risk quantification, and communication of uncertainty for which physicians to date are largely ill equipped (Versus 2017).

Our understanding of the implications of artificial intelligence for clinical practice suggests that practice will be far more consumer-centric and consumer-driven than it is today, utilizing virtual cognitive systems and large social media networks to form educational and supportive care communities. The healthcare workforce as we know it will undergo considerable redesign and automation, first focusing on routine pattern recognition tasks and then moving gradually into middle-level and upper-level skills. Physicians, working as leaders of newly configured

healthcare teams, will need to master the skills of managing the full range of delegated responsibilities within multi-professional healthcare teams; of monitoring and interpreting the vast amounts of patient data generated by ubiquitous wearable and implantable technologies, and of understanding the meaning of probabilities generated by smart machines and clearly communicating the implications of the probabilities and uncertainties.

The Educational Challenge

A recent article captures some of the angst these changes are causing thoughtful practitioners (Beck 2016). Siddhartha Mukherjee recounts conversations with Geoffrey Hinton of the University of Toronto and David Bickers of Columbia University. Hinton said, "if you work as a radiologist you are like Wile E. Coyote in the cartoon…You're already over the edge of the cliff, but you haven't yet looked down. There's no ground underneath." Deep learning systems for breast and heart imaging have already been developed commercially. "It's just completely obvious that in five years deep learning is going to do better than radiologists," Hinton continued.
David Bickers, the chair of dermatology at Columbia, also talked with Mukherjee about the automated future. "Will dermatologists be out of jobs? I don't think so, but I think we have to think hard about how to integrate these programs into our practice. How will we pay for them? What are the legal liabilities if the machine makes the wrong prediction? And will it diminish our practice or our self-image as diagnosticians, to rely on such algorithms? Instead of doctors, will we end up training a generation of technicians?"

The practitioners of the future will need continuous CME that helps them to perform at the top of their licensure, that incorporates a solid understanding of the capabilities of health professionals across the care continuum, that enhances teamwork in their professional practice, that provides a comfortable knowledge of information platforms and intelligence tools, that strengthens their consumer service skillset, and that reinforces the effective use of information and intelligence to improve performance and outcomes.

In other words, education of physicians in practice will need to move beyond updates on emerging diagnostic and therapeutic trends and on condition-focused best practices. It will need to evolve to include more systematic attention to the organization of professional effort among a variety of health professionals, the use of information and intelligence tools such as machine learning and robots, and a relentless focus on improving performance and outcomes. That is, the governing concept of professionalism will need to evolve to address artificial intelligence directly.

Professionalism implies the process of a group of individuals setting themselves off from others on the basis of values and expertise. This is usually accomplished by identifying a discrete body of knowledge, a code of acceptable behavior, a defined scope of practice, a process of internal review and certification of the competence of the group members, a process of remediation for members whose competence fails, and a commitment to continuing education and continuous improvement. Most health care delivery involves interaction between practitioners and patients in a private encounter where the patient is at a disadvantage in terms of knowledge and his/her health status at the time. Given this clinical context, professionalism has long been identified as the best means of assuring the quality of the practitioners who deliver healthcare (Institute of Medicine, 2003).

In general, this concept has served the health care system well. However, critics are correct to note the limitations of professionalism (Jacox 1997). The process of setting a group apart from other groups inevitably involves a sense of tribalism, a too keen sense of who belongs and who does not, coupled with all the sorts of group building behaviors—separate uniforms, different titles, different status, defining exclusive areas of practice, profession-based recognition for career advancement, etc.—that make working well with other types of professionals a secondary concern. The process of self-policing is too often compromised by the urge to maintain the status and image of the profession at the expense of allowing less competent or incompetent practitioners to continue to be members of the profession in good standing. Too often, the process of continuing education is linked solely to demonstration of continuing competence in practice.

Indeed, this combination of limitations creates concern about whether the benefits of professionalism are beginning to be eclipsed by its costs. Unfortunately, the professionalism of individuals often impedes their capacity to work effectively in teams whose members have different competencies and whose work together is a more important determinant of success than the work of any single member of the team (Bhutta 2010). The increasing use of artificial intelligence as a part of the professional team will require rethinking current roles.

Political and social proposals for reforming health care delivery systems include incentives for new models of care that change and blur traditional professional roles. Based on the formation of interactive collaborative teams, systems will be managed through venues that share information and address the full continuum of care to achieve integrated outcomes. Established notions of professionalism, including the dominance of the health practitioner, are pushed into the past by the networks,

rapid communication systems and applications of artificial intelligence, which now empower the patient to engage in shared decision-making and to be at the center of managing their own health.

In addition to impacting current concepts of professionalism, artificial intelligence will challenge the ability of individual practitioners to demonstrate maintenance of competence. The practice of health care involves a variety of individuals with differing levels of education and training. From certification to graduation to licensure and recertification, the focus of the legal and professional regulatory system is on the individual (Citizen Advocacy Center 2006).

Proof of competence has historically been based on the successful completion of a course of study ranging from some months to as many as eleven years of post-collegiate study; the successful completion of national and/or state written exams; and some process of continuing education that may or may not involve a periodic re-examination by either the state, the profession or both. This process of demonstrating competence holds generally true for laboratory technicians, physical therapists, pharmacists, dentists, nurses, physicians, administrators and the manifold public and allied health workers who together constitute the US health workforce. Recent innovations in the process have often focused on ways of assessing continuing competence in practice in addition to assessing the knowledge base. These innovations have arisen from concerns about the capacity of practitioners of all types to be knowledgeable about the plethora of emerging diagnostic and therapeutic technologies and about their ability to continue to practice effectively during decades-long careers.

Effective processes for assuring the continuing competence of individuals is, of course, necessary for maintaining the quality of any health care system. As many observers have noted, however, individual competence is not sufficient to ensure either patient safety or high quality patient care. The ever-increasing specialization of knowledge, the practical limits on how many hours a week can be worked safely, and the fact that patient health problems require competencies held by practitioners of different professions combine to require additional competence in working as a member of a team.

Communication, cooperation, and the recognition and integration of disparate skill sets along with patience, perseverance, and shared responsibility and accountability are central attributes of effective team members. Many reform proposals over many years have urged medical and health education programs to do a better job of incorporating these concepts into their curricula. Similar calls for professional certification, licensure and recertification programs to incorporate an emphasis on multi-disciplinary teamwork have not been heeded.

Unfortunately, as the striking similarity of the reform proposals demonstrates, only minimal changes in the process of medical and health professions education have occurred during the past century. Until individual competence is supplemented by team competence, both in education and in certification, the types of quality and safety problems that have been well documented in the health care systems are inevitable. That many organizations—hospitals, group practices, insurers—are beginning to force change by requiring some evidence of team competence as a condition of the right to work in particular settings and to be reimbursed is again evidence of how the professions, the educators and the regulators lag real world practice. That almost none of these efforts address the practical requirements of increased use of artificial intelligence applications suggest a looming misfit between the knowledge and skills required to demonstrate competence and actual competence in practice.

Everlasting Skills

Regardless of the specific impact of the coming technological changes, it is essential that physicians augment two key aspects of their profession that have lasted for millennia. Indeed, these particular skills may be in greater demand than ever before: respecting the right of patients to make choices according to their values and understanding how these values impact care decisions; and having real and tested abilities to provide the uniquely human services that patients need, most notably empathy and compassion.

Before the era of scientific practice, these skills were arguably the defining characteristic of the profession. As care has evolved – and continues to evolve – empathy and compassion may have lost their place as the prime drivers of the doctor-patient relationship. It is both necessary and ironic that 21st century healthcare returns physicians to their roots.

References

Information. In Oxford online dictionary (2017). Retrieved from https://en.oxforddictionnaries.com/definition/information

Beck, E. H. (2016, September). Training AHC graduates for the 21st century workplace. A presentation to the 2016 Annual Meeting of the Association of Academic Health Centers, San Diego, CA. Retrieved July 27, 2018 from http://www.cacenter.org/cac/continuing_competence_requirements

Bhutta, Z.A., et.al. (2010) Educating health professionals for the 21st century. *The Lancet*, 376:1923-1958

Citizen Advocacy Center. (2006) Implementing Continuing Competency Requirements for Health Care Practitioners.

Copeland, B. J. (2017). Artificial Intelligence (AI). In the Encyclopedia Britannica (January 2017). Retrieved from https://Britannica.com/technology/artificial-intelligence

Hunter, D. J. (2016). Uncertainty in the era of Precision Medicine. *NEJM* 375:711-713.

Institute of Medicine. (2003). *Health Professions Education: A Bridge to Quality*. Washington: National Academy Press.

Jacox, A. (1997) Determinants of who does what in health care. Online Journal of Issues in Nursing. Retrieved July 21, 2018 from http:www.nursingworld.org/ojin/tpe5/tpc5_1.htm

Saurabh, J. & Topol, E. J. (2016). Adapting to artificial intelligence, Radiologists and Pathologists as Information Specialists. *JAMA*, 316(22):2353-2354. doi:10.1001/jama.2016.17438

Susskind, R. & Susskind, D. (2015) The Future of the Professions. Oxford: Oxford University Press

Susskind, R. & Susskind D., op.cit.

Versus, A. I. (2017, April 3). What happens when diagnosis is automated? *The New York Times*. Retrieved from http://www.newyorker.com/magazine/2017/04/03/ai-versus-md

Wartman, S.A. & Combs, C.D. (2017) Medical Education Must Move from the Information Age to the Age of Artificial Intelligence. Acad Med, Nov 1.

Wong, T. Y. & Bressler, N. M. (2016). Artificial Intelligence with deep learning technology looks into diabetic retinopathy screening. *JAMA*, 316(22):2366-2367. doi:10.1001/jama.2016.17563

C. Donald Combs, PhD, FSSH, serves as vice president and founding dean of the School of Health Professions at Eastern Virginia Medical School (EVMS) in Norfolk, VA. In addition to being a Fellow of the Society for Simulation in Healthcare (SSH), Dr. Combs holds senior faculty appointments in the EVMS School of Health Professions, the Department of Modeling, Simulation and Visualization Engineering at Old Dominion University, the University of Paris-Descartes and the Taipei Medical University.

PHASE CONTRAST-MRI INTEGRATED CFD SIMULATION: EFFECT OF CTHRES ON BLOOD FLOW FIELDS FOR PATIENT-SPECIFIC CEREBROVASCULAR

Mohd Azrul Hisham Mohd Adib[(a)], Nurul Najihah Mohd Nazri[(b)], Mohd Shafie Abdullah[(c)]

[(a),(b)]Medical Engineering & Health Intervention (MedEHiT), Human Engineering Group, Faculty of Mechanical Engineering, Universiti Malaysia Pahang, 26600 Pekan, Pahang, Malaysia.
[(c)]Department of Radiology, Hospital Universiti Sains Malaysia (HUSM), 16150 Kubang Kerian, Kelantan, Malaysia.

[(a)]azrul@ump.edu.my

ABSTRACT

Phase Contrast-Magnetic Resonance Image (PC-MRI) measurement integrated computational fluid dynamics (CFD) simulation are used to obtain details information of model boundaries on patient specific hemodynamics. This study focuses the effects of threshold coefficient (C_{thres}) on the solution of error estimation in PC-MRI measurement integrated blood flow simulation using computational fluid dynamics. The investigation involved five patient-specific aneurysm models reconstructed from digital subtraction angiography (DSA) image, where the aneurysm is developed at the bifurcation. To evaluate the effect of C_{thres} on the solution of error estimation, two different of CFD analysis with unphysiological and boundary adjustment method are performed. The quantitative comparison of the flow field between the CFD analysis and PC-MRI measurement data showed significant different were observed in the flow fields obtained between unphysiological and boundary adjustment method. The result shows, the geometry have the strongest influence on aneurysm hemodynamics where the lowest of velocity error was obtained at configuration of the C_{thres} value of 0.3 and the total of velocity error between measurement integrated CFD simulations reduces to less than 25% for all patients using the boundary adjustment method. Hence, this preliminary method is a possible solution to further understanding on error estimation between PC-MRI and CFD simulation for patient hemodynamics.

Keywords: digital subtraction angiography, phase contrast-mri, threshold image intensity, computational fluid dynamics.

1. INTRODUCTION

Quantification of blood flow properties (hemodynamics) is the highest importance in clinical practice for diagnosis of cerebrovascular disorders and intervention planning. In current clinical practice, the most ordinarily equipment used to obtain detailed information on blood flow field in the vessel is phase-contrast MRI. Moreover, PC-MRI measurement itself may have errors in geometry and velocity information due to noise and insufficient resolution. However, the information on the blood flow field obtained from PC-MRI is essential to demonstrate the pathological instrument in cerebrovascular treatment. In previous studies (Antiga 2008; Adib 2015; Hassan 2005; Hoi 2004), validation of computational fluid dynamics (CFD) simulation is extremely important to solve the flow field in hemodynamic problems. Conversely, a combined PC-MRI measurement and CFD simulation introduced the good understanding on hemodynamic studies in prediction of the flow field problems through internal carotid arteries. However, little information is available in the literature about the accuracy of the approach and quantitative differences between PC-MRI measurement and CFD simulation, especially on configuration and boundary condition (Boussel 2008). As for the blood flow simulation in cerebral aneurysm, the computational result depends on the vessel configuration and that simplification of the geometry may possibly have observed the effect on flow field (Chang 2009).

Since we assumed that the blood vessel configuration was accurately reconstructed, the effect of deviance on blood vessel geometry from real one remains to be investigated. Currently, the computational simulation essentially depends on boundary and initial conditions. However, it is difficult to precisely set these conditions in numerical simulation of *in vivo* complicated unsteady blood flow (Ishikawa 1998), resulting in computational result which may be different from the real blood flow. In this context, CFD has been used by many groups to investigate possible correlations between hemodynamics and risk of aneurysm rapture. Some studies use the blood flow in realistic boundary condition constructed between computational simulation and medical imaging measurement to record blood velocity and to infer pressure. From (Adib 2015; Cebral 2011; Cebral 2005; Hoi 2004), the related measurement of the blood flow rate calculated in advances by image measurement technology in recent years. The analysis obtained the inlet boundary conditions and the blood flow information from patient specific aneurysm. On the

other hand, it is possible to get the output boundary conditions such as pressure outlet by the difficult measurement because there have more than one vessel bifurcation in the particular cerebral aneurysm. By implemented the measurement integrated CFD simulation inherently were introduced some error on blood flow field based on inaccurate setting of the boundary conditions. Noise from measurement data also may cause of measurement error (Broussel 2008).

Therefore, the configuration reconstructed and setting of the boundary condition are importance to investigate the effect of velocity error on flow field between PC-MRI measurements integrated CFD simulation. To obtain accurate and detailed information on a real blood flow field by reducing error derived from boundary conditions, we have proposed the PC-MRI integrated CFD simulation using boundary adjustment method. This method an application of flow rate observer in local of velocity error (Adib 2015; Adib 2017).

2. METHOD

2.1 Segmentation process

Medical imaging data were acquired in five (see Figure 1) different patients carrying with two and three branches of internal carotid artery (ICA). The reconstruction of the vessel wall was performed manually from digital subtraction angiology (DSA) image. The geometry model was derived using a DSA sequence of 512 x 512 number of pixels, image resolution 0.12 x 0.12 mm^2 with 512 number of slice and slice thickness 0.12mm in AMIRA™ software.

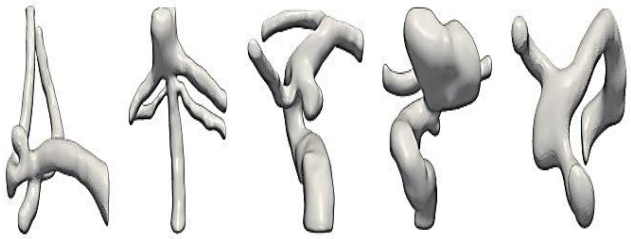

(a) (b) (c) (d) (e)

Figure 1: Geometry of patient-specific aneurysm for (a) patient 1, (b) patient 2, (c) patient 3, (d) patient 4 and (d) patient 5 models.

2.2 Acquisition of threshold image intensity

We employed the equation of threshold coefficient (1) to determine the different five threshold image intensities for respective cases, such that 50 segmented vascular models in total were created. The image intensities from DSA were taken as normalized, and we considered it is from -4119 to 11261 corresponding to the total data of the acceptable threshold image intensity in segmenting the vessel wall boundary from the user defined region of interest. We set a straight line via the cross section of the blood vessel shown in Fig.1a and used the threshold coefficient equation (1) to determine profile curve of the image intensity as follows (Omodaka 2012):

$$C_{thres} = \left(\frac{I_{thres} - I_{\min}}{I_{\max} - I_{\min}} \right) \quad (1)$$

where I_{thres} referred to the threshold image intensity, I_{max} is the highest image intensity, I_{min} is the baseline image intensity and C_{thres} is the threshold coefficient in the range of 0-1.

2.3 PC-MRI measurement

By performs image measurement of cerebral blood vessels and surrounding cerebral aneurysm using PC-MRI continuously taken over a cardiac cycle synchronization and divided into 15 frames of one heart beat were acquired and morphological image taken, the phase image corresponding to the form of the acquired image at the same time and possible to measure only the phase images with velocity information in the one direction of measurement for each of time. In order to obtain a three-dimensional velocity field in a certain axial, cross-section was performed three times measured in the same cross section while changing the speed measurement direction PC-MRI. As shown in Figure 2, the image measured Y-axis direction for the body axis upward after the body in the vertical X-axis. For the coronal plane to the left from the right of the body perpendicular and the sagittal plane as the origin O at the bottom left (X, Y, Z) orthogonal coordinate system as a Z-axis.

2.4 Calculation of the flow rate from PC-MRI

From this section, PC-MRI measurement data setting as the inlet boundary conditions in CFD analysis using the basis of the three-dimensional velocity field to define the flow rate of the cross section of the cerebral blood vessels. Blood can be regarded as incompressible flow but due to the influence of the low resolution in the PC-MRI, the continuity equation used for the flow rate in the cerebral blood vessels in different cross-section area. Therefore, the extracted cross-section in each vessel was used the average value of the flow rate in cross section of the large number.

$$V_k = \frac{1}{L} \sum_{i=1}^{L} |{}_i\mathbf{v}| \quad (2)$$

Here, L represented the number of voxels constituting the blood vessel cross-section. In addition, ${}_i\mathbf{q}$ is flow vector in voxel,

$${}_i\mathbf{q} = \begin{pmatrix} a & 0 & 0 \\ 0 & b & 0 \\ 0 & 0 & c \end{pmatrix} \begin{pmatrix} {}_iv_x \\ {}_iv_y \\ {}_iv_z \end{pmatrix} \quad (3)$$

Here, respectively a, b, c is the area of a cross section perpendicular of voxels, X, Y, and Z axis. Therefore, the Q_k is flow rate in a vessel cross-section,

$$Q_k = \sum_{i=1}^{L} |_i\mathbf{q}| \tag{4}$$

After calculate the flow velocity and flow rate of the cross section for blood vessel region, we calculate the average value,

$$\bar{V} = \frac{1}{N}\sum_{k=1}^{N} V_k \tag{5}$$

$$\bar{Q} = \frac{1}{N}\sum_{k=1}^{N} Q_k \tag{6}$$

Here, N is the number of a section constituting the blood vessel region and used the average flow rate to set at the inlet boundary conditions in CFD analysis.

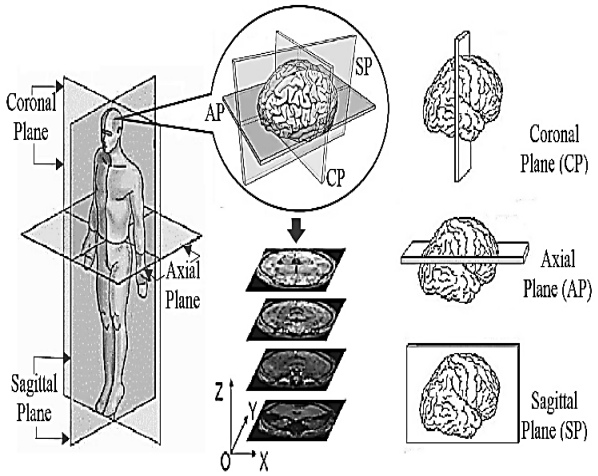

Figure 2: Definition of Cartesian coordinate system (x,y,z).

2.5 Computational setup

The computational fluid dynamics (CFD) analysis was performed by solving steady Navier-Stokes equations and continuity equation using fluid analysis software STAR-CCM+6.04 (CD-Adapco). Blood flow is assumed to be incompressible Newtonian fluids with a density of 1050 kg/m^3 and viscosity of 3.5 x 10^{-3} Pa.s. Arterial walls are expected to be rigid with no-slip. The flat velocity profile of the velocity magnitude obtained from PC-MRI measurement is applied to inlet boundary condition. In the outlet boundary condition, the boundary data assimilation technique was performed, in which the outlet pressure is iteratively changed such that the difference of the boundary flow rate between CFD and PC-MRI is reduced in the outlet branch (Adib 2015; Boussel 2008). As below, two different cases were introduced; case 1, sets the outlet pressure to zero and case 2, control the outlet pressure based on flow rate boundary.

$$^{N}P_{out,j} = {}^{N-1}P_{out,j} + \Delta P_{out,j} \tag{7}$$

$$\Delta P_{out,j} = \frac{KV_{in}}{A_{in}}\left(f^{m}_{out,j} - f^{c}_{out,j}\right) \tag{8}$$

where P is pressure, N represents the number of CFD analysis, j is the number of outlet, $f^{m}_{out,j}$ and $f^{c}_{out,j}$ are flow rate obtained from PC-MRI and CFD respectively, K is proportional gain, V_{in} is velocity inlet and A_{in} represent inlet cross-sectional area.

2.6 Evaluation of error

In order to evaluate the quantitative comparison of the flow solution, the error of velocity vector is introduced as below (Adib 2017):

$$e(U_m, U_c) = \frac{1}{N}\sum_{i=1}^{N}\left|U_i^m - U_i^c\right| \tag{9}$$

where U^m and U^c are velocity vector obtained from PC-MRI measurement and CFD simulation respectively, N is number of voxels in computational domain and $e(U_m,U_c)$ represented as error of velocity vector.

3. RESULT AND DISCUSSION

About twenty-five shape models of internal cerebral aneurysm were designed base on five different C_{thres} level was performed. Refer to the method we used in determination of threshold image intensity, the highest and lowest values were (8572-11261) and (-4119-2698) for AMIRA and (12193-25549) and (44452-83919) for ImageJ respectively. In creating a computational model to predict the hemodynamics in an ICA, assumptions are often made that can adversely affect the numerical results. One of the most important areas where assumptions are required is the application of boundary conditions. Several authors have demonstrated the significant influence of boundary conditions on computed hemodynamics indices (Jou 2008; Adib 2016; Ii 2018; Omodaka 2012) and these studies were observed the effect of C_{thres} on flow field solution in measurement integrated simulation.

3.1 Effect of C_{thres} on flow solution and quantitatively comparison of the velocity on CFD simulation

This investigate focuses on five vascular models with three and two branches as shown in figure 1. In order to investigate the effect of different configurations on flow solution in measurement integrated simulation, we first obtained the real blood flow with velocity vector from PC-MRI (see Figure 3) measurement under systole condition refer table 1. The quantitative comparison of

the different C_{thres} values based on the velocity error between CFD analysis and PC-MRI measurement shown in figure 4. From the result, the lowest and highest values of velocity error were (34%-180%), (27%-62%), (43%-84%), (28%-55%) and (23%-61) for patient 1 to patient 5 respectively. When all the outlet pressures are set to zero, the minimum velocity error was obtained at C_{thres} value of 0.3 which difference between others C_{thres} values were 96%, 14%, 24%, 15% and 16% for patient 1 to 5 respectively.

Table 1: Velocity measurement for patient (P1-P5) at systole and diastole condition

	P1	P2	P3	P4	P5
Systole (m/s)	0.212	0.601	0.201	0.731	0.463
Diastole (m/s)	0.079	0.361	0.083	0.433	0.191

However, after implemented boundary adjustment, the result shows supplementary decreased which 23%, 23%, 21%, 24% and 19% for patient 1 to patient 5 respectively. After C_{thres} 0.3, the velocity error increased when the C_{thres} values increased for all patients. In systole condition, it is difficult to provide a linear correspondence between differences of threshold coefficient (C_{thres}) and flow solution change. However, the flow solution as represented by velocity error present similarity at minimum C_{thres} value of 0.3 for all five patients. For the comparison between unphysiological and boundary adjustment condition at C_{thres} value of 0.3, the largest different is occurred at patient 1 with 18% compare with patient 2 to patient 5 with 3%, 10%, 4% and 3% respectively.

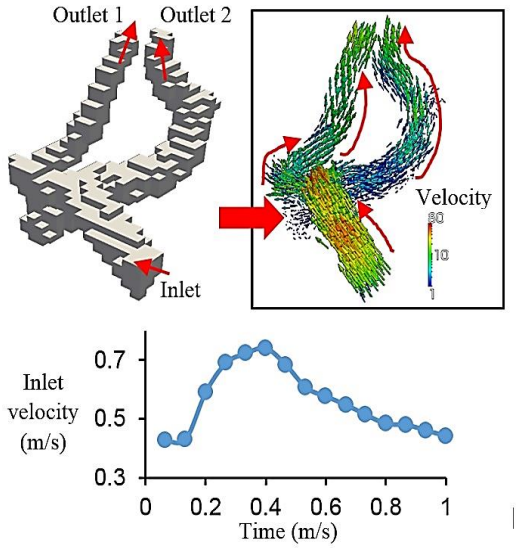

Figure 3: Measurement of velocity vector obtain from PC-MRI for patient 1. Top shows the calculation of velocity vector base on voxel size. Bottom indicate the inlet velocity measurement from 15 frame in 1s cardiac cycle with sampling time of $\Delta t = 0.066s$.

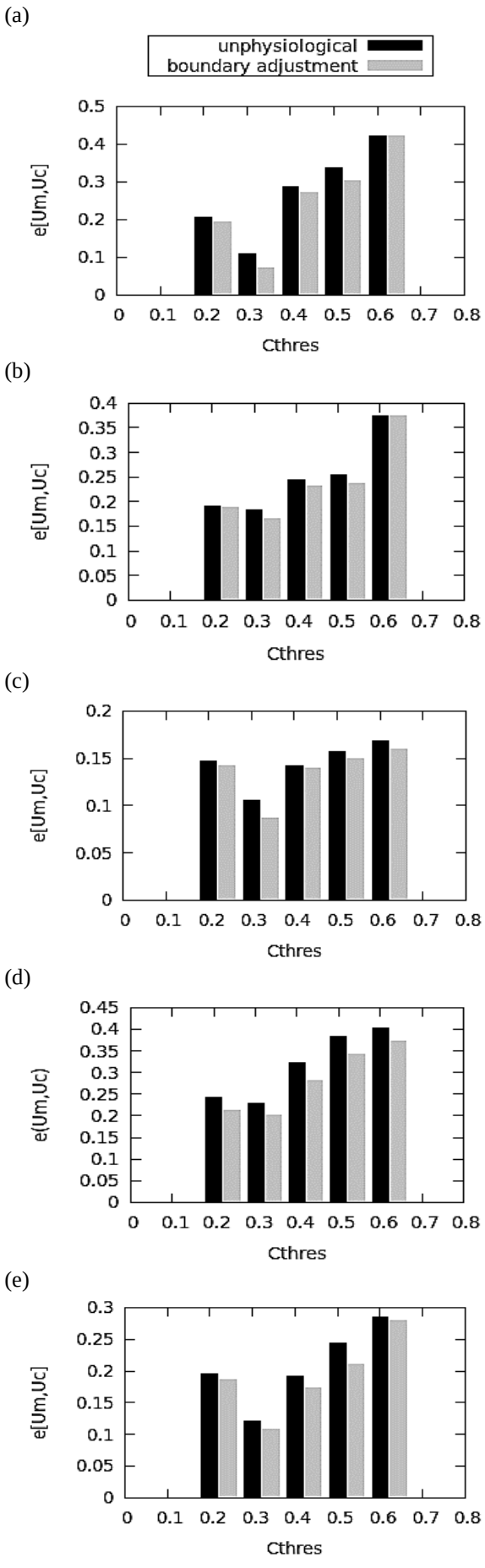

Figure 4: Evaluation in velocity error between PC-MRI measurement and CFD analysis at peak systole for patient-specific cerebral aneurysm for (a) patient 1, (b) patient 2, (c) patient 3, (d) patient 4 and (e) patient 5. Black bars represent CFD analysis with unphysiological condition and grey bars represent CFD analysis with boundary adjustment.

Conversely, the flow solution as represented by velocity error shows the minimum error always occurs at C_{thres} value of 0.3 for all five patients' distribution. The average value of velocity error in identification of the outlet pressure from five patients presented 36% to 63% and there was no significant difference in comparison with the results of the outlet zero pressure condition. In general, the large difference of velocity error between CFD and PC-MRI measurement data still has been found which remain the lowest and highest value were 36% and 82% respectively obtained in patient B and C. Based on these results, the velocity errors are entirely improved using the boundary data assimilation.

3.2 Evaluation of velocity vector

In **figure 5a-b**, velocity vector can be seen is a slight difference between unphysiological and boundary adjustment method. From the color maps, the velocity error distribution in aneurysm (see **figure 5a**) reduced about 10% when applying the adjusted outlet pressure method. This result indicates that setting outlet pressure based on the flow ratio obtained from measurement data enables to analyze aneurysmal hemodynamics in more detail. However, the difference in the aneurysm remains so large because the controlled object of the control approach is only flow rate after branching.

(a)

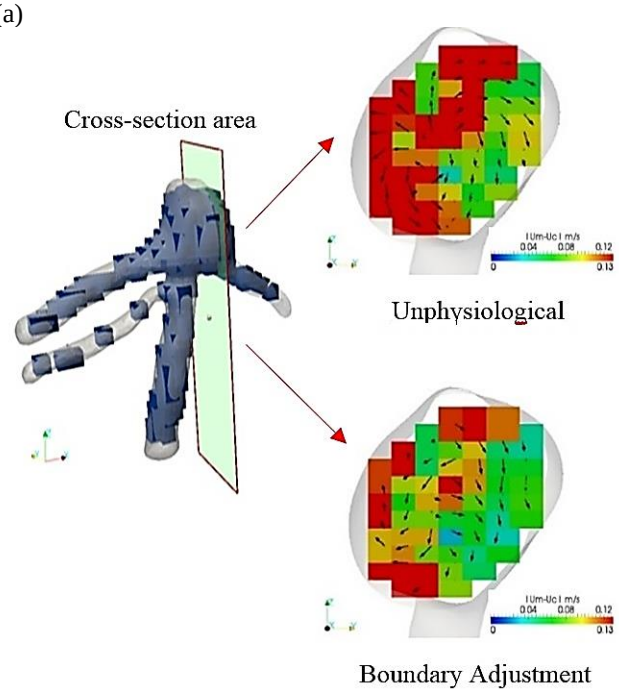

(b)

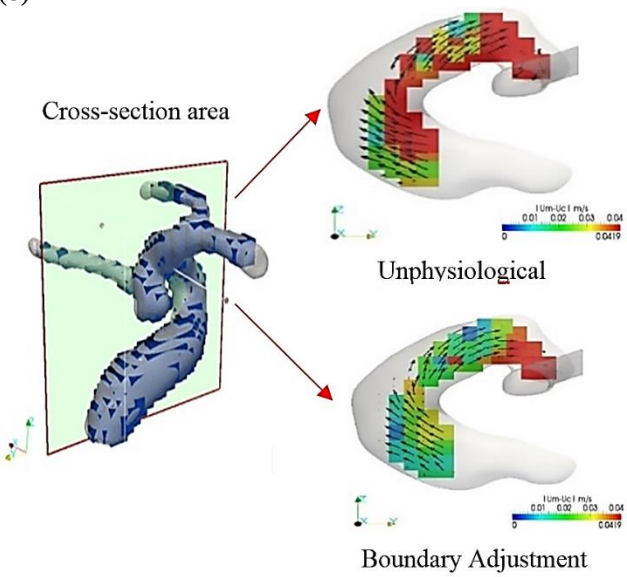

Figure 5: Representative the cross-section of error evaluation between unphysiological and boundary adjustment method for (a) patient 2 and (b) patient 3. Black arrow inside the cross-section indicate the velocity vector of the blood flow and color maps presented the velocity error between measurement and CFD.

3.3 Limitation of the study

We investigated cerebral aneurysms which are classified as a curved artery or side-wall type aneurysms. The flow in such an aneurysm differs from that in an aneurysm at the apex of arterial bifurcations (Chang 2009; Moore 1997; Yim 2002). We set the inlet velocity for all cases base on PC-MRI measurement data with steady-state condition in numerical simulation. The unsteady-state assumption is also a possible limitation of our study. Physiologically, realistic computations should be carried out using patient-specific flow conditions in future investigations. Wall compliance, non-Newtonian properties of blood, outflow conditions and the numeric technique used to solve the governing equations can also affect hemodynamics. The number of patient also a limitation of our investigation. In the future we need to increase the number of data to become more realistic result.

4. CONCLUSION

Our results suggest the good procedure used for threshold determination and can profoundly affect CFD analysis. However, the quantitative comparison of flow solution based on different C_{thres} between the CFD analysis and PC-MRI measurement still indicate the large of the velocity error and maybe in the future, taking into account to improve the current boundary data assimilation technique to the global data assimilation technique.

ACKNOWLEDGEMENT

The support of the University Malaysia Pahang under grant RDU180311 and MedEHiT are gratefully acknowledged. The authors of this paper also would like to express their gratitude to Dr. Nur Hazreen Mohd Hasni and Dr. Nur Hartini Mohd Taib for supporting these research activities.

REFERENCES

Antiga, L., Piccinelli, M., Botti, L., Ene-Iordache, B., Remuzzi, A., Steinman, D.A., 2008. An image-based modeling framework for patient-specific computational hemodynamics. Medical and Biological Engineering and Computing 46, 1097–1112.

Adib, M.A.H.M., Hasni, N.H.M., 2015. Effect on the reconstruction of blood vessel geometry to the thresholds image intensity level for patient aneurysm. Journal of Biominetics, Biomaterials and Biomedical Engineering, 22, 89-95.

Hassan, T., Timofeev, E.V., Saito, T., Shimizu, H., Ezura, M., Matsumoto, Y., Takayama, K., Tominaga, T., Takahashi, A., 2005. A proposed parent vessel geometry-based categorization of saccular intracranial aneurysms: computa- tional flow dynamics analysis of the risk factors for lesion rupture. Journal of Neurosurgery 103, 662–680.

Hoi, Y., Meng, H., Woodward, S.H., Bendok, B.R., Hanel, R.A., Guterman, L.R., Hopkins, L.N., 2004. Effects of arterial geometry on aneurysm growth: three- dimensional computational fluid dynamics study. Journal of Neurosurgery 101, 676–681.

Boussel, L., Rayz, V., McCulloch, C., Martin, A., Acevedo-Bolton, G., Lawton, M., Higashida, R., Smith, W.S., Young, W.L., Saloner, D., 2008. Aneurysm Growth Occurs at Region of Low Wall Shear Stress Patient-Specific Correlation of Hemodynamics and Growth in a Longitudinal Study Stroke 39, 2997-3002.

Chang., H.H., Duckwiler, G.R., Valentine, D.J., Chu, W.C. 2009. Computer-assisted extraction of intracranial aneurysms on 3D rotational angiograms for compu- tational fluid dynamics modeling. Medical Physics 36, 5612–5621.

Ishikawa, T., Guimaraes, L.F.R., Oshima, S., Yamane, R., 1998. Effect of non-Newtonian property of blood on flow through stenosed tube. Fluid Dynamics Research 22, 251-264.

Cebral, J.R., Mut, F., Weir, J., Putman, C., 2011. Quantitative Characterization of the Hemodynamic Environment in Ruptured and Unruptured Brain Aneurysms, AJNR Am J Neuroradiology 32, 145-151.

Cebral. J., Castro, M., Burgess, J., Pergolizzi, R., Sheridan, M., Putman, C., 2005. Characterization of cerebral aneurysms for assessing risk of rupture by using patient-specific computational hemodynamics models. Am J Neuroradiol 26, 2550–2559.

Adib, M.A.H.M., Ii, S., Watanabe, Y., Wada, S., 2017. Minimizing the blood velocity differences between phase-contrast magnetic resonance imaging and computational fluid dynamics simulation in cerebral arteries and aneurysms. Medical & Biological Engineering & Computing, 55,9, 1605-1619.

Omodaka S, Inoue T, Funamoto K, Sugiyama S, Shimizu H, Hayase T, Takahashi A, Tominaga T (2012) Influence of surface model extraction parameter on computational fluid dynamics modeling of cerebral aneurysms. J of Biomech 45: 2355-2361.

Jou, L.D., Lee, D.H., Morsi, H., Mawad, M.E., 2008. Wall shear stress on ruptured and unruptured intracranial aneurysms at the internal carotid artery, AJNR Am J Neuroradiology 29, 1761-1767.

Adib, M.A.H.M., 2016. Measurement of threshold image intensities on difference of vascular model: Effect on computational fluid dynamics for patient-specific cerebral aneurysm. Jour. Of Biomimetics, Biomaterials & Biomedical Eng., 27, 55-59.

Ii, S., Adib, M.A.H.M., Watanabe, Y., Wada, S., 2018. Physically consistent data assimilation method based on feedback control for patient-specific blood flow analysis. Int. Jour. For Numerical Methods in Biomedical Engineering, 34, 1, e2910.

Adib, M.A.H.M., Ii, S., Watanabe, Y., Wada, S., 2016. Patient-Specific blood flow simulation on cerebral aneurysm based on physically consistency feedback control. Proceeding-IEEE 16th Inter. Conf. on Bioinfo. & Bioeng. 2016, 7790006, 334-337.

Moore, J.A., Steinman, D.A., Ethier, C.R., 1997. Computational blood flow model- ling: errors associated with reconstructing finite element models from magnetic resonance images. Journal of Biomechanics 31, 179–184.

Yim, P.J., Vasbinder, B., Ho, V.B., Choyke, P.L. 2002. A deformable isosurface and vascular applications. Progress in biomedical optics and imaging 3, 1390–1397.

AN APPROACH FOR ATTENUATION CORRECTED 3D INTERNAL RADIATION DOSIMETRY

Werner Backfrieder

Dept. Biomedical Informatics, University of Applied Sciences Upper Austria, Hagenberg, Austria

Werner.Backfrieder@fh-hagenberg.at

ABSTRACT

The key to individual patient dose calculation is a good estimate of isotope kinetics in organs of observed metabolism. Kinetics can be measured by organ specific time activity curves (TACs), derived from a series of planar whole body szintigrams, representing temporal evolution of radioactive uptake. Overlaps in projections and photon attenuation deteriorate directly measured counts in regions of interest (ROIs).

In this work, corrections of TACs, based on three-dimensional (3D) SPECT and CT scans, are developed. An automated volume of interest (VOI) segmentation strategy combines local thresholds and topographic form-features from SPECT data with high-resolution CT morphology. VOIs are registered to whole body scans, allowing the differentiation of overlapping organs in projections. Photon attenuation is corrected based on CT scans, transformed to isotope specific linear attenuation coefficients. A simulation study is performed, based on real patient morphology, comparing native and uniformly attenuation corrected data, to non-uniform 3D attenuation correction. Its influence on effective patient dose is studied, and finally the new algorithms are applied to measured patient data.

Attenuation correction, based on 3D data achieves substantially better results. Automated processing avoids time-consuming manual segmentation, giving raise to application in a clinical workflow.

Keywords: medical internal dosimetry, image registration, segmentation

1. INTRODUCTION

Modern nuclear medicine therapy uses many different bio-tracer molecules for treatment of a broad range of tumors. Radioactive isotopes are carried like in a back-pack to the tumor area and deposit a lethal radiation dose directly into the tumor. This combination of specific bindings and radio-active labelling is the mechanism of individual cancer treatment. The distribution radioactive particles is not restricted to the pathologic tissue of the tumor, radiation is distributed all over the body. Therapy planning shall reduce collateral damage. For risk assessment the radioactive exposure of other organs is determined by Monte-Carlo dose calculations, based on standardized phantom geometries. The effective dose per administered activity is calculated respectively for various different human models, e.g. pediatric, female, pregnant, and male body phantoms. Results for all relevant body compartments are published in the ICRP reports. The principles are implemented in the software package MIRDOSE (Stabin 1996), the clinical standard until 2004, before OLINDA was deployed (Stabin and Siegel 2004).

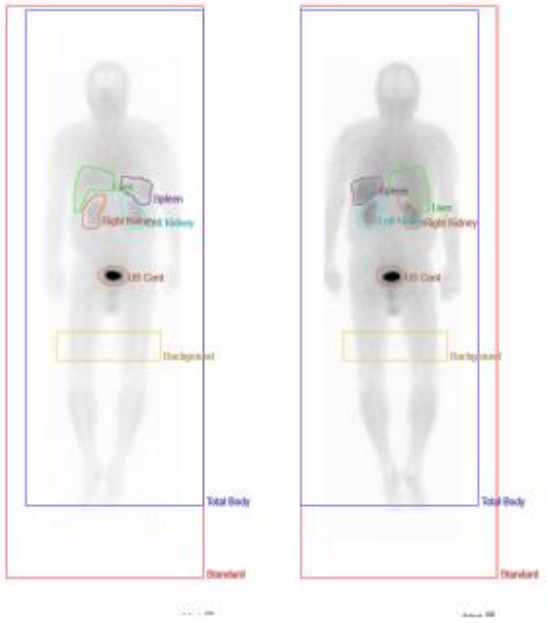

Figure 1: Manually drawn regions used in the standard approach for dose calculation. Regions are drawn and displayed on the anterior and posterior projection: kidneys (brown, cyan), liver (green), spleen (purple), bladder (ocher), body background (gold), total body (blue), and the reference standard (orange).

With the further development of imaging modalities, anthropomorphic models were refined towards realistically shaped organs, segmented in 3D from real model 3D data sets (Schläger 2011).

Individual dose planning focuses on the assessment of pharmacokinetics and accumulation of the radioactive isotope in every single patient. Most therapeutic radiopharmaceuticals are mainly beta emitters and have no or only weak gamma lines in their emission spectra, inhibiting assessment of radioactive uptake. A work around is to substitute an isotope with similar pharmacokinetics but strong gamma spectrum in the dose estimation scans. Time activity curves for all relevant organs, providing the essential information for the following dose calculation, are estimated from emitted

cumulative counts. Regions of interest (ROIs) are drawn manually on the whole body images and evaluated at each point in time, cf. Fig1. To correct for the latter applied therapeutic isotope the summed counts are modified, reflecting the physical half-life-time of the therapeutic isotope (Mizarei et al 2013).

Projection may lead to overlapping ROIs in 2D scans making accurate rating of concerned TACs very difficult. Approaches with factor analysis were made for distinguishing overlapping regions, utilizing small differences in tracer dynamics (Backfrieder et al. 2015, Sámal et al. 1987, 1989)

More recent approaches for individual dose planning are based on hybrid data SPECT-CT or PET-CT in combination with whole body data series for estimation of temporal evolution dose distribution (Lee 2014), but until now costly image acquisition and data processing in 3D are drawbacks in clinical application of 3D dosimetry.

In the current approach a method for automated segmentation in 3D and volume based attenuation correction based on complementary CT Data is developed. Information is transferred to a common whole body time series, thus fostering 3D dosimetry in clinical procedures.

2. MATERIALS

Materials comprise anthropomorphic phantom data to show the accuracy of the methods, with respect to attenuation correction and accurate separation of organs, and clinical patient data, to demonstrate the reliability and usability of the methods.

2.1. Patient Data

Data from 6 patients, three male and three female, age ranging from 52 to 79 years, are examined. Each patient study comprises a SPECT and CT volume image, and 6 planar whole body scans.

2.1.1. Whole body scans

After administration of 60 MBq In-111, whole body scans are acquired 20 min, 90 min, 24h, 48h, 72h, and 96 h after injection. Image data are measured with a double-headed gamma camera, Philips BrightView, detectors are in 180 degree position. Anterior and posterior data are stored in a 1024x512 image matrix, 2.8mm pixel-size and scan-speed 10cm/min. Figure 2 shows the full whole body series in anterior view.

Images are scaled to individual data ranges. In early images, the content of the urinary bladder dominates the image dynamics, thus diminishing organ contrast. In latter frames, kidneys show higher relative intensity indicating the washing out of radioisotopes from blood. Uptake of liver and spleen is increasing; urinary bladder shows still substantial filling. The following frames show main residence of the radioactive substances in liver, spleen and kidneys. The residence times in spleen and liver are slightly higher than in kidneys, indicated by higher count rates. Accumulation in these organs is responsible for main dose stress.

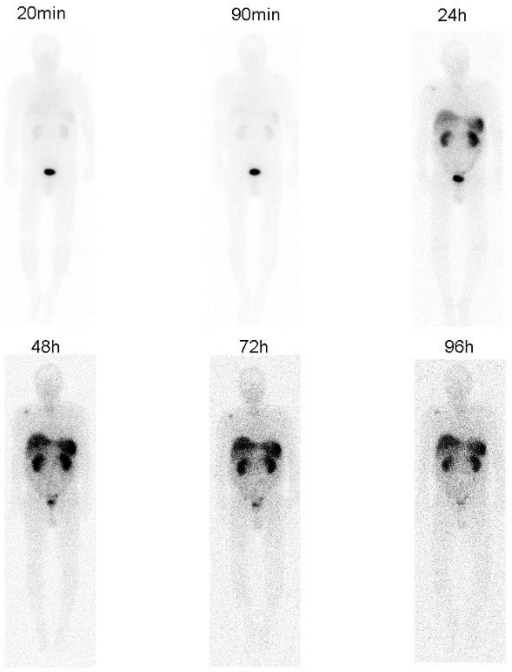

Figure 2: Anterior projection of the whole body time-activity study, i.e. six scans over a period of 96 hours. Projection images are acquired on a 1024 by 512 matrix, with 10cm/min scan speed. The intensity window is scaled to 45% of the maximum in each individual frame.

2.1.2. Volume scans

SPECT and CT data are acquired directly following the 90 min planar whole body scan. SPECT projections are acquired on an elliptical, body approaching orbit with 3 degrees rotational increment and 20s acquisition time on a 130x130 matrix, squared FOV with 605mm length, 90 slices, thickness 4.66mm. Images are reconstructed with an OSEM algorithm and attenuation corrected. CT data are on a 512x512 matrix, isotropic voxel-size 1mm. The volume comprises 406 slices. Figure 3 shows an identical slice from both SPECT (a) and CT (b).

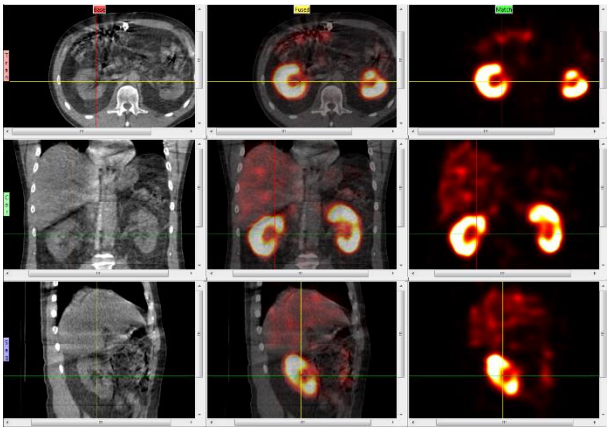

Figure 3: CT and SPECT scans in a dosimetry study acquired by a Philips BrightView hybrid camera. Data sets are co-registered. Columns show CT, CT-SPECT overlay, and SPECT images in transversal, coronal, and sagittal slice orientation.

2.2. Mathematical Phantom Data

Mathematical phantom data are used to verify the effects of attenuation correction and overlapping VOIs, compared to well-known data. The phantom comprises the organs of the abdomen essential for dose calculation, i.e. liver, spleen, kidneys, and the urinary bladder. Manual VOIs are drawn carefully over these regions in real SPECT data, building anthropomorphic binary masks. Each organ VOI is associated with a bi-exponential TAC. From this 3D temporal model whole planar projections are calculated for anterior and posterior view, at 20min, 90min, 24 h, 48h, 72h, and 96h. Attenuation is considered based on mapping HUs to isotope specific attenuation coefficients.

3. METHODS

The MIRD approach of internal dosimetry considers the dose contribution of each radioactive particle, emitted by a source organ, to all relevant target organs. For each target and source a specific *S* value is calculated by Monte Carlo simulation, listed in MIRD pamphlet 11 (Snyder et al. 1975). For estimation of effective dose, totally emitted counts are calculated from TACs, cf. Figure 3.

In common image based dosimetry TACs are assessed from accumulated counts in ROIs, drawn over organs in whole body scans. These measures derived from planar dosimetry are mainly deteriorated by attenuation of gamma rays by penetrated tissue. In this work, an attenuation correction algorithm is developed based on complementary 3D information from SPECT and CT. The images in CT volumes are generated by interaction of x-rays and matter, the linear attenuation coefficients are scaled in Hounsfield units (HUs) a measure with reference to attenuation in water. These images allow a conclusion to underlying attenuation coefficients. SPECT data provide functional information in form of specific bindings of radioactive tracer. 3D tracer distribution is derived by segmentation of specific VOIs.

3.1. Segmentation

In this approach VOIs over liver, spleen, kidneys, and urinary bladder (if already filled) are determined based on SPECT and CT data. In the first step, a global threshold is applied to SPECT data, defining a super-set containing all voxels belonging to the considered organs. This set still contains false voxels. In the second step, all voxels selected before, are classified, determining its probability of membership derived from the HU in the related CT volume and a topologic distance map.

3.2. Attenuation correction

A hybrid camera, providing co-registered image volumes, acquires both SPECT and CT data. Image volumes are resampled to the same resolution. An image volume consists of N_k slices, with N_i by N_j pixels. Summing the voxels along the *j*-direction, i.e. the columns of the slice, yields a projection image. Considering attenuation and the order of summation, distinguishes between anterior and posterior projection. The tensors of third order M, with elements $m_{i,j,k}$, and X, with respective elements $x_{i,j,k}$, represent the CT and SPECT volumes, with subscripts $k=1$ to N_k for slices, $i=1$ to N_i for rows, and $j=1$ to N_j for columns. Summing along the columns yields a simple projection image

$$p_{i,k} = \sum_j x_{i,j,k} \tag{1}$$

An alternative method for pixel indexing, counting from upper left to lower right in the projection image, concentrates indices *i* and *k* to a new index *i* ranging from 1 to N_i times N_k. With this notation the anterior *ant* and posterior *post* projections, considering attenuation read

$$ant_i = \sum_j x_{i,j} \cdot e^{-\sum_{l=1}^{j} m_{i,l}}, \tag{2}$$

$$post_i = \sum_j x_{i,j} \cdot e^{-\sum_{l=j}^{N_j} m_{i,l}}. \tag{3}$$

Where each activity voxel *x* is multiplied with the attenuation factor along its way to the detector.

Figure 4 shows an attenuation map used for registration, derived from the CT image. HUs are mapped to isotope specific linear attenuation coefficients (Bai et al. 2003).

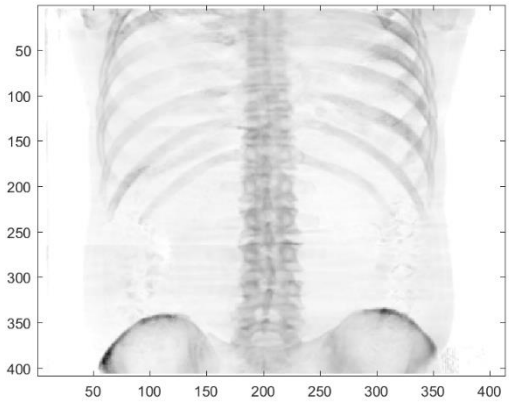

Figure 4: Attenuation mask calculated from HUs mapped to linear attenuation coefficients.

Rewriting the above equations with attenuation matrix ATT reads

$$ant_i = \sum_j ATT_{i,j} \cdot x_{i,j}, \tag{4}$$

$$ATT_{i,j} = e^{-\sum_{l=1}^{j} m_{i,l}}, \tag{5}$$

and respective for the posterior image. This leads to a position dependent attenuation correction factor *f*, allowing an estimate of real counts *p*, based on the known attenuation factors

$$p_i = f_i \cdot \sqrt{ant_i \cdot post_i}. \tag{6}$$

This correction factor image is registered to planar whole body images by mutual information image registration.

The method is also used for registration of whole body images against each other.

3.3. Registration

Mutual information is a statistical measure from information theory; it describes the relation of symbols in two coherent data sets, respective tissues or morphologies. It is extensively used in image registration of multimodal data, where correlation methods are not applicable to modality specific manifestation of tissue. In perfectly registered images mutual information is maximized (Studholme et al. 1996, Hill et al. 1998, Crum et al. 2003).

For alignment of two-dimensional images, *X* and *Y*, the global maximum in a three-dimensional variable space, one rotational and two translational degrees of freedom, is determined. Mutual information of both images is maximized by steepest gradient search

$$MI(X;Y) = \sum_{y \in Y} \sum_{x \in X} p(x,y) \log\left(\frac{p(x,y)}{p(x)\,p(y)} \right). \qquad (7)$$

In the above equation $p(x,y)$ denotes the joint probability of images *X* and *Y*, the probabilities of both single images are represented by $p(x)$ and $p(y)$.

4. RESULTS

Image segmentation based on functional and morphological images provides reasonable results. As an example, real patient data, as shown in Figure 3, are segmented. In case of a combined Indium 111 scan, serving as planning basis for an Yttrium 90 treatment, kidneys are the critical organs, and must be prevented from lethal dose. For this planning procedure left and right kidneys, liver and spleen are segmented. Figure 5 shows a rendering of the regions in the SPECT data set. For orientation a transparent rendering is shown on the left (a) and an exclusive display (b) of liver (blue), spleen (orange), right kidney (red), and left kidney (green).

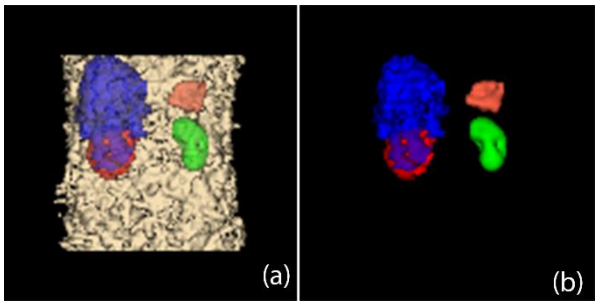

Figure 5: Automated segmentation based on morphological, shape, and functional information. Relevant organs for nuclear medicine radiation therapy are segmented; liver (blue), spleen (orange), kidneys (red and green). Objects are shown as transparent renderings relative to the body surface (a) and as exclusive 3D display (b).

For testing the reliability of the developed methods, mathematical phantom data are generated based upon these segmentations. The development of an anthropomorphic phantom provides realistic activity data as a reliable reference for evaluation of the methods, not accessible from in vivo data.

For simulation purposes the left kidney was masked, cf. the green object in Figure 5, providing a natural activity distribution. The dynamics of the TAC is characterized by a bi-exponential function with amplitudes 5GBq and 3GBq and half-life times 16h and 61h. The region is calibrated to 8GBq at application time. Image volumes are calculated at 20min, 90min, 24h, 48h, 72h and 90h, adding Gaussian noise with 7% of individual pixel intensity as standard deviation. Considering non uniform attenuation, derived from the CT scan, anterior and posterior projection images are calculated. From this image data TACs are simulated by the following categories:

- uncorrected: the geometric mean of the native summed ROI counts,
- uniform attenuation correction: the geometric mean of summed ROI counts is corrected assuming homogeneous attenuation by water,
- non-uniform attenuation correction: anterior and posterior images are corrected on a pixel basis by the correction mask f_i derived in equation 6.

A comparison of the different methods is repented in Figure 6. The dashed line shows true activity simulated in the organ.

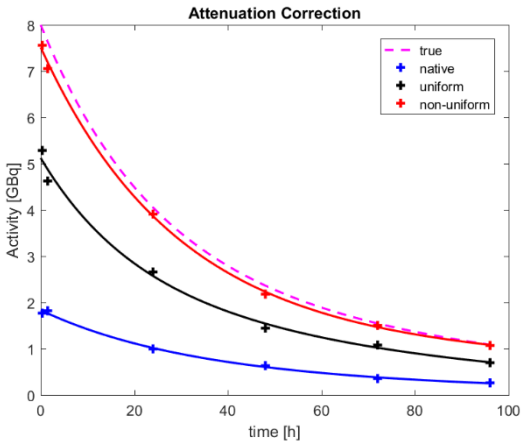

Figure 6: Simulation study for comparison of attenuation correction methods in internal dosimetry. True total counts are indicated by the dashed magenta line. Simulated data are represented by cross marks. The solid lines show the bi-exponential curve fits. The uncorrected counts are drawn blue, the homogeneous H_2O correction is black and the non-uniform 3D based correction is drawn red.

Assessment of radiation dose from native ROI data shows a substantial underestimation of counts, at least uniform attenuation correction is recommended. Non-uniform attenuation correction and derivation of VOIs from 3D SPECT and CT data is most accurate.

5. DISCUSSION

Internal dosimetry raises its importance with the increasing availability of a great variety of tracer molecules, enabling individual tumor therapy. Ethic and legal constraints put focus on reliable and accurate dosimetry. With common whole body scintigraphy, problems of overlapping organs in projections and deterioration of counts by attenuation are inherent to the method. The installation of modern 3D imaging modalities allow a three dimensional sight of the problem, at the cost of at least two additional scans and some time consuming data processing. This work proposes a reasonable approach for automated definition of 3D VOIs in contrast to manual drawing organ ROIs. With VOIs a strict separation of organs is possible overcoming the problem of merged projected regions. The simultaneous acquisition of a CT study allows the development of an accurate and individual non-uniform attenuation correction approach.

After additional clinical evaluation and careful comparison to results of standard whole body dosimetry, this method may be a further step towards accurate individual dosimetry, based on organ specific time activity curves.

ACKNOWLEDGEMENTS

The author thanks Univ.-Prof. Dr. Michael Gabriel and the clinical staff of the Institute of Nuclear Medicine and Endocrinology of the Med. Campus III of Keppler University Clinicum, Linz, Austria, for providing in-vivo data and medical expertise.

REFERENCES

Backfrieder W, Baumgartner R, Sámal M, Moser E, Bergmann H, 1996. Quantification of intensity variations in functional MR images using rotated principal components. *Phys Med Biol.* 1996, 41(8), 1425-38.

Bai CY, Shao L, Da Silva AJ, Zhao Z, 2003. A generalized model for the conversion from CT numbers to linear attenuation coefficients. IEEE Trans Nucl Sci. 2003, 50, 1510–5.

Crum WR, Hill DL, Hawkes DJ, Information theoretic similarity measures in non-rigid registration. *Inf Process Med Imaging*. 2003 Jul, 18, 378-87.

Hill DL, Maurer CR , Jr, Studholme C, Fitzpatrick JM, Hawkes DJ, 1998. Correcting scaling errors in tomographic images using a nine degree of freedom registration algorithm. *J Comput Assist Tomogr*. 1998 Mar-Apr, 22(2), 317-23.

Mirzaei S, Sohlberg A, Knoll P, Zakavi R, Diemling M, 2013. Easy-to-use online software package for internal dose assessment after radionuclide treatment in clinical routine. *Clin Nucl Med*. 2013, 38(9), 686-90.

Lee JA, Ahn YC, Lim DH, Park HC, Asranbaeva MS, 2015. Dosimetric and clinical influence of 3D versus 2D planning in postoperative radiation therapy for gastric cancer. *Cancer Res Treat*. 2015 Oct, 47(4),727-37.

Sámal M, Kárný M, Sůrová H, Maríková E, Dienstbier Z, 1987. Rotation to simple structure in factor analysis of dynamic radionuclide studies. *Phys Med Biol.* 1987, 32(3), 371-82.

Sámal M, Kárný M, Sůrová H, Pěnicka P, Maríková E, Dienstbier Z, 1989. On the existence of an unambiguous solution in factor analysis of dynamic studies. *Phys Med Biol*. 1989, 34(2), 223-8.

Schläger M, 2011. Comparison of various anthropomorphic phantom types for in vivo measurements by means of Monte Carlo simulations. *Radiat Prot Dosimetry*, 2011 Mar, 144(1-4),384-8.

Snyder WS, Ford MR, Warner GG, Watson SB, 1975. "S," Absorbed dose per unit cumulated activity for selected radionuclides and organs. Oak Ridge National Laboratory, Oak Ridge, Tennessee, USA

Stabin JA, 1996. MIRDOSE: personal computer software for internal dose assessment in nuclear medicine. *J Nucl. Med.* 1996, 37(3), 538-46.

Stabin JA, Siegel MG, 2003. Physical models and dose factors for use in internal dose assessment. *Health Physics*, 2003 Sep, 85(3), 294-310.

Studholme C, Hill DL, Hawkes DJ, 1996. Automated 3-D registration of MR and CT images of the head. *Med Image Anal.* 1996 Jun, 1(2), 163-75.

AUTHORS BIOGRAPHY

Werner Backfrieder received his degree in technical physics at the Vienna University of Technology in 1992. Then he was with the Department of Biomedical Engineering and Physics of the Medical University of Vienna, where he reached a tenure position in 2002. Since 2002 he is with the University of Applied Sciences Upper Austria at the division of Biomedical Informatics. His research focus is on Medical Physics and Medical Image Processing in Nuclear Medicine and Radiology with emphasis to high performance computing. Recently research efforts are laid on virtual reality techniques in the context of surgical planning and navigation.

SKILL-BASED ROUTING PROBLEM IN EMERGENCY CALL CENTERS: TOWARD AN IMPROVEMENT OF RESPONSE TIME

Eva Petitdemange [(a)], Franck Fontanili[(a)], Elyes Lamine[(a,b)], Matthieu Lauras[(a)]

[(a)]Industrial Engineering Center, IMT Mines Albi, France
[(b)] ISIS, University National Institute Champollion, France

[(a)]eva.petitdemange@mines-albi.fr, [(a)]franck.fontanili@mines-albi.fr, [(a, b)]elyes.lamine@univ-jfc.fr.fr
[(a)]matthieu.lauras@mines-albi.fr

ABSTRACT

Emergency Call Centers (ECCs) have now to manage different streams of calls (vital emergencies, general medicine regulations…). To do so, ECCs use different workforce organizations based on dedicated or polyvalent skills on one hand, and based on different management rules for waiting queues of incoming calls. The purpose of this paper is to objectively study these different approaches in terms of waiting time and quality of service. Using a Discrete Event Simulation model, we demonstrated the clear benefits of merging queuing lines and developing multi-skilled human resources.
Keywords: Emergency Call Center, Discrete Event Simulation, Workforce Management.

1. INTRODUCTION, RESEARCH QUESTION AND METHODOLOGY

In a matter of pre-hospital care, the Emergency Call Center (ECC) is indeed a significant link in the chain of emergency. When a patient is in an emergency situation, he/she can call for help using a national phone number (112 or 15 in France). This call will be routed to the nearest local ECC where it will be treated. Depending on the situation, ambulances and medical staff will be sent to provide help to the caller. In France, the Emergency Medical System (EMS) is managed by the *Service d'Aide Médicale Urgente* (SAMU). The purpose is to offer a 24/24 answering service for each call as fast as possible with the most suitable way. ECCs are confronted to a growth of the number of calls because of the ageing of the population, the democratization of the use of emergency number and to the creation in some countries like France, of a non-emergency medical service number: the General Medicine Regulation (GMR). The purpose of this last phone line is to handle general medicine calls when the general physician offices are closed. This new stream of calls combined with the funding limitations in healthcare organizations leads to redesign the way workforces are managed in ECCs. In the next few years, the different flows of inbounding demands for the emergency will diversify further through the appearance of *e-calls* which are automated calls send by cars when an accident occurs (Castrén et al. 2008), or with new streams such as videos, text messages or e-mails. These new streams will increase the workload that can have a critical impact on the response time. In such a situation, the response time is defined as the time between the dialed number (112 for emergency or specific number for GMR) and the picked up call. This time is crucial because it can impact the patient survival. To maintain a suitable response time threshold, there is a need to study and potentially adapt how ECC' workforces are managed. In the French ECCs, there are several human resources. Incoming calls are firstly picked up and sorted by an Emergency Call Operator (ECO) or a Medical Call Operator (MCO) depending on the inbound stream. Then it is transferred to a physician who can be a Medical Regulator (MR) for an emergency case or a General Practitioner (GP) for GMR calls. With the creation of the GMR, workforce management has not been unified yet between local ECCs. Some have a dedicated staff of ECO and MCO handling incoming calls from their respective stream. Others have one team of ECO considered as 'multi-skilled' who handle all calls regardless of the inbound stream.

This problem of multi-sources call centers is known as '*routing problem*' in the literature (Aksin Zeynep et al. 2009). A call center can handle multiple types of calls from different sources that will need different skills to be adequately answered. This induces some complexity to choose how to manage workforces efficiently. The use of multi-skilled agents can produce economies of scale for organizations (Gans et al. 2003). However, it needs to determine which type of call is treated by which agent and how many kinds of calls an agent must be able to manage. The same issue occurs in ECCs with

the diversification of call streams. Finally, the goal of this research work is to investigate the following Research Question:

RQ: Does the use of multi-skilled ECO in ECCs reduce the response time of emergency calls?

To answer this question, we decided to use Discrete-Event Simulation (DES) models to test different workforce management configurations and assess the impact on ECC's service level: (1) ECC with two dedicated queues; (2) ECC with one shared queue for the two incoming streams and multi-skilled ECO and MCO; (3) Two separate queues but the MCO can take calls from the emergency queue; (4) Two separate queues but each ECO and MCO can pick up calls from both if he/she does not have calls in his/her own.

In section 2, we will develop a literature review on skill-based routing in a multi-sourcing call centers and on ECCs. In section 3 we present the DES and how it is structured. The scenarios and the results are discussed in section 4

2. BACKGROUND

2.1. Skill-Based Routing in Call Center

Call centers are a growing part of the global economy because it is the easiest and the cheapest way to provide support to the customer (Aksin Zeynep et al. 2009). With the growth of demand and the diversification of inbounding stream, call centers must handle several types of calls which can be due to the language of communication or the level of skills needed to answer the request (Gans et al. 2003). Call center is asked to provide the highest quality of service possible with attempting the fewer costs. As a consequence, training all the agents in order to allow them treating all type of calls is not the better way to be cost-effective (Gans et al. 2003). That is why today call centers are designed as *multi-skilled* call centers. It is defined as several types of calls and several kinds of agents who can handle one or multiple families of calls. The problem which tries to optimize the assignation of call type to an agent is called *Skill-Based Routing (SBR)* or *Routing* (Koole and Mandelbaum 2002). (Wallace and Whitt 2005) propose an algorithm to find how many skills an agent must have to improve the global performance of a center. The purpose of their research work is to find the appropriate combinations through six types of calls and only two skills per agent, but they assume that the service times do not depend on the call type. They add some flexibility in the routing of a call to improve the quality of service. The flexibility is defined as the capability of an agent to handle several types of calls.

(Ahghari and Balcioğlu 2009) worked on a call center dealing with several types of inbounding calls/e-mails and agents using a simulation model. They proved the benefits of using multi-skilled agents for call center performances looking at the mean sojourn time. (Jaoua et al. 2013) try to give more insight to determine which calls must be merged into one specific type. This study was conducted on a real dataset from an electric company call center.

2.2. KPI to evaluate Call Center

The *Quality of Service* (QS) is a standard KPI to evaluate the response time of a call center (Avramidis et al. 2009). It is a KPI widely used to evaluate call centers (Passmore and Zhan 2013) even ECC (Penverne et al. 2017). It is usually defined as the fraction of calls served under a specified threshold on the total of incoming calls. Some definitions reduce the number of calls served by the calls abandoned before *x* seconds of waiting. They consider that calls abandoned before a certain amount of time are mistakes and don't need to be served.

The *Abandon Rate* is the part of calls which interrupted the communication before being served by and agent. Some abandoned calls will try to call back later and then will increase the incoming flow of the call center. (Dai and He 2010) studied the length of the waiting queue to manage the number of the abandoned call.

The *Occupation Rate* or *Occupancy* measures the availability of a resource. It is often calculated as the fraction of the busy time of an agent on the total time of the agent. It contains the time the agent is handling a call with the customer or the time he is achieving a task linked to the customer's service. (Penverne et al. 2017) worked on the link between the *Occupation Rate* and the *QS*. These two KPI are strongly correlated.

The *Customer satisfaction index* is another KPI, more qualitative but still used and considered as important by the managers of call centers (Robinson and Morley 2006).

The *Average Speed of Answer* or the *Waiting time before pick up* is an important measure of call centers (Passmore and Zhan 2013) because if it increases then the *Abandon rate* will also increase, and *the Customer satisfaction* and the *Quality of Service* will decrease.

The Call duration is the time taken to serve a call. It includes the on-call time, the on-hold time, and the activity after the end of the call for closing the customer request.

The Number of calls per agent might be evaluated as well to measure the performance of each agent. However, it is considered as less relevant by the manager after the survey of (Robinson and Morley 2006).

2.3. Emergency call center

As far as we know, there are only a few studies on that topic in the healthcare field. (Van Buuren et al. 2017) designed a DES model of an ECC to evaluate the communication processes and the performances of the ECC. They have worked on the staffing problem to determine how many agents of each type is needed to reduce the average duration until the dispatch of an ambulance. In an ECC, the time is crucial because more than the satisfaction of the caller, it can have an impact on his/her survival. The treatment of an emergency call

can be divided into two stages (see Figure 1): *Upstream* and *Downstream* (Belaidi et al. 2009). The *upstream* stage goes from when the call is received to the decision to dispatch or not a mobile medical unit for the patient. It contains three tasks: (1) the *Answering* of the call with an initial sorting, *(2)* the *Recording* of the medical files and (3) the *Regulating* part managed by the MR or the GP. The *downstream* stage is about the management of the care of the patient, the choice of the hospital of destination, his/her transport to the hospital and his/her registration. In this paper, the focus is on the upstream stage.

Figure 1: A global process of an emergency call

(Aringhieri et al. 2017) demonstrate in their literature review, a gap of studies between the *upstream* and the *downstream* parts. Indeed the *downstream* part is well documented with location and dispatching problem of the ambulances, dynamics re-dispatching and staffing of the mobile units (Aboueljinane et al. 2013). However, the literature is sparse on the *upstream* stage. The treatment of the call before dispatching a medical unit should be an interesting topic of research because some treatment times might be reduced (Lamine et al. 2015). (Aboueljinane et al. 2014), for instance, found that a decrease of 30 seconds in the treatment before the dispatch can improve the total response time of the call significantly. The management of workforces in an ECC has been treated by (Montassier et al. 2015). They studied the impact of work shift on the time performance of the ECO and MCO in a French Call Center using a statistical analysis. It can be interesting to look at the cross-training problem in an ECC to validate that multi-skilled agent is a benefit.

2.4. Call Center and Simulation

Most of the time, call center issues are addressed using the queuing theory (Gans et al. 2003), (Koole and Mandelbaum 2002). However, the queuing theory is more adapted for a single type of call and agent. When it comes to multi-sourcing call center and multi-skilled agent, DES seems more appropriate as shown by (Bhulai 2009) and (Roubos and Jouini 2013).

3. MODEL PRESENTATION

In this section, we present the models designed for the experimental part. These have been implemented on Witness® package.

3.1. Assumptions

The "As-Is" model was built from a real ECC: SAMU 31 (Toulouse, France). For this model, we have set the rules of all the waiting queues except the one before the *ANSWERING* task that is the one we want to challenge.

We have considered the different tasks are not interruptible: they cannot be stopped. If the agent begins the task, he/she has to finish it.

Based on what is really done in SAMU 31, we worked on one ECC with two types of incoming streams. To simplify the analysis, the model includes only one ECO or MCO for each stream, one Medical Regulator (MR) and one General Practitioner (GP). According to the number of calls, several ECOs, MCOs, MRs and GPs can work in parallel.

We are considering only the incoming calls and not the outgoing ones. Considering them will reduce the availability time of the agent, but this problematic is not studied in this paper.

3.2. Model

3.2.1. The agents

We are considering four types of agents in the ECC: the ECO and the MCO who pick up the calls and the MR and GP who regulate the calls. They have different tasks which cannot be disrupted when they have already begun. The first two tasks are performed for each call, regardless of the severity:

ANSWERING: The call is picked up and the severity of the call is evaluated.

RECORDING: A medical or non-medical record is open and fulfilled by the ECO/MCO with basics information: the name of the caller, the location, the purpose of the call, etc.

According to the severity of the call, the following four tasks can be performed:

ADVISING: The caller needs a piece of information that can be given without the skills of a physician.

EMERGENCY DISPATCHING: The call needs mobile unity care as soon as possible. It is a life-threatening case. In this situation, the ECO/MCO dispatches an ambulance or a mobile intensive care unit and after he/she sends the call to the MR.

MED. REGULATION: Calls that needs regulation by a MR who is an emergency doctor dedicated to urgent matters and life-threatening calls.

GMR REGULATION: Calls that needs regulation by a GP who regulate the calls for general medicine.

3.2.2. The inbounding streams and call severity index

In our study, there are two streams of incoming calls:

- *Call_112:* calls dialed by the national or European emergency number (15 or 112).
- *Call_GM:* calls dialed by the general medicine number (3966 in France)

These two streams can receive 4 types of calls with a different severity index (S) (see Table 1), but the percentage of each type varies from one stream to another.

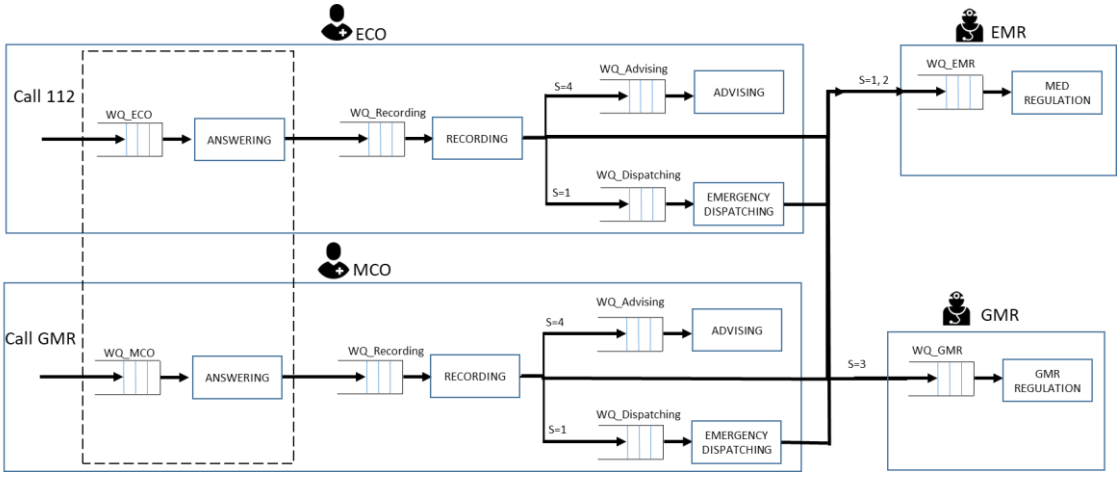

Figure 2: Flow diagram of an emergency call

The process flow diagram of an emergency call is provided on Figure 2 to explain the service process of an emergency call treated by an ECO (the business process is the same for a MCO). When a call arrived in the system and if there is no ECO available for answering then it waits in the *WQ_ECO* waiting queue until it can be picked up by an ECO. Then it goes to the *RECORDING* task with the same principle for WQ_Recording waiting queue than before. Depending on its severity index S, the call will take different paths (see Table 1 for the synthesis):

If S=1: Life-threatening situation that needs an ambulance or a mobile intensive care unit as quickly as possible. The call will go to the *EMERGENCY DISPATCHING* task and will be taken by the MR as soon as he/she is available.

If S= 2: Urgent situation which needs to be regulated by an MR but can wait a few seconds before dispatching units. The call will go to the *MED_REGULATION* task or to the *WQ_EMR* waiting queue depending on the *MR* availability.

If S=3: General Medicine that needs to be regulated by a GP, the processing time can be longer without being life-threatening. The call will go to the *GMR_REGULATION* task or the *WQ_GMR* waiting queue depending on the GP availability.

If S=4: Non-medical advice that needs information that can be given by an ECO/MCO. The call will go to the *ADVISING* task after the WQ_Advising waiting queue.

Table 1: Specification of the severity of a call (S)

TYPE	DEFINITION	NEXT ACTION
1 – Life-threatening	Need a "reflex" departure	*EMERGENCY DISPATCHING*
2 – Urgent	Need to be regulated by an MR	*MED_REGULATION*
3 – General Medicine	Need to be regulated by a GP	*GMR_REGULATION*
4 – Advice	Need advice which can be given by an ECO or MCO	*ADVISING*

3.2.3. The waiting queues

As mentioned earlier, a particularity of the model is when a task has begun it cannot be interrupted. But an ECO or MCO should not handle a call from the beginning (picked up) to the end (transmitted to EMR or GMR). If there is at least one call in the incoming waiting queue (WQ_ECO or WQ_MCO), he/she can place the call being processed on hold between two tasks and switch to the first call in the incoming waiting queue. The flow diagram (Figure 2) shows several waiting queues with different priority levels (1 is the highest, 4 is the lowest):

- *WQ_ECO (or WQ_MCO)*: This queue has a priority level of 2. Calls need to be picked up as fast as possible to evaluate their gravity. So, if there is a call in this queue and no call in WQ_Dispatching, the agent will take a call from this queue.
- *WQ_Recording:* This queue has a priority level of 3. If there is no call in the WQ_ECO (or WQ_MCO) and WQ_Dispatching queues, the agent will take a call from this queue. To select the call he/she will handle, the agent looks at the severity of each call in the queue and takes the call with the lowest severity index because it is the most urgent.
- *WQ_Dispatching*: It is the queue with the highest priority level (=1). If there is a call in this queue, that means that its severity S is equal to 1 and it must be treated as a priority by the resource.
- *WQ_Advising*: Finally, if there is no call in another waiting queue, the agent will take a call from this queue (its priority level is the lowest) to realize the *ADVISING* task. Only calls with a severity index of 4 go in this queue.

The priority of the tasks (and their upstream queues) is summarized in the Table 2.

Table 2: Priority of the tasks (or upstream queues)

Task	Priority
EMERGENCY_DISPATCHING	1
ANSWERING	2
RECORDING	3
ADVISING	4

Finally, the Figure 3 illustrates the flow chart of an agent to know in which queue he/she must pick up a call.

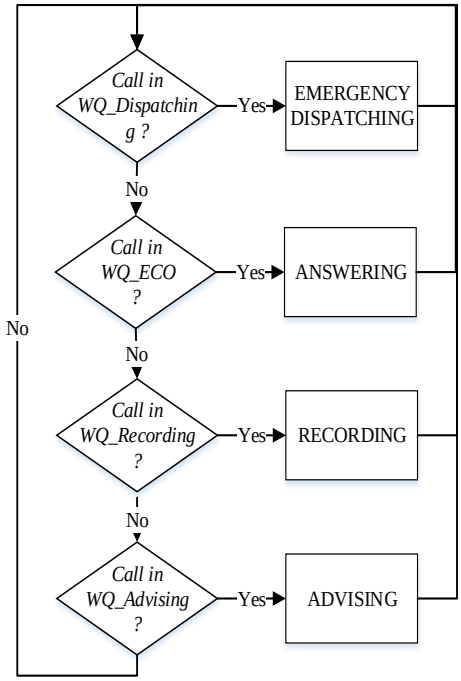

Figure 3: Flow chart of an ECO

3.3. KPI and evaluation methodology

To measure the performances of the model, we looked at several KPIs. ECC has the particularity not to look only at the mean value when it comes to performance measures. For the response time, it is more interesting to reduce the maximum value than the average. Indeed, even if there are only a few calls that do not respect the threshold, they might be life-threatening calls as well. The exception is not allowed in the healthcare field.

Consequently, we decided to focus specifically on time performances. We evaluated the Quality of Service QS, and the waiting time before picks up. For the waiting time before picking up, we looked at the mean value and the maximum value. We evaluated two QS, QS_{20} and QS_{60}. We can remark there than QS_{60} is used as a national KPI to evaluate the French ECCs with the recommendation that QS_{60} must be superior to 99%. Even though QS_{20} is not used in France, it is used in the USA where at least 95% of the calls must reach in less than 20 seconds. Therefore, it is interesting to look at it as a comparison factor.

Table 3: Types of KPIs

KPI	Objective Value
Quality of Service QS_{20}	95%
Quality of Service QS_{60}	99%
Mean waiting time before pick-up	Minimum
Maximum waiting time before pick-up	Minimum

4. SCENARIOS AND RESULTS

To execute our test-run, several scenarios have been established in close collaboration with the physicians of four French ECCs. As a consequence, considered scenarios are representative of the field. We have taken one ECC as a starting point, and then we have elaborated different ways to manage the incoming calls and the waiting queues before the *ANSWERING* task. The first scenario corresponds to the "As-Is" situation of a French ECC (SAMU 31 in Toulouse).

4.1. Scenarios

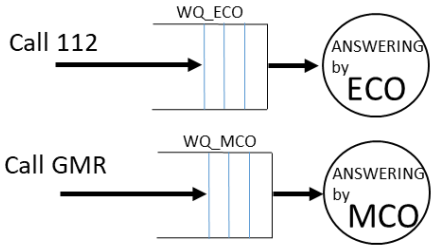

Figure 4: Scenario 1 (As-Is)

In Figure 4, we have two types of resources. ECO who manages calls from the stream *Call 112*, and MCO who takes only calls from the stream *Call GMR*. As shown in Figure 3, ECO or MCO will receive a call in the waiting queue just if they have not an *EMERGENCY DISPATCHING* task on process. Then the *ANSWERING* task can be done. Calls are picked up with a First-In-First-Out (FIFO) rule from the queues.

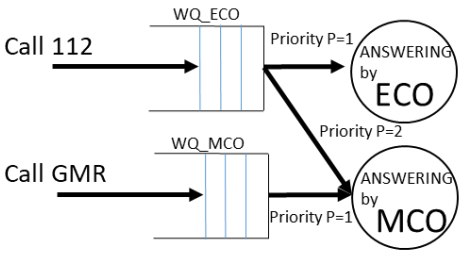

Figure 5: Scenario 2

Scenario 2 suggests letting MCO handles calls from the *Call 112*. In Figure 5, calls from *Call GMR* are served by a MCO. *Call 112* is served by an ECO but a MCO can take calls in the *WQ_ECO* if his/her own *WQ_MCO* is empty and if he/she is not busy in another task with a higher priority. Consequently, the MCO can support the

ECO if only he/she has no call from his/her stream to handle.

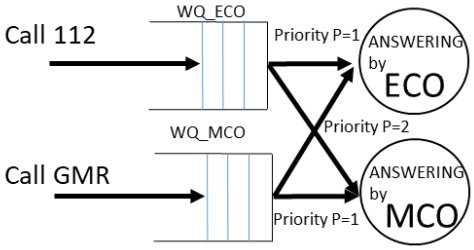

Figure 6: Scenario 3

Scenario 3 is illustrated in Figure 6. In this one, we let the two pools of agent, ECO and MCO, able to pick up calls in the two waiting queues. However, a priority is applied for each kind of agent. ECO must pick up firstly calls from *WQ_ECO*. If this queue is empty, then he/she can pick up call from *WQ_MCO*. *MCO* follows the same principle: firstly he/she picks up calls from *WQ_MCO;* if empty, he/she can pick up calls from *WQ_ECO*.

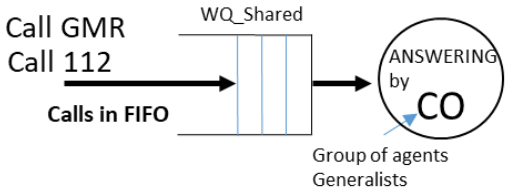

Figure 7: Scenario 4

For the next two scenarios, we create a new pool of agents: *Call* Operator (CO) who is a generalist and multi-skilled agents able to handle a call from both incoming streams. In Figure 7, we merge the two previous waiting queues in one shared queue (*WQ_Shared)* for both streams of calls. The queue manages calls with a FIFO rule without considering the flow. We assume that the two kinds of agents skilled enough to handle both streams with the same treatment time, because analyzing the severity of the calls is the same task from one stream to another.

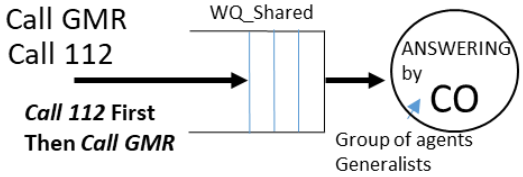

Figure 8: Scenario 5

For Scenario 5 (Figure 8), instead of applying a FIFO rule to the *WQ_Shared* we put a priority on the call from the *Call 112* stream. As this stream has a higher proportion of emergency calls which should be treated in priority, addressed them in priority might improve the pick-up time.

4.2. Data Input

To feed the model, we used data from the SAMU 31 from Toulouse (France) for three months from January to March 2018. The data set includes the number of calls per hour for the whole period. We decided to focus on a critical day (Sunday) to assess the extreme behaviors. Sunday is the day with the most significant amount of calls due to the GMR that is open all day long. Number of incoming calls profiles (*Call 112* and *Call_GMR)* on Sunday are represented on Figure 9. We have described each stream and the cumulative of both as it is the cumulate profile that is used for the scenarios 4 and 5. The peak of calls is between 8 AM and 9 AM.

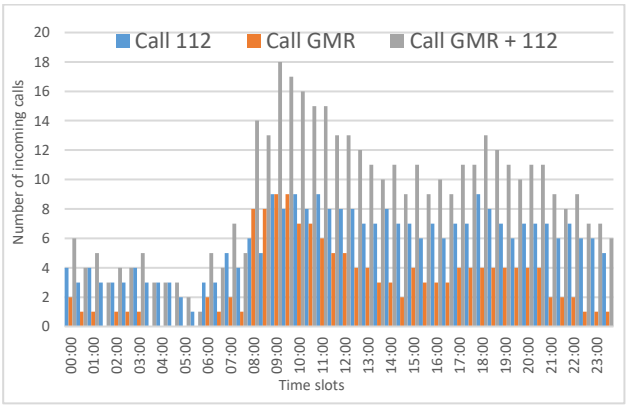

Figure 9: Profile of incoming calls

To model the processing time of each task, we have looked at the communication time per call, hour by hour from the historical data set of the SAMU 31. According to this data set, the fittest distribution is a *uniform (min, max)* distribution to model the processing time. The Table 4 summarizes the different processing times by task.

Table 4: Processing Time (in sec.) of each task

Ress.	tTask	Processing Time (sec.)
ECO /MCO	ANSWERING	*UNIFORM(30,60)*
	RECORDING	*UNIFORM(20,60)*
	ADVISING	*UNIFORM(100,140)*
MR	MED_REGULATION	*UNIFORM(80,225)*
GP	GMR_REGULATION	*UNIFORM(90,245)*

4.3. Results and discussions

The Figure 10 presents the results of the five scenarios with a box and whisker plots chart (Tukey 1977) for the time before picking up call.

The table 5 presents the QS_{20} and QS_{60} for the five scenarios.

Table 5: Results for the Quality of Service QS

		QS_{20}	**QS_{60}**
Scenario 1	AsIs	78.65%	92,13%
Scenario 2	Value	86,38%	96,48%
	Delta AsIs	*10%*	*5%*
Scenario 3	Value	93,43%	**100%**
	Delta AsIs	*19%*	*9%*
Scenario 4	Value	93,10%	**100%**
	Delta AsIs	*18%*	*9%*
Scenario 5	Value	92,13%	**99,55%**
	Delta AsIs	*17%*	*8%*

The scenario 1 is the *As-Is* scenario in which there are six outliers:

- Two calls with a pickup time of 02:39 and 02:36. These calls can be explained as following: the ECO is doing the *ADVISING* task and these calls are waiting in the *WQ_ECO* during this time. We can notice that during this time the MCO is waiting, he/she has no call to handle. It reflects an unbalanced workload.
- There are four other calls that have their pickup time between 02:12 and 02:01. This group corresponds to calls at 08:14:15 where there is a peak of activity for the GMR (see Figure 9). MCO must treat six calls and during this time, the ECO has no call to handle. As a consequence, there is an unbalanced distribution of the workload.

If we looked at the QS, neither QS_{20} nor QS_{60} would reach the objective targeted (95% and 99%).

The scenario 2 allows solving the situation when the ECO has several calls to handle. In this situation, the MCO can help the ECO to pick up calls. As a consequence, the maximum waiting decreases of 26 seconds. The third quartile is reduced to 13 seconds. This means that 75% of calls are picked up in less time than in the first scenario. The call with the maximum waiting time is the same than for the scenario 1. This is consistent because in this scenario, we allowed the MCO to take a call from the WQ_ECO. But the ECO cannot help the MCO. So, the MCO can be overwhelmed and the waiting time is still high.

The scenario 3 leads to a significant decrease of the interquartile range of 19 seconds. This scenario has a QS_{60} of 100%. Indeed, the maximum waiting time reaches 56 seconds. The QS_{20} is improved by 19%. It reached to 93,10%. The possibility for both MCO and ECO to pick-up calls in each queue increase the performance of the agent to pick-up the calls quickly. 75% of the calls are picked up in less than 28 seconds that means that the third quartile is reduced to 29 seconds compared to scenario 1. Moreover, in this scenario, the median is near the mean value. There are less exceptional values that increase the mean value as in scenarios 1 and 2.

If we compare scenarios 1 and 4 now, the call that was picked up in 2:38 in scenario 1 is now picked up after 41 seconds. Scenario 4 leads to better results thanks to a better distribution of calls between resources. This scenario reached a QS_{60} of 100%. There are few differences between scenarios 3 and 4. The FIFO rule in the shared queue induces a maximum waiting time lower than scenario 3, however, the third quartile is higher in scenario 4 than in scenario 3.

Scenario 5 compared to scenario 1 reduced the maximum waiting time from 02:12 to 01:41, so a reduction of 31 seconds. Let now have a look at the call which has the highest waiting time in scenario 3 (call 84 at 08:38:51) from the stream *Call GMR*. When it arrives, both of the CO is doing an *ADVICE* task that cannot be interrupted. But when the first CO has finished his/her task, then he/she picks up the call #85 instead of the #84 because the #85 comes from the stream *Call 112* (priority). However, call #84 has a severity of 2 and call #85 has a severity of 3. So, in this particular case, a call more urgent is waiting for more than a less urgent call. This shows the limits of this approach. As we have calls from the four severities in both streams, if we put a priority on a stream rather than the other, we run the risk of keep waiting for an urgent call, even if this scenario improves the mean pickup time of 74% and let us reach the objective for QS_{60}.

If we look only at the QS values, scenario 3 has the best results. However, if we look only at the maximum waiting time, scenario 4 gives the lowest value.

As we can have urgent calls coming from the two streams of calls, it is not interesting to let just the MCO pick-up call from the WQ_ECO. Scenarios with all the resources that are multi-skilled give the best results in a matter of QS and waiting time before picking up calls.

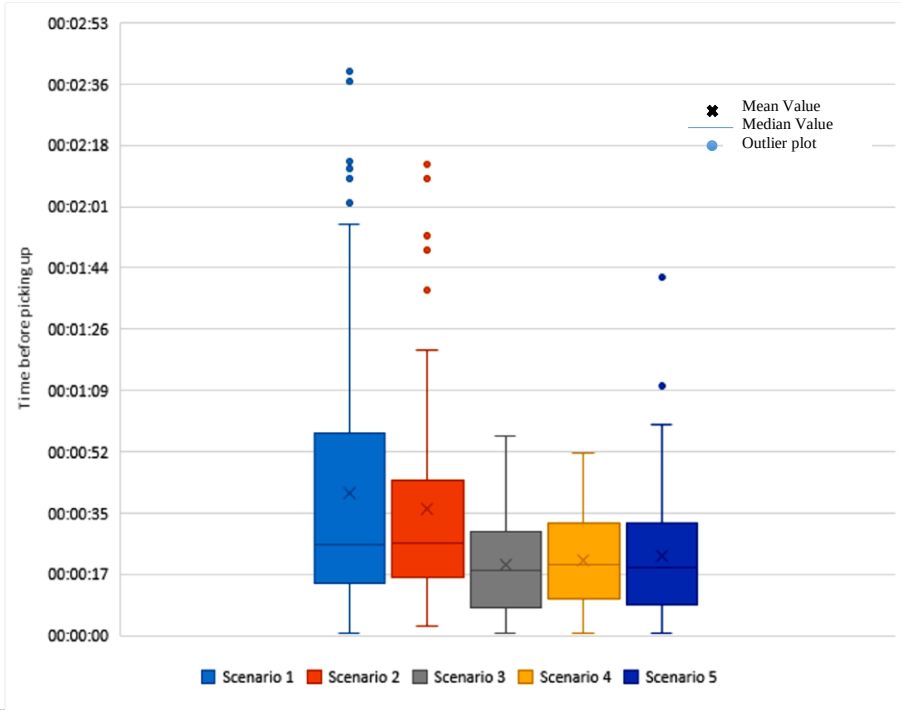

Figure 10: Box and Whisker Plots of the Five Scenarios

5. CONCLUSION AND FUTURE WORKS

The purpose of this article was to investigate the following research question: *Does the use of multi-skilled ECO in ECCs reduce the response time of emergency calls?* To solve this issue, we have developed a discrete event simulation model dedicated to the treatment of calls in an ECC. Starting from the management of a real ECC, we have tested several resources organizations' scenarios to assess their impacts on time performances. We have seen that adding flexibility in the management of resources let reduces the maximum waiting time before picking up. However, rooms for improvement remain to conclude on the most appropriate ECC's organization.

Firstly, a more thorough study of real data sets might improve the model and make it more accurate. This could allow confirming (or not) that a correlation exists between the treatment time and the occupation rate of resources. With more real data, profiles of calls should be more precise and it would be possible to study the impact of the seasonality depending on the type of ECC.

Secondly, the current study only challenges the management of the incoming waiting queue. We can imagine working on the operations of the others waiting queues for the different types of calls to reduce the time for the most urgent calls promptly.

Thirdly, adding the outgoing calls that was ruled out in this study will improve the accuracy of the model. It can also be interesting to create a link between calls and medical files because one medical file can have several incoming and outgoing call linked to it.

Fourthly, in the current research, we only focused on response time of an ECC. However, other KPIs have to be studied in detail, as the occupation rate of resources, the abandon rate or the total treatment time. This will lead us to have an overall insight into ECC performances. It can be interesting to make allowances for the correlation between the different KPIs too.

Finally, for this research work we have enlightened one type of ECC. Working with several ECCs could help us to extract some distinctive characteristic in order to propose clusters. Maybe the management of workforces and business processes have a different improvement depending on the characteristics of the ECC. This study might help to provide recommendations that are adapted to different types of ECCs. Moreover, working with several ECC will let us investigate further the collaboration between different ECCs to assess the collaboration and see the impact on different KPIs.

ACKNOWLEDGMENTS

We would like to thank Dr. Vincent Bounes, Dr. Laurent Gout (SAMU 31), Dr. Pierre Rodriguez (SAMU 12) and Dr. Emmanuelle Gomez (SAMU 81) for their expertise and knowledge about French ECC.

REFERENCES

Abouelijnane L, Sahin E, Jemai Z (2013) A review on simulation models applied to emergency medical service operations. *Comput. Ind. Eng.* 66(4):734–750.

Abouelijnane L, Sahin E, Jemai Z, Marty J (2014) A simulation study to improve the performance of an emergency medical service: Application to the French Val-de-Marne department. *Simul.*

Model. Pract. Theory 47(Supplement C):46–59.

Ahghari M, Balcioğlu B (2009) Benefits of cross-training in a skill-based routing contact center with priority queues and impatient customers. *IIE Trans.* 41(6):524–536.

Aksin Zeynep, Armony Mor, Mehrotra Vijay (2009) The Modern Call Center: A Multi-Disciplinary Perspective on Operations Management Research. *Prod. Oper. Manag.* 16(6):665–688.

Aringhieri R, Bruni ME, Khodaparasti S, van Essen JT (2017) Emergency medical services and beyond: Addressing new challenges through a wide literature review. *Comput. Oper. Res.* 78:349–368.

Avramidis AN, Chan W, L'Ecuyer P (2009) Staffing multi-skill call centers via search methods and a performance approximation. *IIE Trans.* 41(6):483–497.

Belaidi A, Besombes B, Marcon E, Guinet A (2009) Toward a Decision Support Tool for Emergency Networks in France. *Intell. Patient Manag.* Studies in Computational Intelligence. (Springer, Berlin, Heidelberg), 25–37.

Bhulai S (2009) DYNAMIC ROUTING POLICIES FOR MULTISKILL CALL CENTERS. *Probab. Eng. Informational Sci.* 23(1):101–119.

van Buuren M, Kommer GJ, van der Mei R, Bhulai S (2017) EMS call center models with and without function differentiation: A comparison. *Oper. Res. Health Care* 12:16–28.

Castrén M, Karlsten R, Lippert F, Christensen EF, Bovim E, Kvam AM, Robertson-Steel I, et al. (2008) Recommended guidelines for reporting on emergency medical dispatch when conducting research in emergency medicine: The Utstein style. *Resuscitation* 79(2):193–197.

Dai JG, He S (2010) Estimating customer patience-time density in large-scale call centers. *2010 7th Int. Conf. Serv. Syst. Serv. Manag.* 1–5.

Gans N, Koole G, Mandelbaum A (2003) Telephone Call Centers: Tutorial, Review, and Research Prospects. *Manuf. Serv. Oper. Manag.* 5(2):79–141.

Jaoua A, L'Ecuyer P, Delorme L (2013) Call-type dependence in multiskill call centers. *SIMULATION* 89(6):722–734.

Koole G, Mandelbaum A (2002) Queueing Models of Call Centers: An Introduction. *Ann. Oper. Res.* 113(1–4):41–59.

Lamine E, Fontanili F, Mascolo MD, Pingaud H (2015) Improving the Management of an Emergency Call Service by Combining Process Mining and Discrete Event Simulation Approaches. *Risks Resil. Collab. Netw.* IFIP Advances in Information and Communication Technology. (Springer, Cham), 535–546.

Montassier E, Labady J, Andre A, Potel G, Berthier F, Jenvrin J, Penverne Y (2015) The Effect of Work Shift Configurations on Emergency Medical Dispatch Center Response. *Prehosp. Emerg. Care* 19(2):254–259.

Passmore CM, Zhan J (2013) Determining Appropriate Staffing Adjustments in a Call Center Staff Group. *2013 Int. Conf. Soc. Comput.* 1046–1053.

Penverne Y, Leclere B, Labady J, Berthier F, Jenvrin J, Javaudin F, Batard E, Montassier E (2017) Key performance indicators' assessment to develop best practices in an Emergency Medical Communication Centre. *Eur. J. Emerg. Med. Off. J. Eur. Soc. Emerg. Med.*

Robinson G, Morley C (2006) Call centre management: responsibilities and performance. *Int. J. Serv. Ind. Manag.* 17(3):284–300.

Roubos A, Jouini O (2013) Call centers with hyperexponential patience modeling. *Int. J. Prod. Econ.* 141(1):307–315.

Tukey J (1977) *Exploratory Data Analysis* (Pearson).

Wallace RB, Whitt W (2005) A Staffing Algorithm for Call Centers with Skill-Based Routing. *Manuf. Serv. Oper. Manag.* 7(4):276–294.

TRHEE DIMENSIONAL MODEL OF LEFT VENTRICLE: COMPUTATIONAL INVESTIGATION OF FLOW IN PRESENCE OF PATHOLOGY

Lina T. Gaudio[(a)], Gionata Fragomeni[(b)]

[(a),(b)] Department of Medical and Surgical Sciences, Magna Graecia University, Catanzaro

[(a)]l.gaudio@unicz.it, [(b)]fragomeni@unicz.it

ABSTRACT

The left ventricle is the most prone to diseases. Among these the dyssynchrony constitutes a pathology of considerable epidemiological relevance, it is caused by a disorder cardiac contraction. The purpose of the following study is to investigate blood flow during the systole phase within the left ventricle both in physiological conditions and in the presence of dyssynchrony. The three-dimensional reconstruction of the left ventricle is used to perform the numerical simulations through computational fluid dynamics (CFD) analysis. The fluid-structure interaction, with wall motion, was conducted on the physiological left ventricle and in presence of dyssynchrony, to investigate the LV-flow in terms of volume, pressure, and deformation. The results show the comparison between the ejection curve of the physiological ventricle and that in the presence of pathology. The result of this study indicates that the dyssynchrony causes incomplete left ventricular filling with reduced ejected volume and reduced output pressure in the aorta.

Keywords: left ventricle 3D, dyssynchrony, CFD analysis, hemodynamic

1. INTRODUCTION

Heart disease is the cause of death of 17.7 million people every year, 31% of all global deaths (Weir 2016). Among these, heart failure is responsible for most hospitalizations (Bleeker 2006). Heart failure is associated with structural and ultrastructural cardiac changes that are responsible for a heterogeneity of electrical impulse propagation and the onset of contraction dyssynchrony at different levels (Bleeker 2006). Besides the prolongation of the systolic times and reduction of the diastolic ones, the dyssynchrony causes and asynchronous contraction of the left ventricle (Khidir 2016). Consequently, there is incomplete left ventricular filling with reduction of the ejected volume and reduction of the outlet pressure to the ventricle (Khidir 2016). For a correct understanding of the pathology in question, it is useful to have accurate predictive models, for this purpose the three-dimensional modeling of the entire left ventricle is of increasing interest. 3D modeling allows a detailed study of cardiac problems of particular interest with the support of fluid-dynamics simulation (Mazzitelli 2016). So the computational fluid-dynamics (CFD) allows studying high flow dynamics resolution, particularly in areas that do not are visually accessible (Caruso 2016). The CFD analysis is used for the advantage of creating in silico product to study its behavior with the reduction of development time and cost (Condemi 2017). Through this numeric-physical approach, any physical quantity of interest can be detected and sampled in any area of the domain (Condemi 2016). In this context, many authors have focused their attention on the 3D modeling of the physiological ventricle. Taylor & al. have reconstructed the 3D left ventricle first in systole and then in diastole to evaluate the ejection fraction, pressure drop and calculation of velocity and vortices but in distinct different phases without considering the movement (Taylor 1995). Other authors have instead modeled both the flow and the heart muscle and simulated the phases of cardiac cycle evaluating the fluid-structure interaction (Watanabe 2004). More recently by other authors have been studied different pathologies, such as dilated cardiomyopathy, that involving geometric changes in the left ventricle, nothing has been done yet about the dyssynchrony (Mangual 2013). The purposes of the following study are primarily to evaluate the fluid-structure interaction in the physiological ventricular 3D model and, secondly, to evaluate the variations in the presence of dyssynchrony.

2. MATERIALS AND METHODS

The geometry of the 3D ventricle was created by the CT scan of a patient acquired for clinical reasons. Two models were reproduced one to study the physiological ventricle and one to reproduce the situation of dyssynchrony.

2.1. Geometry reconstruction

To build a model of the left ventricle using finite element method (FEM) starting from CT images, the different step must be executed (Caruso 2017). To represent the systole phase, the image was taken at the beginning of the compression. During this phase, the internal radius of the left ventricle decreases and the wall thickness increases as the volume of the muscular wall is kept constant as the volume of the ventricle decreases. Scan data must be appropriately processed to be used for creating numerical models. To this end, an image has

been segmented on the coronal plane to outline both the ventricle and the aorta and cardiac muscle. Another image, that intersecting the centerline path, has instead been segmented to define the volumes on the sagittal plane to define the apex of the ventricle, the central part and the entrance with the aorta. Subsequently, the contour curves were extruded and the entire three-dimensional geometry comprising: the ventricle and the aorta, covered by the heart muscle, were created using RHINOCEROS v.4.0 software (Robert McNeel & Associates, Seattle, WA, USA).

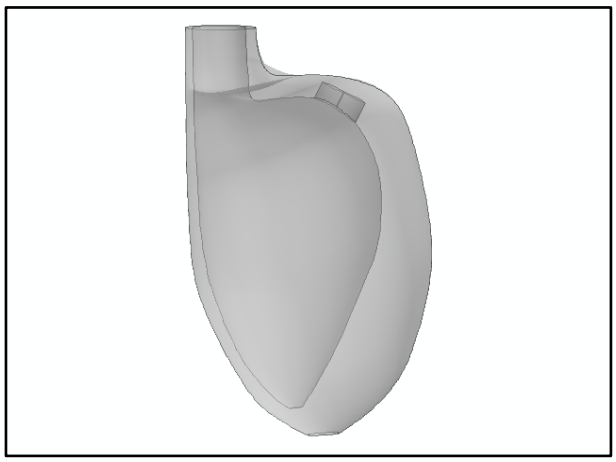

Figure 1: 3D Left Ventricle geometric reconstruction

Following is the entry for the flow coming from the left atrium. In Figure 1 the final model.

2.2. Computational Simulation

To perform the fluid-structure interaction simulations was used the software COMSOL Multiphysics 5.3 (COMSOL Inc., Stockholm, Sweden). The coupling is chosen to represent the fluid and the interaction structure is two-way Multiphysics. Moving Mesh application for computing the deformation/movement of the finite element mesh was applied.

2.2.1. Flow equations

For the fluid domain, the blood was assumed as Newtonian with a density of 1.060 (Kg/m^3) and viscosity of 0.0035 (Pa*s) (Gaudio and De Rosa 2017). The other assumption is that the flow is considered to be laminar and 3D incompressible Navier-Stokes equation was used as governing laws (Mazzitelli 2016 and Gramigna 2015). The incompressible condition as follow for the conservation of mass:

$$\nabla . u = 0 \tag{1}$$

and momentum:

$$\rho \frac{\delta u}{\delta t} + \rho(u.\nabla)\mathrm{u} = \nabla.\{-pI + \mu[\nabla \mathrm{u} + (\nabla \mathrm{u})^T]\} \tag{2}$$

where ρ is the fluid density, u is the fluid velocity, p is the pressure, I is the unit diagonal matrix and μ is the viscosity (Caruso 2015).

2.2.2. Structural equations

For the structural domain, the mechanical properties of cardiac muscle are considered being made of Neo-Hookean hyperelastic behavior, defined by density $\rho = 1200\ (kg/m^3)$ and Lamè constants (Caruso 2016). Lamè constants, $\lambda\ and\ \mu$, are respectively:

$$\mu = 7.20 * 10^6\ (\mathrm{N/m^2}) \tag{3}$$

while the bulk modules equal:

$$\lambda = 20 * \mu - 2\mu/3\ (\mathrm{N/m^2}) \tag{4}$$

And corresponds to value for Poisson's ratio $\nu = 0.45$ an equivalent Elastic modulus E= 1.16*10^6 (N/m^2).
The governing equations are given for momentum:

$$\rho \frac{\partial^2 u}{\partial t^2} - \Delta\sigma_s = Fv \tag{5}$$

Where ρ is the density of the material, u is the displacement vector, σ_s is the Cauchy stress tensor given by the Lagrangian elasticity tensor and the infinitesimal strain tensor for a linear elastic isotropic material, finally Fv is the body load in (N/m^3) (Mazzitelli 2016).

2.2.3. Moving Mesh

The two domains (fluid and solid) were discretized with tetrahedral elements for a total of 150.000 elements with the presence of some hexahedral and prismatic elements. To optimize the analyses, the fluid domain is discretized with a finer mesh and the solid domain with a normal mesh (Figure 2).

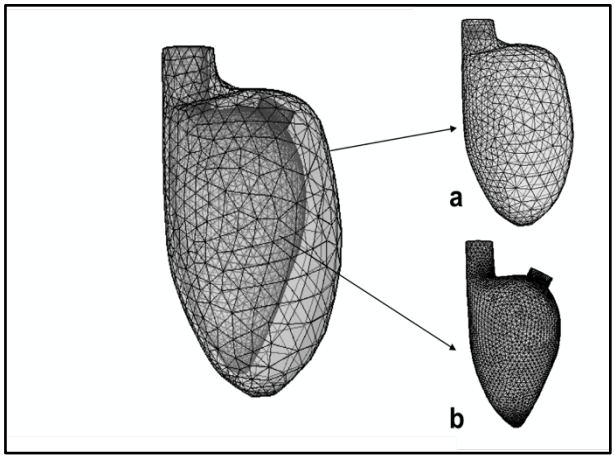

Figure 2: 3D Left Ventricle mesh a)muscle b)fluid

Two types of mesh were compared, a finer and a fine mesh, whose statistics are visible in the Table 1.
Due to the higher quality of the elements and the higher number, a mesh finer was chosen.

Table 1: Finite Element Mesh

Domain Element Statistic		
Mesh Type	Finer	Fine
Number of elements	161825	83538
Average element quality	0.6714	0.6631
Mesh volume [mm^3]	$8.61e^{-4}$	$8.58e^{-4}$

With the aim of reproducing the ventricular movement during the systole phase it was necessary to make use of the arbitrary Lagrangian-Eulerian (ALE) moving mesh technique. In which the mesh velocity is calculated from the Laplace equation (Monnier 2007):

$$\nabla^2 \vec{v} = 0 \qquad (6)$$

The velocity $\vec{v}$, calculated at the interface, depends on the boundary conditions at the interface:

$$\vec{v} = (\vec{u}.\vec{n})\vec{n} \qquad (7)$$

where u is the fluid velocity and $\vec{n}$ is the normal vector.
The advantage of this method lies in the fact that it allows solving problems that require the change of geometry over time. Through the ALE method the dynamics of the deforming geometry and the moving boundary are handles with a moving grid. The new mesh coordinates are calculated for the movement of structure's boundaries form the Navier-Stokes equations that solve the flow (Bruyere 2016).

2.2.4. Boundary conditions

As for the physiological model, a flow rate of 5 (l/min) was imposed at the inlet to the ventricle and a curve pressure with a maximum value of 120 (mmHg) was output of the model in aorta. When in inlet the model with dyssynchrony, a flow rate of 3.5 (l/min) was imposed to reproduce the failure to completely fill the ventricle. The no-slip boundary condition is applied to the fluid-solid interface.
Taking into account the ventricular geometry model, the value of the ventricular wall tension can be traced back to the pressure inside it. During the ejection, the internal radius decreases and the wall thickness increases as the volume of the muscular wall is kept constant as ventricle volume decreases (Pironet and Desaive 2013). The same pressure is therefore obtained with an average minor wall stress. Then, a load on the boundaries of different directions adjacent to the ventricular walls equal to 2 (N/m^2) was imposed on the solid domain. A fixed constraint has been placed in the aorta to simulate the normal contraction that involves movement in the other structures. The two physicists of laminar flow and structural mechanics have been connected through a complete coupling of the fluid and solid interfaces that provides deformation in both directions. A time dependent study was performed and the equation was solved through the use of the direct MUMPS solver.

3. RESULTS

This study aims to investigate the effects of blood flow in the 3D model of the left ventricle. Two cases were considered: a physiological model and a pathological model.
First the velocity streamlines at the systolic peak (t1) were calculated, that as shown in Figure 3.

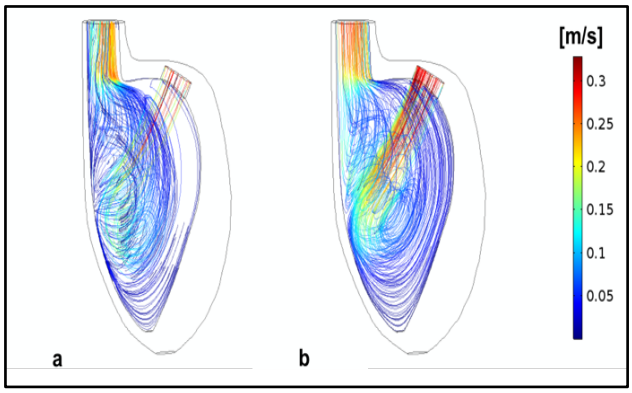

Figure 3: 3D Left Ventricle velocity streamlines at peak time instant t1 a) pathologic case b) physiologic case

Figure 3b shows the presence of vortices given by the physiological movement of blood flow inside the physiologic ventricle with trend coming from the atrium and outgoing in the aorta with a speed of 30 (cm/s). Figure 3a shows the trend of the streamlines in the case of the pathologic ventricle, as it observes the velocity are reduced in some points even near the aorta and the presence of greater vortices. The velocity was also calculated during the initial instant (t0), in which the blood flow is coming in from the atrium. As we note from Figure 4b in the case of the physiological ventricle it notices better streamlines, because they are more linearly distributed with respect to the pathological case (Figure 4a). Moreover, the presence of vortices for the physiological case, Figure 4b, is reduced compared to the presence of dissynchrony, in which the vortices are more appreciable.

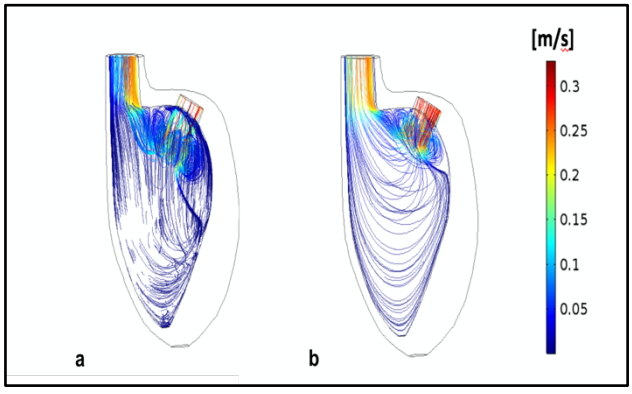

Figure 4: 3D Left Ventricle velocity streamlines time instant t0 a) dyssynchrony case b) physiologic case

Subsequently the pressures were observed, which appear to be greater in the case of the physiological ventricle and, as expected, the pressures decrease because they are due to a lower flow in the ventricular chamber. The data show an average aorta pressure of 125 (mmHg) for the physiological model and in the pathological model about 100 (mmHg) at the systolic peak. In particular, there is a medium reduction, in the case of dyssynchronization, with pressures of 20%.

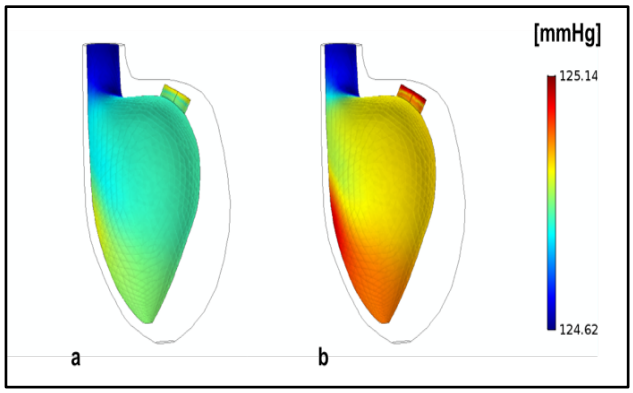

Figure 5: 3D Left Ventricle pressure a) dyssynchrony case b) physiologic case

Table 2 shows the value of the hemodynamic parameters calculated in the output section for both the physiological case and in the presence of dyssynchrony, as can be seen there is a decrease in pressure, flow rate and ejected volume.

Table 2: Average Hemodynamic Value

Average Hemodynamic Value		
Hemodynamic Parameter	LV physiologic	LV pathologic
Flow rate [l/min]	5	3.5
Pressure [mmHg]	124	100
EjectedVolume [ml]	70	45

Below is shown, in Figure 6, the deformation of the heart muscle and the ventricular chamber, in two times of the systolic phase. At the initial instant t0 and subsequently when the force acts at the time instant t1, as we see, the deformation is highest first in the intraventricular septum and subsequently also on the lateral faces of the left ventricle. As can be seen in Figure 6b, the heart muscle and the ventricular chambers contract as a result of the impressed force.

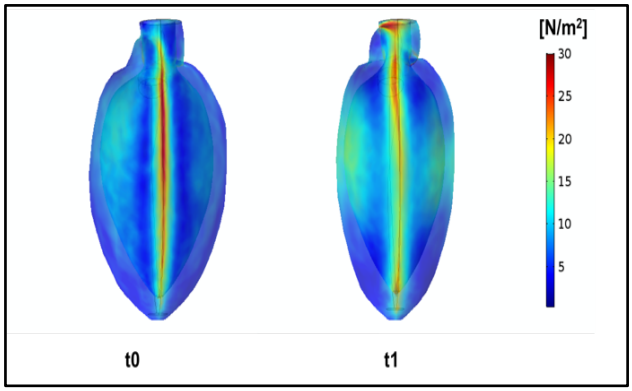

Figure 6: 3D Left Ventricle deformation a) time instant t0 b) time instant t1

In addition, the ejected volumes in systole in the aorta were evaluated for both cases: with regard to the physiological case in the aorta 70 ml of blood are ejected and in the pathological case 45 ml. Through the pressure and volumetric curves the pV-loop ejection curve was calculated and shown in Figure 7.
Respectively, referring to the ejection curve of the physiological 3D left ventricle, the highlighted points correspond to:

- A: diastolic blood pressure (DBP), pressure of the expulsion start phase which corresponds to the end diastolic volume (EDV)
- B: systolic blood pressure (SBD), phase of expulsion of the flow
- C: end systolic pressure (Pes) which corresponds to the end systolic volume (ESV)

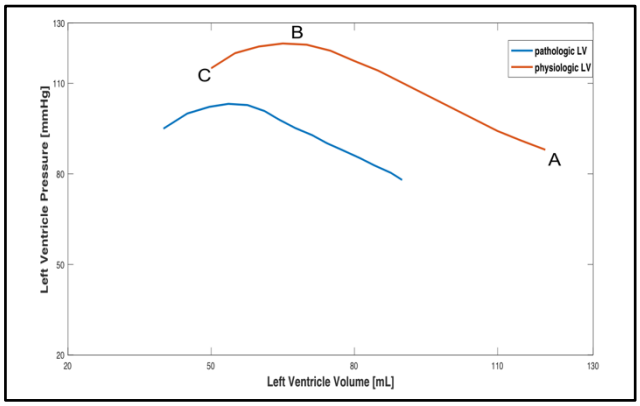

Figure 7: Ejection curve pV-loop

The ejection curve of the physiological model has been compared with the curve obtained from experimental data. The trend is correct form a qualitative but also quantitative point of view with a maximum error of 5%.
As can be seen, the pressures and volumes in the pathologic case are reduced, and the ejection curve lowers and moves to the left.
This is the result of the mechanics of the ventricular filling, as the duration is reduced dramatically and the systolic range is reduced. This also justifies the reduction

of the volume in the ventricle as well as the pressure due to a lower flow in the left ventricular chamber.

4. CONCLUSION

The purpose of this analysis was to be able to ascertain the clinical manifestation of this pathology using the CFD analysis of a 3D model of the left ventricle, which made it possible to identify the variation compared to the physiological model.

The data obtained shows that in case of pathology there is a reduction of the output flow from the left ventricle, with a consequent reduction in volume and pressure.

This preliminary study is aimed at demonstrating that the use of 3D models combined with CFD analysis can be a good starting point for deeper future investigations.

The pV-loop diagram is an important tool for the study of cardiac mechanics and for the definition of pressure/volume relationships in the various moments of the cardiac cycle.

For this purpose, future studies will include the integration of the model with the atrium and the two aortic and mitral valves to simulate all the phases of the cardiac cycle.

REFERENCES

Bleeker, G. B., Bax, J. J., & Van Der Wall, E. E. (2006). Left ventricular dyssynchrony in patients with heart failure: pathophysiology, diagnosis and treatment. Nature Reviews Cardiology, 3(4), 213.

Bruyere, V., Touvrey, C., & Namy, P. (2013). Comparison between Phase Field and ALE methods to model the keyhole digging during spot laser welding. In Proceedings of the 2013 COMSOL Conference, Rotterdam.

Caruso, M. V., Gramigna, V., & Fragomeni, G. (2016). Computational analysis of aortic hemodynamics during total and partial extra-corporeal membrane oxygenation and intra-aortic balloon pump support. Acta of bioengineering and biomechanics, 18(3).

Caruso, M. V., Gramigna, V., Serraino, G. F., Renzulli, A., & Fragomeni, G. (2015). Influence of Aortic Outflow Cannula Orientation on Epiaortic Flow Pattern During Pulsed Cardiopulmonary Bypass. Journal of Medical and Biological Engineering, 35(4), 455-463.

Caruso, M. V., Renzulli, A., & Fragomeni, G. (2017). Influence of IABP-Induced Abdominal Occlusions on Aortic Hemodynamics: A Patient-Specific Computational Evaluation. ASAIO Journal, 63(2), 161-167.

Condemi, F., Campisi, S., & Duprey, A. (2017). Fluid- and biomechanical analysis of ascending thoracic aorta aneurysm with concomitant aortic insufficiency. Annals of biomedical engineering, 45(12), 2921-2932.

Condemi, F., Wang, D., Fragomeni, & Zwischenberger, J. B. (2016). Percutaneous double lumen cannula for right ventricle assist device system: A computational fluid dynamics study. Biocybernetics and biomedical engineering, 36(3), 482-490.

Gaudio, L. T., De Rosa, S., Indolfi, C., & Fragomeni, G. (2017, September). Hemodynamically non-significant coronary artery stenosis: a predictive model. In Proceedings of the International Workshop on Innovative Simulation for Health Care (pp. 18-20).

Gramigna, V., Caruso, M.V., Rossi, M., Serraino, G.F., Renzulli, A., Fragomeni G. (2015) A numerical analysis of the aortic blood flow pattern during pulsed cardiopulmonary bypass. Computer Methods Biomechanics Biomedical Engineering 2015;18(14):1574-81.

Khidir, M. J., Delgado, V., & Bax, J. J. (2016). Mechanical dyssynchrony in patients with heart failure and reduced ejection fraction: how to measure?. Current opinion in cardiology, 31(5), 523-530.

Mazzitelli, R., Boyle, F., & Fragomeni, G. (2016). Numerical prediction of the effect of aortic Left Ventricular Assist Device outflow-graft anastomosis location. Biocybernetics and Biomedical Engineering, 36(2), 327-343.

Mangual, J. O., Kraigher-Krainer, E., De Luca, A., Toncelli, L., Shah, A., Solomon, S., ... & Pedrizzetti, G. (2013). Comparative numerical study on left ventricular fluid dynamics after dilated cardiomyopathy. Journal of biomechanics, 46(10), 1611-1617.

Monnier, J. (2007) Navier-Stokes ALE free surface flow with generalized Navier slip conditions. Droplet impact and attempt using Comsol Multiphysics 3.2. Diss. INRIA

Pironet, A., Desaive, T., Kosta, S., Lucas, A., Paeme, S., Collet, A., ... & Dauby, P. C. (2013). A multi-scale cardiovascular system model can account for the load-dependence of the end-systolic pressure-volume relationship. Biomedical engineering online, 12(1), 8.

Taylor, T. W., & Yamaguchi, T. (1995). Flow patterns in three-dimensional left ventricular systolic and diastolic flows determined from computational fluid dynamics. Biorheology, 32(1), 61-71.

Watanabe, H., Sugiura, S., Kafuku, H., & Hisada, T. (2004). Multiphysics simulation of left ventricular filling dynamics using fluid-structure interaction finite element method. Biophysical journal, 87(3), 2074-2085.

Weir, H. K., Anderson, R. N., & Leadbetter, S. (2016). Peer Reviewed: Heart Disease and Cancer Deaths—Trends and Projections in the United States, 1969–2020. Preventing chronic disease, 13.

DEXHELPP HEALTH CARE ATLAS OF AUSTRIA

Matthias Wastian[a], Matthias Rößler[b], Irene Hafner[c], Christoph Urach[d], Nadine Weibrecht[e], Niki Popper[f], Gottfried Endel[g], Michael Gyimesi[h]

[a],[b],[c],[d]dwh GmbH, Neustiftgasse 57-59. 1070 Vienna, Austria
[e],[f]DEXHELPP, Neustiftgasse 57-59. 1070 Vienna, Austria
[g]Main Association of Austrian Social Security Institutions, Haidingergasse 1. 1030 Vienna, Austria
[h]Gesundheit Österreich GmbH, Stubenring 6. 1010 Vienna, Austria
[a]matthias.wastian@dwh.at, [b]matthias.roessler@dwh.at, [c]irene.hafner@dwh.at, [d]christoph.urach@dwh.at
[e]nadine.weibrecht@dexhelpp.at, [f]niki.popper@dexhelpp.at
[g]gottfried.endel@sozialversicherung.at
[h]michael.gyimesi@goeg.at

ABSTRACT
Publicly available data that the Austrian medical associations of the nine Austrian provinces, the so-called Ärztekammern, publish on their respective home page gets scraped, processed and finally saved in a database on the DEXHELPP research server for further analyses. The processing is done in such a way that questions about the supply effectiveness of medical practitioners in Austria can be answered as comfortably as possible. The scraping is repeated periodically to facilitate carrying out a historiography and to investigate the chronological sequence of the answers to many questions of interest regarding the Austrian health care system. Results are published in the DEXHELPP health care atlas using dynamic and interactive D3 visualisations. Thus, the DEXHELPP health care atlas provides insights to local imbalances regarding for example specialisations, opening hours, sex or foreign languages offered by the Austrian medical practitioners. It will also be able to depict systemic changes over time.

Keywords: health care, Austria, data analysis, web scraping

1. INTRODUCTION

As many pieces of information about the Austrian health care system lie scattered on different web pages, the basic idea of the DEXHELPP health care atlas of Austria is to gather them, combine them in a database and analyse them automatically and repeatedly.
Questions that can be answered by database queries include, but are not restricted to:

- How many general practitioners are there in each district/province/Austria? How many of them have got a contract with one of the health insurances and how many do not?
- How many medical specialists are there in each district/province/Austria? How many of them have got a contract with one of the health insurances and how many do not have any?
- What is the female/male ratio of medical practitioners in Austria?
- Which foreign languages, diplomas, additional fields etc. do Austria's medical practitioners offer?
- Which opening hours are published by Austrian medical practitioners? Where is it possible to consult a medical practitioner on Fridays in the afternoon or on the weekend?
- How many contracts with which health insurance do exist?
- What is the proportion of medical practitioners with (panel doctors) and without contracts (private consultants) with any health insurance? What is the proportion of their published opening hours?

The database structure can be seen in figure 1 below.

2. DATA SCRAPING

The database which is used for all the further analyses was retrieved from the openly accessible websites of the medical associations, the so-called Ärztekammern, from all the Austrian provinces since January 2017. A separate scraping algorithm for every province had to be created, as the structure of the websites for the 9 associations differ greatly. The data available on the websites is mostly the same with some details that are different (e.g. office hours are provided in some tabular format in most provinces but can also be in textual form in others), and some data that is not available for certain districts (e.g. data on gender, either explicitly or by a sex-related identifier, is not available in all provinces). The scraping was performed with Selenium (Garg 2014) and resulted in hierarchically structured xml files. As already pointed out, the data retrieval is repeated once every month to allow future investigations regarding changes and trends of the Austrian health care system.

3. DATA PROCESSING

3.1. Sex Allocation

As there was a relevant number of medical practitioner without a specified sex or a sex-related identifier like 'Arzt' (male medical practitioner) and 'Ärztin' (female medical practitioner), we collected the set of all available pairs of first names and sexes that we had successfully scraped from the websites and checked if the sex allocation was unique. Only a single first name – Nikola – was assigned to both a man and a woman and therefore disregarded for further sex allocation.

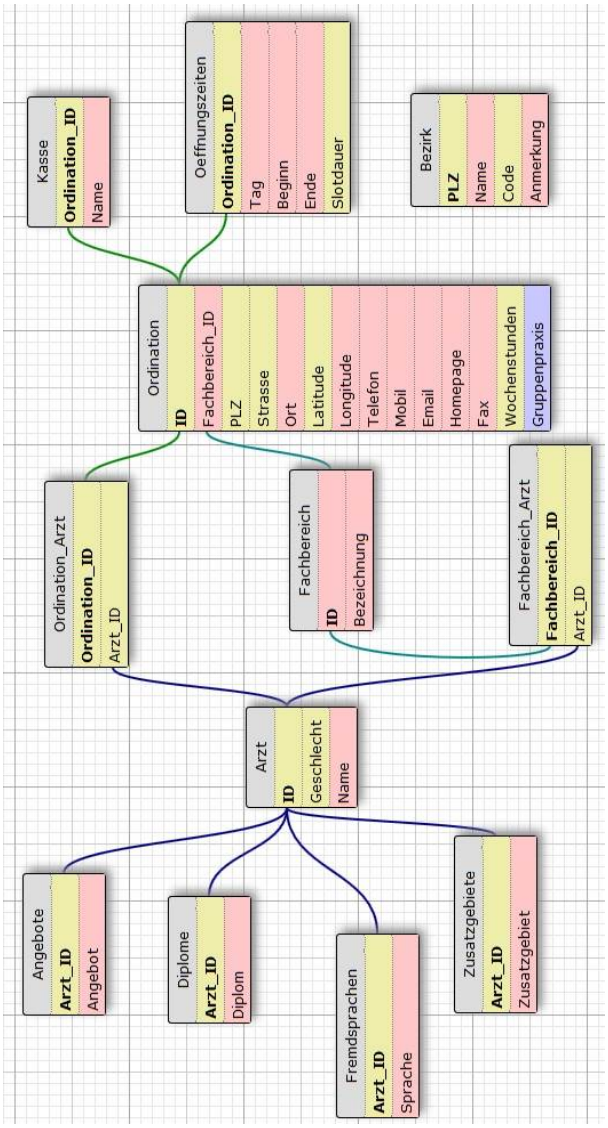

Figure 1: Database Structure

Some first names that were still missing but easily assignable to a specific sex were included into the allocation map by hard-coding (e.g. Jacob – male). This left the following first names unassigned due to a remaining uncertainty: Shamsalddin, Njegos, Kay, Paschoal, Micha, Michele, Orang and Ara. We also excluded names that contained any of the words 'Gruppenpraxis' (group practice), 'Teampraxis' (group practice), 'und' (and), 'Augenärzte' (eye specialists), 'GmbH' (limited liability company) or 'OG' (the German abbreviation for 'general partnership') from the sex allocation. In such a manner we were able to assign 1 136 previously missing sex attributes, leaving only very few entries without a specified sex.

3.2. Area of Expertise Allocation

Based on the scraped textual information about the areas of expertise of all medical practitioners that are presented on the websites of the Austrian medical associations, experts created an allocation map from the scraped texts to the predefined areas of expertise. This was done on the medical practitioner level as well as on the doctor's office level, where a medical practitioner can be connected to multiple special fields while an office cannot.

3.3. Contract Allocation

The scraped textual information about the existing contracts with health insurances is mapped to contracts with the project-relevant insurances BVA, GKK, SVA, SVB and VAEB.

3.4. Double Entries of Offices

According to the criterium that a medical practitioner cannot have more than one office with the same area of expertise and with the same kind of contract with health insurances at the same location, we checked for double entries of offices within our xml files. Such double entries occurred for example, if multiple free texts implying the same area of expertise were scraped (e.g. 'Neurologie und Psychiatrie' – neurology and psychiatry – and 'Psychiatrie und Neurologie' – psychiatry and neurology). By applying this checking routine, we could identify and ignored 105 double entries.

3.5. Handling of Group Practices

For some provinces like e.g. Lower Austria the information whether a certain medical practitioner works in a group practice or not was provided directly on the website. E.g. in Vienna we made use of additional textual information provided on the website (For example 'Doctor John Smith shares a group practice with doctor Max Mustermann.'). Whenever the group practice was already split into entries belonging to several medical practitioners and different opening hours, this split was retained, and the group was treated like a set of offices.

3.6. Office Hours

Most of the 9 Austrian provinces provide the office hours for doctors' offices in a tabular format that is quite easily readable and convertible. But the websites of Vorarlberg and Tyrol only provide free text similar to the German equivalent of 'Monday 8-11 and 13-16; Thu 12-14.' By using regex (Goyvaerts 2006), distinct time slots were separated and transformed into a machine-readable format. E.g., the regular expression

((?:täglich|Mo(?:ntag)?|Di(?:enstag)?|Mi(?:ttwoch)?|Do(?:nnerstag)?|Fr(?:eitag)?|Sa(?:mstag)?|So(?:nntag)?)(?:Mo(?:ntag)?|Di(?:enstag)?|Mi(?:ttwoch)?|Do(?:nnerstag)?|Fr(?:eitag)?|Sa(?:mstag)?|So(?:nntag)?|Feiertag(?:e)?|\\s|,|;|\\+|und|\\-|von|bis|\\:|v\\.|u\\.|\\.)*\\d(?:\\d|\\-|\\.|\\:|Uhr|u\\.|und|bis|\\+|\\s|,|;|u|sowie)*)

was the basis for the extraction of the time slots of the office hours. Since some of the office hours are provided in free text form, it is almost impossible to automatically detect and represent all of them in an adequate mathematical manner. We decided to consider only office slots that were provided with both a start and an end time – time specifications like 'ab 17:00' (i.e. 'from 5pm') were not considered for further analyses – as well as to ignore time specifications with the annex 'nach Vereinbarung' (i.e. on appointment). A standard week is used in our current data model. Thus, neither holidays nor expressions like "17-18 on every second Friday during the winter season" are considered.
A correctness check was applied on the gathered time slots: We decided to consciously ignore 18 provided office hours, because the start or the end time included a clear typo (e.g. 07:00-110:00 or 15-10) or was specified to be midnight. The latter only occurred in Lower Austria, indicating that midnight is an internal default value.

4. DATA ANALYSIS

The collected data includes 17 710 medical practitioners with 21 943 offices in Austria. 7 452 medical practitioners possess at least one contract with a §2 health insurance (Gebietskrankenkasse) or a nationwide health insurance, 10 258 do not have such a contract. 7 528 offices contracted with the BVA, 7 248 with the SVA, 7 411 with the VAEB and – according to the database – 4 069 with the SVB. The latter number is considerably less than the other numbers due to the fact that not all the medical associations explicitly list contracts with the SVB: Burgenland, Styria, Vienna and Vorarlberg do not list the SVB at all, Lower Austria and Tyrol indicate only very few contracts with it.
Opening hours are available for 7 551 out of 7 755 offices with a health insurance contract, while 4 055 of 14 188 offices of private consultants are provided with opening hours. The maximum opening time is 84 hours per week, the minimum 0.5 hours. Panel doctors specify 154 280.9 total opening hours per week, in contrast to 53 825.15 total weekly opening hours of private consultants. The average opening time of panel doctors that indicate opening hours amounts to 20.43 weekly hours, the corresponding average opening time of private consultants is 13.27 hours.
The recorded medical practitioners work in 36 different areas of expertise or are assigned to an unknown or a miscellaneous category. The only recorded area of expertise that does not provide any meaningful information is dentistry, oral medicine and orthodontics, as it is only stated with Carinthian doctors as a secondary discipline. This is due to the fact that in Austria dentists are organized in another association than the other medical professionals. An excerpt of this analysis can be seen in table 1.

Table 1: Excerpt of the distribution of Austrian medical practitioners with respect to their area of expertise and contract type

Area of expertise	Panel doctor	Private consultant
General practitioners	3 955	4 405
Internists	515	1 398
Gynaecologists	446	904
Otorhinolaryngologists	245	216
Radiologists	236	183
Psychiatrists	89	528
Virologists	0	1

5. VISUALISATION RESULTS

The visualisation is carried out with D3 (Bostock et al. 2011), a JavaScript library for creating dynamic interactive data visualisations in web browsers.
In the first visualisation version we distinguished between three different contract types: contracts with the §2 health insurances – the so-called Gebietskrankenkassen (GKK), contracts with one of the health insurances BVA, SVA, SVB or VAEB but not with a GKK, and no contract with any of the named health insurances. The user can also switch between absolute and relative (that are per 100 000 inhabitants) values via a dropdown menu as well as between different areas of expertise and sex.
While most of the structural results are visualised as maps or as bar charts, most of the temporal results are presented as heat maps. For the moment, we stuck with the granularity on a provincial level, but all data is already mapped to the Austrian districts (Bezirke) and would therefore be easily visualisable. Furthermore, we used geocoding to gather the exact latitude and longitude of all offices and can use these for upcoming visualisations.
Almost all results presented in this paper refer to the data captured in June 2017, but we dispose of all the data from January 2017 till today on a monthly basis and plan to present visualisations that allow insights into systemic changes in the future. In general, darker colours indicate higher values.

5.1. Structural Results

Figures 2 and 3 show the distribution of the area of expertise among the male and female medical specialists in Austria. It stands out that the most prevalent specification among women is gynaecology while among men it is clearly internal medicine. Interestingly, the picture changes drastically when only looking at doctors with §2 contracts: Under this constraint, more women are oculists than gynaecologists.

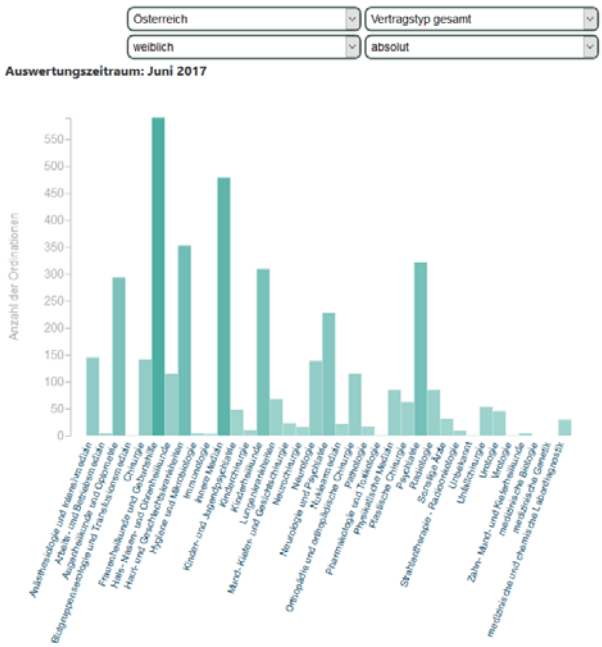

Figure 2: Female Medical Specialists by Expertise

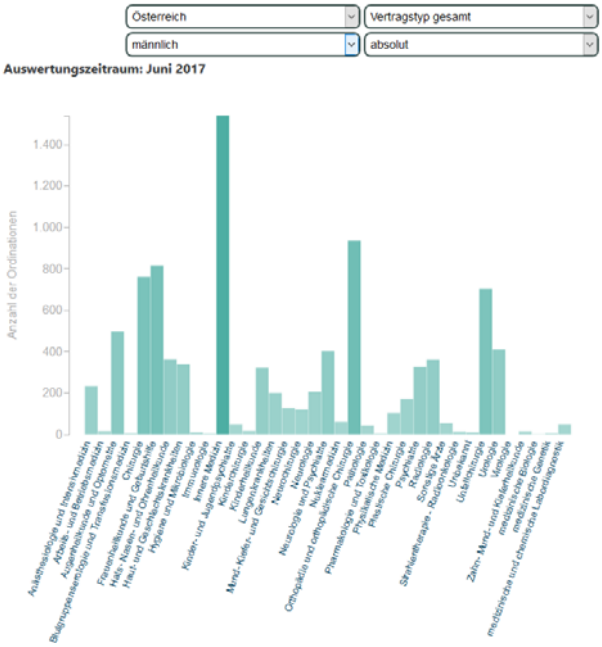

Figure 3: Male Medical Specialists by Expertise

When looking at the differences between the geographic distributions of general practitioners with a contract with a GKK in Austria per 100 000 inhabitants with respect to their sex by comparing the visualisations in figures 4 and 5, a clear east-west decline can be noticed: While Vorarlberg and Tyrol in the west exhibit the lowest relative female numbers, it is remarkable that the relative numbers in Lower Austria are the highest for both sexes and that Vienna is the only province that gets very close to a gender balance (21 offices are run by male, 20 offices run by female general practitioners.).

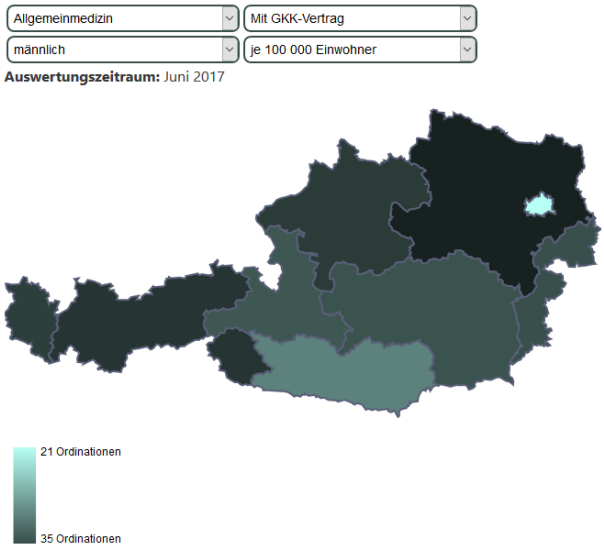

Figure 4: Male General Practitioners with a §2 Contract per 100 000 Inhabitants

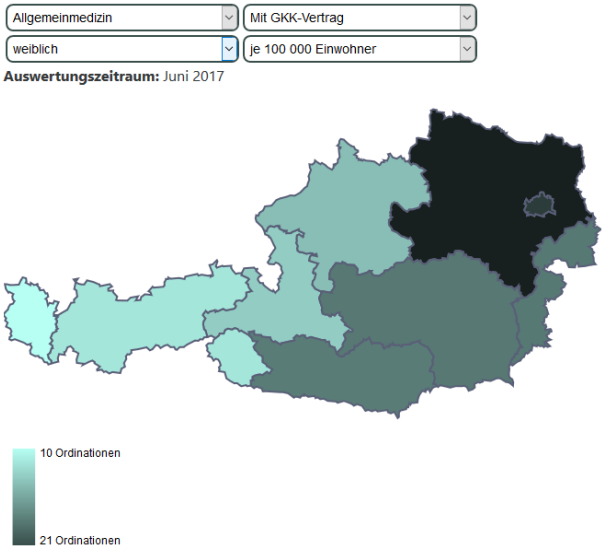

Figure 5: Female General Practitioners with a §2 Contract per 100 000 Inhabitants

Figures 6 and 7 show a comparison between the relative numbers of gynaecologists with a contract with a GKK and without any contract. While the numbers of those gynaecologists without a contract with any of the big Austrian health insurances is more or less double in all the provinces, it can easily be seen that people living in Vorarlberg have the most GKK-gynaecologists per person available. Salzburg and Vienna show the highest relative numbers of gynaecologists in general.
Additionally, some of the possible interactivity with the visualisations of the DEXHELPP health care atlas of Austria is shown in these figures: During a mouseover event the colour of the selected province changes to blue and the exact number of offices is displayed together with the name of the province (in this case Upper Austria – Oberösterreich).

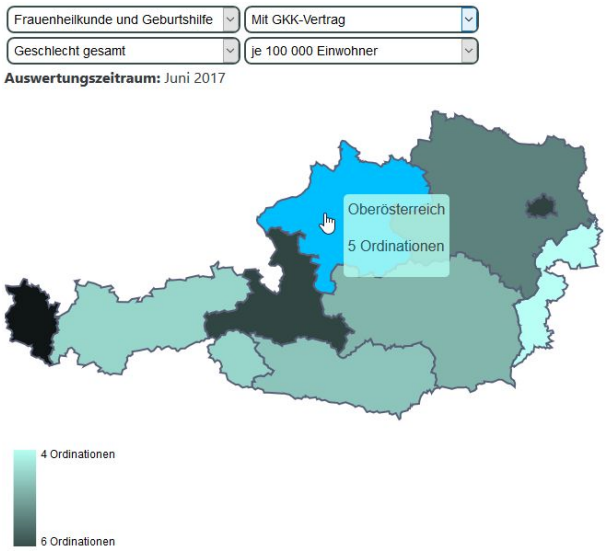

Figure 6: Gynaecologists with a §2 Contract per 100 000 Inhabitants

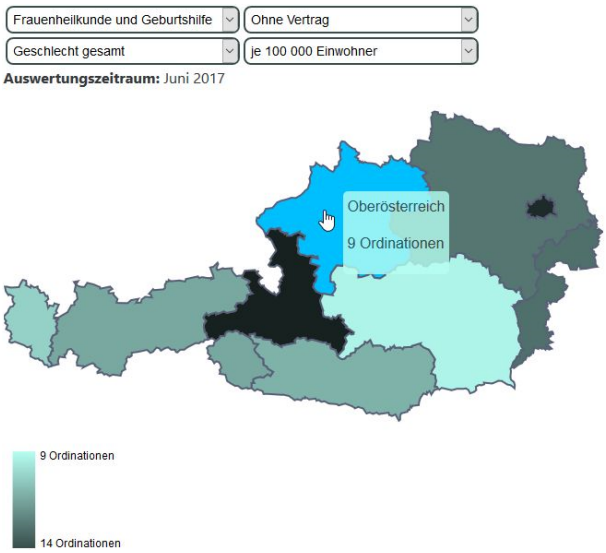

Figure 7: Gynaecologists without a Contract with a Big Austrian Health Insurance per 100 000 Inhabitants

As a final structural result, we show that very rare areas of expertise like medical genetics are agglomerated in Vienna, just as expected because Vienna is Austria's only megacity. For example, the offices of all 4 geneticists registered at the Austrian medical associations are located in the Austrian capital (shown in figure 8).

5.2. Temporal Results

Regarding the working hours of Austrian medical practitioners, a main research question was if the rising number of private consultants coincides with a rise in the corresponding working hours. In June 2017, the Austrian medical associations registered 7 452 medical practitioners with at least one contract with one of the 5 big health insurances and 10 258 without such a contract. However, regarding the published working hours, the 10 258 doctors without a contract only sum up to 25.86% of the 208 106 published working hours per week. The corresponding pie chart is shown in figure 9.

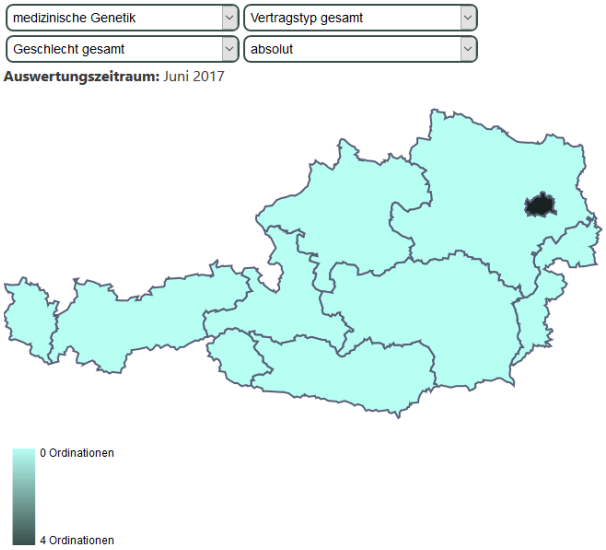

Figure 8: Medical Geneticists in Austria

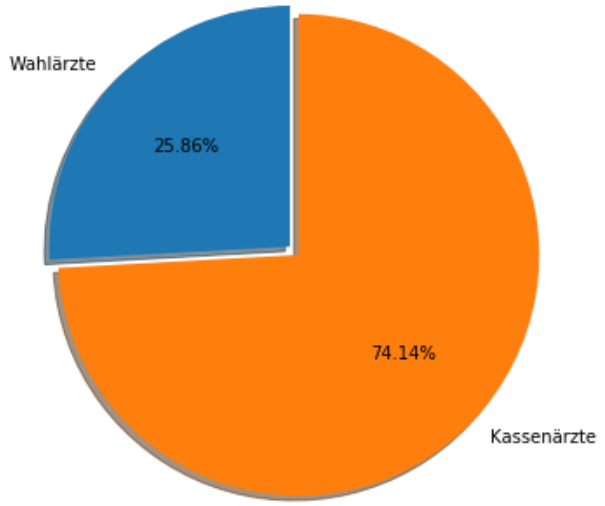

Figure 9: Ratio of Working Hours of Panel Doctors (Kassenärzte) and Private Consultants (Wahlärzte), April 2018

We have identified three main reasons leading to this result:

- The average weekly opening hours of private consultants – if published – are significantly lower (13.27 in contrast to 20.43). In fact, Austrian panel doctors are obliged by their contracts to open their offices at least 20 hours per week, private consultants are not.
- Private consultants offer their services more likely based on appointments than at fixed times.
- Private consultants are much less likely to publish any office hours at all. In our model we

could only consider office hours of a little bit more than 28.5% of all private consultants.

Another interesting temporal result is shown in figure 10: When comparing the heat maps of the office hours of general practitioners in Vienna and Lower Austria, the clear shift from the antemeridian focus in Lower Austria to the postmeridian focus in Vienna becomes visible. Many general practitioners in the Austrian capital open their offices on Monday afternoons.

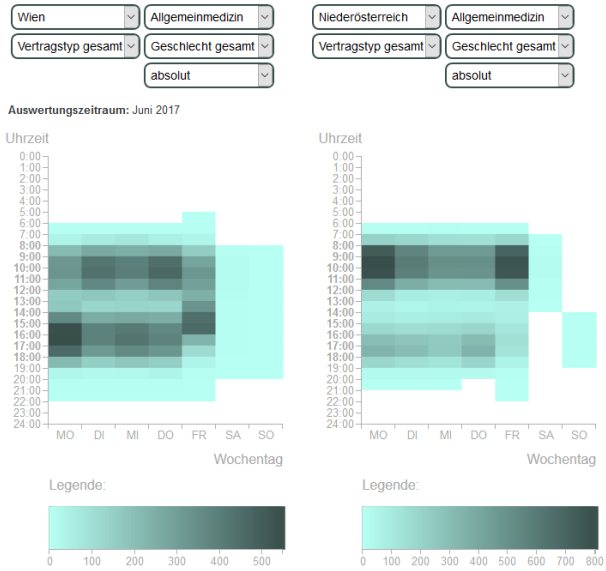

Figure 10: Office Hours Comparison of General Practitioners in Vienna and Lower Austria

Regardless of the fact that Vienna disposes of many offices of private gynaecologists per 100 000 inhabitants (see figure 7), the following comparison in figure 11 shows that the Styrian equivalents indicate more office hours at the scraped webpages.

Our health care atlas also provides the possibility to conduct a detailed analysis of a specific time slot as shown in figure 12: Day and time in the heat map of the office hours of all Austrian radiologists are selectable by a mouse click that leads to additional bar charts. These allow to compare the specified time slot with other time slots of the same week day as well as to compare it with the same time slot on the other days of the week.

The DEXHELPP health care atlas of Austria can be openly accessed via:

http://www.dexhelpp.at/de/versorgungsatlas/

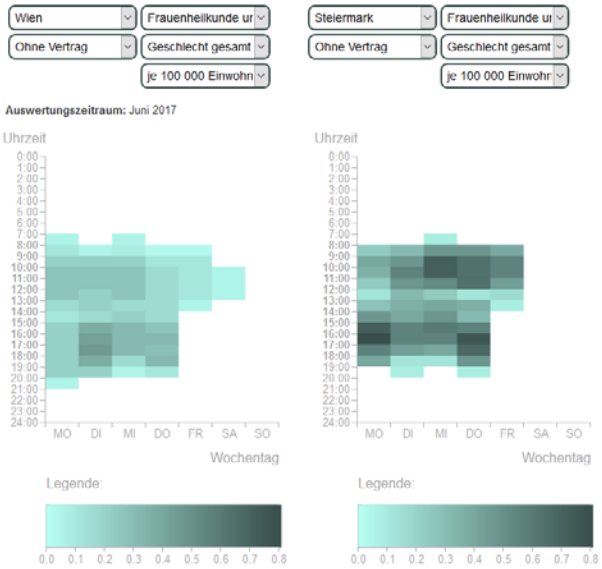

Figure 11: Comparison of Office Hours per 100 000 Inhabitants of Gynaecologists without a Contract with a Big Austrian Health Insurance in Vienna and Styria

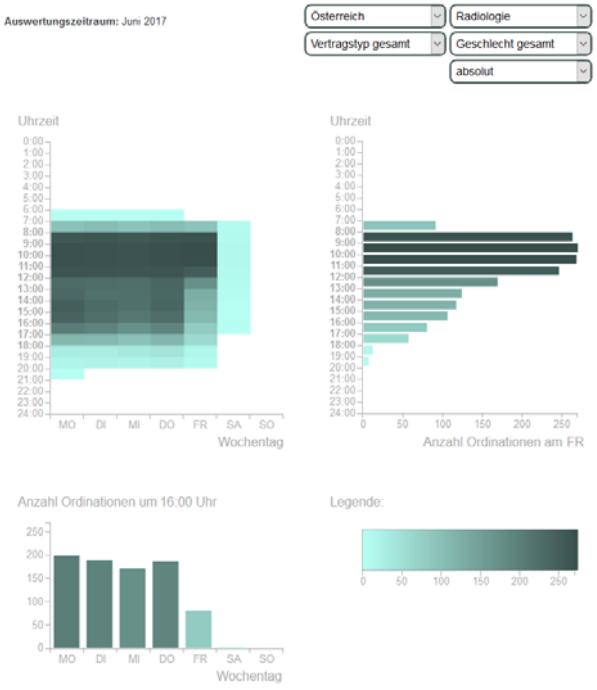

Figure 12: Detailed Analysis of Radiologists' Office Hours, Focusing on Friday 4pm.

REFERENCES

Bostock M., Ogievetsky V., Heer J., 2011. D3: Data-Driven Documents. IEEE Transactions on Visualization and Computer Graphics 17(12): 2301-2309.

Garg N., 2014. Test Automation using Selenium WebDriver with Java: Step by Step Guide. AdactIn Group Pty Ltd.

Goyvaerts J., 2006. Regular Expressions: The Complete Tutorial. Published at http://www.regular-expressions.info/print.html.

THE ASSOCIATION OF DEMOGRAPHIC AND HEALTH FACTORS WITH WORKING CAPABILITY IN ELDERLY

Laura Aponte-Becerra, M.D.[(a)(1)], Antonio Padovano[(b)(1)], Francesco Longo, PhD.[(b)], Vasileios-Arsenios Lioutas, M.D.[(a)], Peter Novak, M.D., Ph.D.[(c)], Long Ngo, Ph.D.[(d)], Regina McGlinchey, PhD.[(g)], Catherine Fortier, PhD.[(g)], Vera Novak, Ph.D., M.D.[(a)].

[(a)] Department of Neurology, Beth Israel Deaconess Medical Center, Harvard Medical School. Boston, MA., USA
[(b)] Department of Mechanical, Energy and Management Engineering (DIMEG), University of Calabria, Arcavacata di Rende (CS), Italy
[(c)] Autonomic Laboratory, Department of Neurology, Brigham and Women's Faulkner Hospital, Harvard Medical School, Boston, MA., USA
[(d)] Division of General Medicine and Primary Care, Beth Israel Deaconess Medical Center, Harvard Medical School, Boston, MA., USA
[(f)] Translational Research Center for TBI and Stress Disorders (TRACTS) and Geriatric Research Education and Clinical Center (GRECC), VA Boston Healthcare System, Boston, MA., USA.

[(a)]laponte@bidmc.harvard.edu, [(b)]antonio.padovano@unical.it,[(b)]f.longo@unical.it,[(a)]vlioutas@bidmc.harvard.edu, [(c)]pnovak2@bwh.harvard.edu, [(d)]lngo@bidmc.harvard.edu, [(f)]regina_mcglinchey@hms.harvard.edu, [(f)]catherine_fortier@hms.harvard.edu, [(a)]vnovak@bidmc.harvard.edu,

[(1)] These authors contributed equally to this article.

ABSTRACT
With an aging work-force, factors determining working capability, such as cognitive functions or communication skills, need to be assessed precisely. We addressed the gap of current knowledge based on self-rated measures by using objective measures and standardized questionnaires. Cross-sectional analysis included baseline data from the Memory Advancement by Intranasal Insulin in Type 2 Diabetes trial (MemAID), which consisted of 168 subjects, 84 men, 67.6±9.05 years old (mean ±SD), 44% diabetic, and 78 currently working. The subjects' working status, demographic characteristics, health factors – including body mass index, hemoglobin A1c (HbA1c - a measure of insulin resistance), number of co-morbidities – and a set of objective measures of their health status – including cognitive speed processing, visual learning, memory, walking speed, depression, and disability scores – were analyzed to detect relevant associations, which were then used to construct a logistic regression model aimed to determine significant determinants of the probability of working in older adults (≥50 years of age). Results show that hemoglobin A1c and normal walking speed have a strong association with the probability of working in older adults.

Keywords: aging, job performance, medical history, health, cognition, walking speed, diabetes

1. INTRODUCTION

The number and proportion of elderly workers is increasing steadily (Pit et al., 2010). Therefore, it is important to determine the impact of aging and co-morbidities on working capability and potential job performance. In the United States, 17.5% of employed civilian labor force is older than sixty years (American Bureau of Labor Statistics, 2017). It is expected that people older than 55 years will comprise at least 25% of workforce in the US (Toossi, 2012), UK, and European countries (Anxo et al., 2012). A decline of cognitive and executive functions with aging (Rabbitt and Lowe, 2000) may negatively impact effectiveness of "real-world functioning" (Salthouse, 2012). However, skills based upon accumulated knowledge tend to remain relatively robust over the life cycle (Skirbekk, 2008). Health risk factors and co-morbidities may further affect job performance (Lee et al., 2018). A greater absenteeism and presenteeism was observed in employees with more severe health risks i.e. poor diet, abnormal body mass index (BMI), high cholesterol, physical inactivity, excessive stress, lack of emotional fulfillment, high blood pressure, diabetes, tobacco use, and alcohol abuse (Boles et al. (2004). Work functioning (assessed through a questionnaire on 622 workers) was significantly lower in obese as compared to overweight and normal weight workers (Nigatu et al. 2016).

Diabetes has a significant impact on many aspects of life and its prevalence is steadily rising across various age groups. Diabetes complications may prevent working entirely, increase absenteeism (Julius et al., 1993), or diminish productivity at work (Lavigne et al., 2003). Both diabetes and impaired glucose tolerance (or higher insulin resistance) were associated with subjective depression and cognitive decline and worse functionality at work (Lee et al. 2018). Hemoglobin A1c (HbA1c) is an indicator of long-term insulin resistance and pre-diabetes. When monitoring diabetic subjects, HbA1c is the preferred marker of long-term glycemic control (Stratton et al. 2000).

Factors affecting job performance have been investigated in several work domains (Kyriakidis et al., 2015) and human factors models have been proposed in industrial and business processes (Bruzzone et al., 2007). A comprehensive list (Kim & Jung 2003) was compiled, for instance, for human reliability analysis of emergency tasks in nuclear power plants. In this study, self-rated factors include cognitive (e.g. attention, intelligence), physical (e.g. disabilities), and psychological measures (e.g. clarity in speaking). However, an objective quantitative approach

of these factors and its relation with the probability of working is currently lacking. Factors are often assessed with subjective questionnaires, interviews, or self-rated scales, thus lacking the implementation of objective and scientific methodologies. Therefore, we used validated medical tests combined with standardized questionnaires to quantify factors that are considered crucial for any type of worker. In summary, physical and psychological impairments correlate with unfavorable work outcomes, absenteeism, presenteeism, and errors, which are the main markers of job performance (Iverson et al., 2010).

The aim of this study was to assess the association among demographic characteristics, medical history variables (such as body mass index, HbA1c and number of co-morbidities) and a set of objective measures of the factors influencing work capability (including cognitive speed processing, visual learning, memory, walking speed, depression, and disability scores) with the probability that subjects older than 50 years are currently working. To this end, a preliminary analysis is performed to determine associations among demographic characteristics, medical histories and health status variables assessed by objective medical measures and standardized questionnaires in elderly people.

We analyzed baseline data of participants in the Memory Advancement by Intranasal Insulin in Type 2 Diabetes (MemAID) trial. MemAID is a five year, randomized, double-blinded, controlled clinical trial (ClinicalTrials.gov NCT02415556) conducted at the Syncope and Falls in the Elderly (SAFE) Laboratory and the Clinical Research Center (CRC) at the Beth Israel Deaconess Medical Center (BIDMC). Eligible participants signed an informed consent approved by the BIDMC Committee on Clinical Investigations, and were enrolled. MemAID aims to determine the long-term effects of 40 international units (IU) of intranasal insulin (Novolin® Novo Nordisk, Inc. Bagsvaerd, Denmark) as compared to placebo (sterile saline) on cognition and memory when administered once daily over 24 weeks with 24 weeks of follow-up in older diabetic and non-diabetic adults.

The trial is taking place in the Greater Boston Area and the inclusion criteria are: men and women between 50 and 85 years old with the ability to walk for six minutes, and either diagnosed type 2 diabetes (T2DM) treated with non-insulin agents or non-diabetic controls. At the baseline assessment, medical history and fasting laboratory samples were collected, and neurocognitive and gait tests were conducted. We cross-sectionally analyzed data of 168 subjects who were enrolled, randomized, and completed baseline assessment by May 2018. This sample includes subjects with a mean age of 67.65 years (SD±9.05), 78 of which are currently working and 90 subjects not working. Demographic, medical history, and health status variables and questionnaires at baseline are available for every subject.

2. METHODS

2.1. Selection of the factors associated to the job performance latent construct

The MemAID sample includes workers from different domains, with different skills, working capability and employment status. We were able to classify them according to the International Standard Classification of Occupations (ISCO-08) in more than six broad categories, including managers, professionals, technicians, clerical workers, service and sales workers, and craft and related trades workers. Due to the heterogeneity of occupations, job performance could not be uniquely and quantitatively defined. Furthermore, Standard classification of employment status (i.e. retired, employed, unemployed, and homemaker) was not used in this study, because it is not a reliable equivalent of the capability of working in people older than 50 years. For example, a retired person may continue to work or an unemployed individual may have an informal job. Besides their employment status, subjects were then asked "Do you currently work either paid, non.-paid or self-employed?" during the implementation of WHODAS questionnaire and their response was used to classify working status. Frequencies of people working and not working by employment status in our sample reported in Table 1 shows that working status classification is indeed a more reliable indicator than an employment status classification.

Table 1. Employment Status vs. Working Status

Working Status / Employment status	Yes	No
Retired	24	66
Employed	50	3
Unemployed	3	17
Homemaker	1	4

In order to identify a set of potential etiologic factors and health-related determinants of job performance, we refer to it as a "latent construct" to indicate that job performance is a measure that is not observable because no specific job is defined (Campbell et al., 1990) but it can be inferred from other variables. For the purpose of this analysis, the following set of factors determining working capability has been considered:

1. Cognitive factors, such as attention, reasoning, and memory.
2. Teamwork-related factors, such as communication and relationship skills.
3. Personality factors, representing worker's feelings and emotions.
4. Physical factors or mobility, such as the ability to walk and perform simple executive tasks.

2.2. Definition of objective medical measures and standardized questionnaires used to assess factors determining working capability

In order to objectively assess and determine the factors mentioned above, validated standardized methods and tools have been used in this study:

- *Mini-mental state examination (MMSE):* an 11-question measure that tests 5 areas of cognitive function: orientation, registration, attention and calculation, recall, and language. The maximum score is 30. A score of 23 or lower is indicative of cognitive impairment. (Tangalos, E.G. et al. 1996)

- *World Health Organization Disability Assessment Schedule (WHODAS 2.0):* an aggregated score of the level of health, disability, and functioning difficulties experienced by the respondents in six domains of life (understanding and communicating, getting around, self-care, getting along with people, life activities, and participation in society) during the 30 days prior to implementing the questionnaire (Üstün, T. B. 2010). WHODAS also includes three variables that are considered of great interest for their potential impact on job performance:
    - The number of days that the subjects identified difficulties,
    - The number of days that the subjects were unable to carry out usual activities or work due to any health condition,
    - The number of days that the subjects cut back or reduced usual activities or work because of any health condition.
- *Geriatric depression scale (GDS):* A screening test for depression in elderly populations (Yesavage, J. A. 1982). Score goes from 0-30; where 0-9 is normal, 10-19 indicates mild depression, and 20-30 severe depression.
- *Cambridge automated neuropsychological test battery (CANTAB) version 7.0:* the following main variables have been considered:
    - Spatial working memory (SWM): requires retention and manipulation of visuospatial information with executive function demands (Benedict et al. 1996). The outcome measure is named "Between errors", meaning the number of times that the subject executes an error in succession; the lower the number is, the better.
    - Paired associate learning (PAL): assesses visual learning with one trial representation (Rabbitt and Lowe 2000). The outcome measure is named "first trial memory score", meaning the number of patterns correctly located immediately after the first trial, summed across the stages that the subject completes throughout this section; the higher the number is, the better.
    - Verbal memory (named in CANTAB as VRM): measures the ability to encode and subsequently retrieve verbal information. The outcome measure is named as "free-recall total correct", meaning the total number of distinct words correctly recalled; higher is better.
    - Rapid visual information processing (RVP): assesses sustained attention and processing speed (Soares et al. 2015). The outcome measure is named as "RVP mean latency", which details the mean time taken to respond correctly and is reported in milliseconds; lower is better.
- *Mobility Lab System (APDM, Inc., Portland, OR.):* measures gait speed during 6 min walking at usual pace (Normal Walk, NW) (Steffen T.M. 2002) and 6 min walking while counting numbers backward subtracting 7 (Dual-Task, DT). These measures were used as markers of their physical state.

2.3. Selected demographic characteristics and medical history variables

For the purpose of the present analysis, the demographic characteristics considered are the following:

- *Sex*: male and female.
- *Race*: white, African-American, Asian, and other.
- *Age:* young-old (<65 years) and old-old (≥65 years).
- *Education:* high-school (0-12 years of school), undergraduate (13-16 years of school), graduate (17-18 years of school), doctoral (> 18 years of school).

Medical history variables were:

- *Body mass index* (BMI, kg/m^2): underweight (<18.5), normal weight (18.5 - < 25), overweight (25 - < 30), obese (≥ 30).
- *Diagnosis of diabetes*: subjects were classified as no diabetes, pre-diabetes, and T2DM based on diagnosis and HbA1c levels (American Diabetes Association's classification guidelines - 2018).
- *Co-morbidities categories*: Classification of co-morbidities was done as using a self-reported medical history, which was verified when possible. Diagnoses and/or chief complaints were counted in each of the following categories: neurological, cardiovascular, musculoskeletal, sensorial, gastrointestinal, hemato-oncological, respiratory, unconsciousness, falls, psychiatric, genitourinary, extremities, and endocrine (other than diabetes) (Palmer et al. 2008). The number of affected categories was further grouped as less than three, three-to-five, and more than five.

2.4. Statistical analysis

Data analysis was done using SAS 9.4.

A preliminary analysis of the associations was performed by a non-parametric Kruskal-Wallis test, which has been used to determine whether there is a statistically significant difference (and therefore whether an association exists) between the median of all the variables considered with the working status of the subjects in the study. The same test was then used:

- To assess whether there is a statistically significant difference among the medians of medical variables in groups of subjects classified by demographic characteristics: Age (young-old and old-old); Race (White, African-American, Asian and other); Sex (male and female), Education level (high-school, undergraduate, graduate, doctoral).
- To assess whether there is a statistically significant difference among the medians of health status variables in groups of subjects with different medical history: BMI (underweight, normal weight, overweight, obese); diagnosis of diabetes (no diabetes, pre-diabetes, and T2DM); affected

comorbidity categories (less than 3, between 3 and 5, more than 5).

As subjects' statements to current working status is expressed as a binary response ("Yes" or "No"), binary logistic regression was used to assess relationship (if any) between this binary response and a set of explanatory variables. The probability of the event Working Status = "Yes" is modeled. The LOGISTIC procedure used in SAS fits linear logistic regression models for discrete response data by the method of maximum likelihood, using the Fisher scoring algorithm. Based on the significant associations established through the non-parametric tests, we modeled the probability of working using the following parameters:

- People classified by age, as Young-old vs. Old-old (i.e. <65 and ≥ 65, respectively);
- Years of school completed;
- Medical history variables: BMI and HbA1c;
- Relevant measures of factors influencing working capability: WHODAS total score for team-work related and personality factors, VRM free recall total correct as a cognitive factor and NW gait speed as physical factor.

Significance level of the factors and odds ratios estimates were calculated in order to offer further insights about the potential association of these variables with the subjects' working status and their capability to predict it.

3. RESULTS

Table 2 reports a descriptive summary (frequencies, mean, standard deviation, confidence interval with alpha = 0.05, minimum and maximum value) of the demographic characteristics, health factors and measures of factors determining working capability of our sample, classified by working status. Significant differences found in non-parametric tests between the means of the demographics, health variables and factors influencing working capability among subjects working and not working, are also reported (p-value ≤ 0.05).

Different prevalence of the diagnoses or chief complaints by affected health system were observed; being the cardiovascular system the most commonly affected (71%) and the respiratory system the least commonly affected (11%) in our study sample.

Non-parametric tests comparing people with different working status has shown that:

- Education level was significantly different by one year of schooling between people who are working and those who are not working.
- People who are working have lower HbA1c (6.02% vs. 6.53%) compared to those who are not working.
- Slower gait speed and higher number of days unable to do activities were observed in people who are not working.

Comparing the differences among health status by demographic characteristics (Table 3) has shown that:

- BMI was higher in African-American people (mean=31.48) compared to White people (mean=28.46) and Asian (mean=23.5). BMI was also significantly higher in Young-old people (mean=30.13) compared to Old-old subjects (mean=27.85).
- The number of affected comorbidity categories differed by race. African-American people reported on average less affected comorbidity categories (mean=2.34) compared to White (mean=4.09) and Asian (mean=4.00) subjects. The number of affected comorbidity categories was also different between age categories (young-old subjects reported 3.17 Young-old and Old-old (3.17vs.4.41).
- HbA1c was significantly different in subjects with different education level. Subjects with high-school education showed HbA1c of 6.99% compared to subjects with higher education (undergraduates 6.22%, graduates 6.00%, doctoral level 6.15%).

Non-parametric tests to assess differences in measures of current factors influencing working capability by health status have shown that:

- RVP Mean Latency, NW Gait Speed, WHODAS Total Score, days with difficulties, days cut back on activities, and the days unable to do activities were different by BMI categories. We observed that obese and underweight subjects had the lowest performance (higher RVP mean latency, slower NW gait speed, more days with difficulties, cut back on activities and unable to do activities), followed by overweight people. Normal weight subjects had the best performance on measures of factors influencing working capability.
- The HbA1c or T2DM diagnoses affect significantly several factors influencing working capability. Diabetics had lower performance (e.g. higher GDS total score, higher RVP mean latency, lower PAL first trial memory score, lower VRM free recall total correct, slower NW gait speed, higher number of days with difficulties, cut back on activities and unable to do activities) compared to people with pre-diabetes or without diabetes.
- Measures of factors influencing working capability: differed significantly according to the affected co-morbidity categories. Subjects who reported more than five affected categories had higher total GDS score, higher RVP mean latency, slower gait speed (both NW and DT) and more days with difficulties, cut back on activities and unable to do activities.

These results suggest that medical history and the current health status have significant influence on working capability.

Table 2. Demographics, health status variables and factors influencing working capability in by working vs. non-working groups

Variable	Statistic	Total	Working	Nonworking	p-value
Sex	N - Men	84	41	43	-
	N - Women	84	37	47	
Race	N - White	130	60	70	-
	N - AfricanAmerican	29	14	15	
	N - Asian	4	2	2	
	N - Other	5	2	3	
Age (categorical)	N - Young-old	83	45	38	-
	N - Old-old	85	33	52	
Age (continuous)	Mean ± SD	65.67 ± 9.05	64.36 ± 8.78	66.80 ± 9.17	0.09
	Min - Max	50.00 – 84.00	50.00 - 84.00	50.00 - 84.00	
Education (categorical)	N - High school	28	8	20	-
	N - Undergraduate	68	32	36	
	N - Graduate	31	14	17	
	N - Doctoral	41	24	17	
Education (continuous)	Mean ± SD	16.21 ± 3.38	16.85 ± 3.41	15.67 ± 3.28	**0.03**
	Min - Max	8.00 – 28.00	10.00 – 28.00	8.00 – 26.00	
BMI (categorical)	N - Underweight	2	1	1	-
	N - Normal Weight	42	16	26	
	N - Overweight	62	35	27	
	N - Obese	62	26	36	
BMI (continuous)	Mean ± SD	28.98 ± 5.90	29.04 ± 6.03	28.92 ± 5.82	0.98
	Min - Max	17.50 – 48.00	17.60 – 44.70	17.50 – 48.00	
Diagnosis of Diabetes (categorical)	N - No Diabetes	53	31	22	-
	N - Pre-diabetes	41	22	19	
	N - Diabetes	74	25	49	
Hemoglobin A1c (%)	Mean ± SD	6.29 ± 1.20	6.02 ± 0.87	6.53 ± 1.38	**0.01**
	Min - Max	4.90 - 11.20	4.90 – 10.10	5.00 – 11.20	
Affected Comorbidity Categories (categorical)	N - Less than 3	65	33	32	-
	N - From 3 to 5	59	27	32	
	N - More than 5	44	18	26	
Affected Comorbidity Categories (continuous)	Mean ± SD	3.80 ± 2.63	3.50 ± 2.43	4.06 ± 2.79	0.23
	Min - Max	0.00 – 11.00	0.00 – 11.00	0.00 – 10.00	
MMSE	Mean ± SD	28.27 ± 1.81	28.41 ± 1.71	28.16 ± 1.90	0.56
	Min - Max	21.00 – 30.00	21.00 -30.00	23.00 – 30.00	
GDS Total Score	Mean ± SD	5.70 ± 5.51	5.55 ± 5.67	5.82 ± 5.40	0.56
	Min - Max	0.00 – 26.00	0.00 – 26.00	0.00 - 25.00	
RVP Mean Latency	Mean ± SD	551.28 ± 139.18	530.37 ± 151.54	569.39 ± 151.18	0.17
	Min - Max	319.20 - 967.67	320.78 – 894.47	319.20 - 967.67	
PAL First Trial Memory Score	Mean ± SD	9.26 ± 3.65	9.76 ± 3.90	8.82 ± 3.37	0.11
	Min - Max	0.00 – 19.00	2.00 – 19.00	0.00 – 17.00	
SWM Between Errors	Mean ± SD	20.59 ± 9.10	19.08 ± 9.63	21.90 ± 8.45	0.09
	Min - Max	0.00 - 40.00	0.00 -35.00	4.00 - 40.00	
VRM Free Recall - Total Correct	Mean ± SD	7.10 ± 1.98	7.04 ± 2.12	7.14 ± 1.86	0.77
	Min - Max	0.00 – 11.00	0.00 – 11.00	3.00 – 11.00	
NW Gait Speed	Mean ± SD	115.14 ± 22.12	120.58 ± 19.54	110.43 ± 23.22	**0.01**
	Min - Max	111.77 – 118.51	70.01 – 189.16	36.81 – 161.89	
DT Gait Speed	Mean ± SD	103.15 ± 23.71	107.77 ± 19.86	99.15 ± 26.05	**0.04**
	Min - Max	0.00 – 160.81	56.73 – 160.81	0.00 – 153.69	
WHODAS Total Score	Mean ± SD	15.78 ± 16.68	13.53 ± 15.11	17.73 ± 17.78	0.12
	Min - Max	0.00 – 88.00	0.00 – 61.00	0.00 - 88.00	
Days with Difficulties	Mean ± SD	6.18 ± 9.07	5.45 ± 8.59	6.81 ± 9.46	0.49
	Min - Max	0.00 – 30.00	0.00 – 30.00	0.00 – 30.00	
Days Unable to do Activities	Mean ± SD	1.65 ± 4.16	1.14 ± 3.73	2.09 ± 4.48	**0.02**
	Min - Max	0.00 – 24.00	0.00 – 20.00	0.00 – 24.00	
Days Cut Back on Activities	Mean ± SD	2.51 ± 4.70	1.87 ± 3.89	3.06 ± 5.27	0.19
	Min - Max	0.00 – 30.00	0.00 – 20.00	0.00 – 30.00	

SD = standard deviation; N = number of individuals; P-values were calculated by Kruskall-wallis non-parametric test of demographic factors, health status variables and factors influencing working capability by working status.

Table 3. Significant differences between the medians of the study variables

Health variables **Demographic Categories**	BMI (kg/m^2)	HgA1c (%)	Number of Affected Comorbidity Categories
Age	0.03	-	0.0015
Race	0.01	-	0.01
Sex	-	-	-
Education	-	0.01	-
Health variables **Indicators of working capability**	BMI classification	Diagnosis of Diabetes category	Affected Comorbidity Categories
MMSE	-	-	-
GDS Total Score	-	0.00	0.0001
RVP Mean latency	0.04	0.01	0.01
PAL First trial memory score	-	0.04	-
SWM Between errors	-	-	-
VRM FreeRecall/TotCorrect	-	0.01	-
NW Gait speed	0.003	0.02	0.001
DT Gait Speed	-	-	0.03
WHODAS Total Score	0.03	0.0049	0.0001
Days with Difficulties	0.02	0.0008	0.0001
Days Cut Back on Activities	0.001	0.01	0.0001
Days Unable to do Activities	0.0009	0.0019	0.0002

SD = standard deviation; N = number of individuals; P-values were calculated by Kruskall-wallis non-parametric test of health status variables by demographic factors and of factors influencing working capability by health variables categories.

In order to attain our primary aim, we used a binary logistic regression to model the probability that a subject answers “Yes” to the question "Do you currently work?”

Since we are dealing with continuous variables, odds ratios that are greater than 1 indicate that the event where working status is equal to “Yes” is more likely to occur as the predictor increases. Odds ratios that are less than 1 indicate that the event is less likely to occur as the predictor increases. In the case of the categorical variable, i.e. age, the odds ratio for the contrast between the categories will be provided.

Table 4 reports the P-value and odds ratio estimates for each variable in the model. Results suggest that the best predictors of an affirmative response of working status were HbA1c and normal walking speed (NW Gait Speed p-value < 0.05). The C statistic of this model is 0.71, meaning that the model predicts with a moderate level of discrimination.

Table 4. Maximum Likelihood Estimates of the probability of working

Effect	**P-value**	**Odds Ratio**
c = 0.707		
Age category	0.06	0.52
Education	0.13	1.08
BMI	0.13	1.05
Hemoglobin A1c	**0.01**	**0.62**
WHODAS Total Score	0.98	1.00
NW Gait Speed	**0.01**	**1.02**
VRM Free Recall/TotCorrect	0.10	0.86

- For every 1% increase in the HbA1c, we expect to see about 38% decrease in the odds of being employed when controlling for other factors in the model;
- For every 1 cm/s increase in NW Gait Speed, there is likely to be a 2.1% increase in the odds of been currently working when controlling for other factors in the model.

Please note that the p-value of the age category is “on the edge”, meaning that there is good chance that belonging to the young-old or old-old category has an impact on the working status. The odds ratio reported in Table 4 indicates that the odds of being currently working is almost 2 times higher for young-old subjects compared to old-old subjects.

4. DISCUSSION

This study has shown that HbA1c levels and normal walking speed were associated with the probability of working in older subjects with different demographic characteristics and medical history. HbA1c is a significant predictor of long-term complications of diabetes and it has been postulated as predictive of insulin resistance (Borai et al. 2011). This study showed that one percent increase in HbA1c would decrease the odds of working by 38%. These findings are clinically significant, because those people with pre-diabetes and diabetes are less likely to work, and the odds of working decline further for those with poorly controlled T2DM.

Gait speed is an important predictor of well-being in older adults. In our study, an increase of walking speed by 10 cm/s, would increase the probability of working by 2%.

A pooled analysis of over 34,000 community-dwelling subjects older than 65 years has shown increasing survival rates per 10 cm/sec increase of walking speed (Studenski et al.2011). The significance of gait speed as a measure of survival might also be extrapolated to the capability to handle activities of daily living, and in this case, to the probability of working in elderly people. Individuals with better results are expected to have a higher probability of working than people with worse scores.

Age can be also considered a relevant factor from a clinical point of view affecting the working status as the p-value is almost equal to 0.05. In the light of the difference between the working status and the employment status underlined at the beginning of the paper, this study shows that young-old subjects have a probability 2 times higher than old-old subjects of being currently working.

Our study also suggests that demographic factors, such as age, race, and education level are associated with BMI, HbA1c levels, and number of comorbidity categories. BMI and the number of affected comorbidity categories have been found to be higher in African-American people and in young-old subjects of our sample, while HbA1c level resulted to be higher in people with lower education level (high-school). Medical history variables were also associated with health status variables assessed by objective and standardized validated tools, such as cognitive processing speed, memory, visual learning, and mobility in terms of gait speed, depression, and disability scores. Subjects with higher BMI (obese or overweight), with a T2DM diagnosis or with a high number of self-reported affected comorbidity categories have been found to have lower performance in the validated medical tools used in this study.

Job performance is indeed a compound of diverse cognitive, physical, and psychological skills and is affected by demographic characteristics, medical history, and health conditions. Considering that health status differs among subjects with different race, age and education level, we conclude that health dissimilarities among people make it more likely to find significant differences in factors influencing job performance.

Therefore, models of working status and job performance should take workers' characteristics that are inherent to their daily living into account, including demographics, medical history, and health conditions. Research in human behavior modeling can benefit from these results, not only because standardized questionnaires and objective scientific measures are suggested to model factors affecting job performance, but also because it is distinctly shown that future models cannot disregard the role of demographics and medical history.

The variables collected in the context of the MemAID study represent quantitative data for a preliminary analysis of the association of demographic characteristics, medical history variables, health status variables and working status, however the lack of information about the subjects' occupation and direct measurements of effectivity and success in job performance is one of the limitations of this study. Linear assumptions made to apply the binary logistic regression model also represent another limitation of the present study. Indeed, we assume that the increase in the odds of being employed is linear when the factors considered increase. This is not generally applicable: anyway, the current model can provide valid and interesting insights in its current shape.

When assessing the study variables, further research initiatives are needed to determine the subgroups among categories, such as demographics, number of co-morbidities, BMI, and diagnosis of diabetes that perform differently and establish estimates for those differences. Furthermore, questions regarding the likelihood of improvements in job performance by achieving a better control of a subject's medical conditions and the applicability of survival measurements such as gait speed in occupational health rise from this study.

ACKNOWLEDGMENTS

The authors acknowledge the contributions of the research team at the Syncope and Falls in the Elderly (SAFE) Laboratory and the clinical research center nursing staff at Beth Israel Deaconess Medical Center. The Memory Advancement by Intranasal Insulin in .Type 2 Diabetes study is being conducted by Dr. Vera Novak as principal investigator, who received the grant from the NIH–National Institute of Diabetes and Digestive and Kidney Diseases (NIDDK) (1R01 DK103902-01A1). Supplemental funding was received from Novo Nordisk, Inc. Bagsvaerd, Denmark (ISS-001063), and Medtronic Inc. Minneapolis, MN USA (NERP15-031)). This work was conducted with support from Harvard Catalyst | The Harvard Clinical and Translational Science Center (National Center for Advancing Translational Sciences, National Institutes of Health Award UL 1TR002541, ULTR001102) and financial contributions from Harvard University and its affiliated academic healthcare centers. The content is solely the responsibility of the authors and does not necessarily represent the official views of Harvard Catalyst, Harvard University and its affiliated academic healthcare centers, or the National Institutes of Health.

REFERENCES

American Diabetes Association, 2018. 2. Classification and diagnosis of diabetes: standards of medical care in diabetes—2018. *Diabetes Care*, *41*(Supplement 1), pp.S13-S27.

American Diabetes Association, 2018. 11. Older adults: standards of medical care in diabetes—2018. *Diabetes care*, *41*(Supplement 1), pp.S119-S125.

Anxo, D., Ericson, T. and Jolivet, A., 2012. Working longer in European countries: underestimated and unexpected effects. *International Journal of Manpower*, *33*(6), pp.612-628.

Benedict, R. H., Schretlen, D., Groninger, L., Dobraski, M., & Shpritz, B. (1996). Revision of the Brief Visuospatial Memory Test: Studies of normal performance, reliability, and validity. *Psychological Assessment*, *8*(2), 145.

Borai, A., Livingstone, C., Abdelaal, F., Bawazeer, A., Keti, V., & Ferns, G. (2011). The relationship between glycosylated haemoglobin (HbA1c) and measures of insulin resistance across a range of glucose tolerance. *Scandinavian journal of clinical and laboratory investigation*, *71*(2), 168-172.

Bureau of Labor Statistics, U.S. Department of Labor. Labor Force Statistics from the Current Population Survey - Annual averages for 2017. On the Internet at [https://www.bls.gov/cps/demographics.htm]. Visited on August, 2018.

Boles, M., Pelletier, B. and Lynch, W., 2004. The relationship between health risks and work productivity. *Journal of Occupational and Environmental Medicine*, *46*(7), pp.737-745.

Bruzzone, A. G., Briano, E., Bocca, E., & Massei, M. (2007). Evaluation of the impact of different human factor models on industrial and business processes. *Simulation Modelling Practice and Theory*, 15(2), 199-218.

Campbell, J. P., McHenry, J. J., & Wise, L. L. (1990). Modeling job performance in a population of jobs. Personnel psychology, 43(2), 313-575.

Iverson, D., Lewis, K.L., Caputi, P. and Knospe, S., 2010. The cumulative impact and associated costs of multiple health conditions on employee productivity. *Journal of Occupational and Environmental Medicine*, *52*(12), pp.1206-1211.

Julius, U., Gross, P. and Hanefeld, M., 1993. Work absenteeism in type 2 diabetes mellitus: results of the prospective Diabetes Intervention Study. *Diabetes & metabolism*, *19*(1 Pt 2), pp.202-206.

Kim, J. W., & Jung, W. (2003). A taxonomy of performance influencing factors for human reliability analysis of emergency tasks. Journal of loss prevention in the process industries, 16(6), 479-495.

Kyriakidis, M., Majumdar, A., & Ochieng, W. Y. (2015). Data based framework to identify the most significant performance shaping factors in railway operations. Safety science, 78, 60-76.

Lavigne, J.E., Phelps, C.E., Mushlin, A. and Lednar, W.M., 2003. Reductions in individual work productivity associated with type 2 diabetes mellitus. *Pharmacoeconomics*, *21*(15), pp.1123-1134.

Lee, Y., Smofsky, A., Nykoliation, P., Allain, S.J., Lewis-Daly, L., Schwartz, J., Pollack, J.H., Tarride, J.E. and McIntyre, R.S., 2018. Cognitive Impairment Mediates Workplace Impairment in Adults With Type 2 Diabetes Mellitus: Results From the Motivaction Study. *Canadian journal of diabetes*, *42*(3), pp.289-295.

Lee, W., Yoon, J. H., Koo, J. W., Chang, S. J., Roh, J., & Won, J. U. (2018). Predictors and estimation of risk for early exit from working life by poor health among middle and older aged workers in Korea. *Scientific reports*, 8(1), 5180.

Nigatu, Y.T., van de Ven, H.A., van der Klink, J.J., Brouwer, S., Reijneveld, S.A. and Bültmann, U., 2016. Overweight, obesity and work functioning: The role of working-time arrangements. *Applied ergonomics*, *52*, pp.128-134.

Palmer, K. T., Harris, E. C., & Coggon, D. (2008). Chronic health problems and risk of accidental injury in the workplace: a systematic literature review. *Occupational and environmental medicine*.

Pit S. W., Shrestha R., Schofield D., & Passey M. (2010). Health problems and retirement due to ill-health among Australian retirees aged 45–64 years. *Health Policy*, 94(2), 175-181.

Rabbitt, P. and Lowe, C., 2000. Patterns of cognitive ageing. *Psychological Research*, *63*(3-4), pp.308-316.

Salthouse, t., 2012. Consequences of age-related cognitive declines. *Annual review of psychology*, *63*, pp.201-226.

Skirbekk, V. (2008). Age and productivity capacity: Descriptions, causes and policy options. *Ageing Horizons*, 8:4–12.

Steffen, T. M., Hacker, T. A., & Mollinger, L. (2002). Age-and gender-related test performance in community-dwelling elderly people: Six-Minute Walk Test, Berg Balance Scale, Timed Up & Go Test, and gait speeds. *Physical therapy*, *82*(2), 128-137.

Stratton, I. M., Adler, A. I., Neil, H. A. W., Matthews, D. R., Manley, S. E., Cull, C. A., ... & Holman, R. R. (2000). Association of glycaemia with macrovascular and microvascular complications of type 2 diabetes (UKPDS 35): prospective observational study. *Bmj*, *321*(7258), 405-412.

Studenski, S., Perera, S., Patel, K., Rosano, C., Faulkner, K., Inzitari, M., ... & Nevitt, M. (2011). Gait speed and survival in older adults. *Jama*, *305*(1), 50-58.

Soares, F. C., & de Oliveira, T. C. G. (2015). CANTAB object recognition and language tests to detect aging cognitive decline: an exploratory comparative study. *Clinical interventions in aging*, 10, 37.

Toossi, M., 2012. Labor force projections to 2020: A more slowly growing workforce. *Monthly Lab. Rev.*, *135*, p.43.

Tangalos, E. G., Smith, G. E., Ivnik, R. J., Petersen, R. C., Kokmen, E., Kurland, L. T., ... & Parisi, J. E. (1996, September). The Mini-Mental State Examination in general medical practice: clinical utility and acceptance. In *Mayo Clinic Proceedings* (Vol. 71, No. 9, pp. 829-837). Elsevier.

Üstün, T. B., Kostanjsek, N., Chatterji, S., & Rehm, J. (Eds.). (2010). Measuring health and disability: Manual for WHO disability assessment schedule WHODAS 2.0. *World Health Organization*.

Yesavage, J. A., Brink, T. L., Rose, T. L., Lum, O., Huang, V., Adey, M., & Leirer, V. O. (1982). Development and validation of a geriatric depression screening scale: a preliminary report. *Journal of psychiatric research*, 17(1), 37-49.

A STUDY ON SIMULATION FOR CAPABILITY ASSESSMENT AND SAFETY: MITIGATING THE IMPACT OF NEURODEGENERATIVE DISEASES

Agostino G. Bruzzone[(a)], Paolo Fadda[(b)], Marina Massei[(c)], Gianfranco Fancello[(d)], Kirill Sinelshchikov[(e)] , Antonio Padovano[(f)]

[(a),(c),(e)]Simulation Team, University of Genoa, Italy, [(b),(d)]DICAAR, Cagliari University, [(f),]Simulation Team, UNICAL

[(a), (c), (e), (f)] {agostino.bruzzone, marina.massei, kirill, padovano}@simulationteam.com, [(b), (d)] {fadda, fancello}@unica.it

[(a), (c), (e), (f)] www.simulationteam.com – [(b), (d)] www.unica.it

ABSTRACT

The present study is aimed to broaden progressive methodologies developed to improve road traffic safety while addressing essential aspects like population aging and diffusion of neuro-degenerative diseases. Nowadays, enabling technologies dealing with Simulation, Serious Games, Biomedical Devices and Neurology continuously improve. This research proposes to use these advances to set up an experimentation and to measure the potential in assessing drivers capabilities. Furthermore, the study offers a methodological solution to diffuse these criteria and provide recommendations for controlling the phenomena, which would allow to reduce injuries and even support design of new aids and solutions for drivers in those conditions.

Keywords: HPM Human Performance Modelling & Enhancement, Simulation, Serious Games, Biomedical Devices, Neurology

1. INTRODUCTION

The progressive aging of the European population has led to an increase in the proportion of elderly drivers on the roads and in the number of car accidents (Fancello et al.2008). It follows that age is one of the major risk factors also for multiple diseases which have been found to be related to car accidents, such as: cardiovascular diseases, traumatic brain injury, depression, dementia, diabetes mellitus, epilepsy, hearing impairments, musculoskeletal and motor disability conditions, Parkinson's disease, psychiatric disorders, renal disease, schizophrenia, sleep apnoea and vision disorders. It worth to highlight that these increased risks can also be caused by the medications that are expected to treat these conditions (Polders et al. 2013). The most common neurodegenerative diseases are Parkinson's (PD) and Alzheimer's (AD). Crude prevalence estimates range between 1 and 2 cases per 1000 persons for PD while prevalence of dementia caused by AD amongst individuals over 60 is around 30 cases per 1000 persons. The most important medical hallmark of PD is motion problems, which include slowness (bradykinesia), postural instability and tremor. AD, on the other hand, is mostly paired with cognitive decline with the early memory impairment and involvement of other cognitive features including interest control, making plans, trouble fixing, visuospatial competencies.

Table 1. Principal diagnosis & Corresponding risks of accident

Diagnosis / Impairment	Vaa Relative Risk	Charlton et al. Relative Risk	Dobbs et al. "Red Flags"
Alcohol abuse and dependence	2.00	2.1 – 5.0	Yes
Cardiovascular diseases (all types)	1.23	1.1-5.0	Yes
Cerebrovascular accident / traumatic brain injury (TBI)	1.35	Inconclusive	Yes (stroke) N/A TBI
Depression	1.67	Inconclusive	No
Dementia	1.45	2.1 – 5.0	Yes
Diabetes mellitus	1.56	1.1 – 2.0	Yes
Epilepsy	1.84	1.1-5.0+	Yes
Hearing impairment	1.19	N/A	No
Musculoskeletal and motor disability	1.17	1.1-2.0	No
Parkinson's disease	N/A	Inconclusive	N/A
Psychiatric disorder	1.72	1.1-5.0	Yes
Renal disease	0.87	N/A	Yes
Schizophrenia	2.01	2.1-5.0	Yes
Sleep apnoea	3.71	2.1-5.0+	Yes
Vision disorder	1.09	1.1-2.0	Yes

There are no simple objective criteria for assessing the driving capacity of persons affected by PD and AD, whereas recommendations have already been proposed and verified for other common illnesses consisting of cardiovascular diseases, diabetes, obstructive sleep apnea syndrome and epilepsy. Even if elderly drivers self-regulate their driving by reducing the amount of driving session and avoiding driving in critical situations, however, deficiency of accurate understanding into possible cognitive, sensory or physical limitations might be a risk factor for underperforming driving and crash risk. According to the Annual Accident Report 2017 provided by the ERSO (European Road Safety Observatory) which publishes statistical data and figures based on CARE (Community database on Accidents on the Roads in Europe) the total annual number of injury accidents in 2015 overpasses 1 million while drivers and passengers

fatalities are more than 12.000. Moreover, 2016 annual number of fatalities by age is 5122 for age group 50-64 while for age group over 65 is 6979. Patients with mild PD and AD symptoms are currently allowed to drive in Europe. However, roughly 50% of people with Alzheimer's drive for up to 3 years after diagnosis (Adler & Kuskowski 2003); patients with mild cognitive impairment already drive less safely than others (Frittelli et al. 2009; Wadley et al. 2009). All Alzheimer sufferers, at some point in time as the disease progresses will no longer be fit to drive (Duchek et al. 2003). Furthermore, the findings of a survey (Meindorfner et al, 2005) showed that 82% of PD sufferers had a driving license, of whom 60% drove regularly and 15% of those who drove regularly reported having had accidents in the last five years. Some of main diseases and associated risks obtained from researches conducted by Vaa (2003), Charlton et al. (2010) and Dobbs (2005) are presented in the table 1.

2. CONCEPT AND METHODOLOGY

As scientific evidence has demonstrated, short attention span, high cognitive workload, and many others aspects called human factors, are the main causes of errors. With the introduction of the human factors concept, workers' health and safety have been improved by adapting machines and tools to humans' skills, limitations and anatomy since the increasing complexity and the use of complex machines, processes and systems has impacted significantly on the role of humans within work activities. Also, new technology, namely in the automotive areas such as assistive driving, lane keeping assist and others, when introduced poorly, carries the risk of increasing operators' mental workload thereby increasing the risk of committing errors. The quantification of human factors, and hence the corresponding error risk, is still an open issue. Although studies have shown that drivers with PD or dementia are at increased risk of causing traffic accidents, there is also evidence to suggest that not all elderly persons or persons suffering from neurodegenerative diseases are incompetent drivers. Therefore, it is particularly important to determine what cognitive, functional, emotional, and motor factors contribute to driving impairment among PD and AD patients, as well as in elderly persons with subtle cognitive and movement disabilities. Separating those people who are currently at risk of impaired driving from those who are not yet at risk is crucial for maintaining personal autonomy while also maintaining public safety. As stated by the European Commission "drivers in Europe must meet minimum standards of physical and mental fitness to obtain a driving license". However, these standards are currently not based on objective evaluations and therefore could be improved. Indeed, standard objective measure of safe driving performance is needed for the elderly population with subtle cognitive and movement disabilities, as well as for people with recognized neurodegenerative diseases.

2.1. Methodology

The proposed methodology contains several principal steps which are presented below.

1. Identification of significant factors and variables related to cognitive and movement disabilities requires the assessment of a substantial number of patients with mild AD and PD which are currently driving as well as age and sex-matched healthy controls. Preliminary power calculation based on the few studies dealing with driving simulation in PD and AD sufferers suggests that recruitment of 100 PD patients, 100 AD patients and 100 healthy subjects who currently drive from each participating neurological center would provide adequate power with alpha=0.05(two-sided) and beta>80%. In order to improve further precision of obtained results it is very important to study subjects from different areas, with different social and cultural settings as well as perception of danger and comprehension of rules, which are probably responsible for different mobility behavior and driving styles, while their influence and characteristics respect road safety will be evaluated during the research.
2. Search for clinical markers, which requires development of extensive experimentation, able to assess fitness to drive of all the patients; this needs to be studied using tests for visual perception and attention, visuospatial ability, learning and memory, executive functions, language comprehension, affectivity and daily sleepiness.
3. Full scope simulation utilizing solution developed by Genoa University, which has been already validated and verified, and is currently in use in University of Cagliari Labs. This simulator uses high-fidelity models and is equipped with a driving position that reproduces a regular road vehicle (real dashboard, seat, pedal board, steering wheel, gear, etc.). Behaviors are assessed for different traffic (free flow, traffic jam, urban road junctions, etc.) and weather conditions (rain, wind, glare, dark and half-light, etc.) and for difficult driving maneuvers (reversing, turning left, sudden braking, U-turn, etc.). The Simulator is containerized and could be easily deployed in other areas to carry out Driving tests (Fancello et.al 2010a). The target factors and key performance indexes measurements are performed over specific scenarios for all patients in all scenarios (e.g. braking and stopping distance, path length in bends and/or on straight stretches, the radius of curvature when turning around, etc); the results are compared both in absolute (against standards measured for a sample of "healthy" drivers) and in relative terms.
4. Analysis of cognitive and movement impairments effects on driving performance using the driving simulator with incorporated medical equipment (Fancello et al.2010b). These medical devices allow studying biosignals (biological activities) using neurophysiologic measures.

Obviously these devices include different tools with different roles, capabilities and requiring specific resources. Possible motor and cognitive impairments associated with the performance at the driving simulator should be evaluated using biomedical devices, such as eye-trackers and non-invasive electromyography devices. In fact, eye-trackers are required to reconstruct the sequence of the driver's observations by measuring fixation length of the different images and signals that appear in the visual scene during the tests. In the same time, non-invasive electromyography devices allow to conduct specific analyses on both timing and amplitude of muscular activation of the upper and lower limbs (to evaluate their responsiveness in the use of the steering wheel and the pedal board, respectively) pressure-sensitive mats, surface Electromyography (sEMG). Furthermore, inertial sensors are required for studying postural control features and body-seat interaction, as shown in figure 1 (Bruzzone et al. 2009a; Bruzzone et al. 2009b). The knowledge of human factors involved in driving inability in people with cognitive and movement impairment enables the development of a solution based on a new generation Lean High Fidelity Simulator. This Simulator incorporate modern concepts (serious games) and technologies (immersive technologies and biomedical devices) easy to be deployed and being characterized by low cost for acquisition and service as well as intuitively usable for extensive assessment of driver capabilities.

3. AIM

As was explained, this study focuses on how to increase driving safety by addressing certain human factors that represent a prime cause of accidents in transportations. In fact, special attention is devoted to elderly population affected by neurodegenerative diseases. For instance, driving performance assessment of PD and AD patients will make possible to observe how cognitive and motion disability influences their capacity to drive and may be used as a paradigm for developing new, high performance equipment for detecting risky driving behavior amongst elderly population suffering mild cognitive and motor disabilities (Frittelli et al 2009). Indeed, the overall goal is to increase the knowledge regarding the impact of these factors on driving capabilities and to develop an innovative solution devoted to prevent and mitigate the associated risks of accidents. This revolutionary improvement turns to be possible thanks to the combined use of enabling technologies and advances in neuro-medicine that allows conducting extensive and reliable measurements on virtual drive test carried out on simulators equipped with biomedical devices.

In order to achieve the goals, it is necessary first to perform identification and quantification of most critical targets and elements (i.e. neurodegenerative diseases) for assessing driving capabilities by impaired drivers in order to improve road safety; at this step it could be useful to utilize large data set of insured vehicles.

Figure 1: sEMG. A biomedical device for measurements

After identification of targets, it is possible to perform an experimentation using the driving simulation with a virtual environment, which would allow measurement, easily and with high reliability, the human perception of the road situation and traffic and to test how people interact with the vehicle and the different systems. This allows recreating, on the simulation, different critical boundary conditions, distraction factors and to evaluate the influence of fatigue and stress in addition to cognitive and movement impairment (Bruzzone et al 2011). This approach allows to create an extensive and comparable database based on sufficient and relevant data related to the aforementioned human factors, and consequentially to identify correlations and finalize the measurement protocols and the driving capability assessment procedures. The protocols should include description of methods, models, equipment and measures to be adopted to evaluate the human skills and critical issues for impaired drivers. The experimentation allows to scientifically identify and quantify the factors (e.g. age, gender, pathologies) influencing and degrading the performance of people suffering from cognitive and movement disabilities related to neurodegenerative diseases. Analysis on impediments on movement and cognition related to the control of a vehicle and the measurements are obtained by integrating the simulation with biomedical devices and with intelligent systems able to capture and classify the driver behaviors. Integration of the simulation with biomedical devices allows correlating driving behavior with the drivers' psychophysical parameters; in this way it will be possible to assign, once the task is completed, performance indexes for assisting diagnosis and the patients' performance will be assessed by means of simulated driving tests respect simple and complex tasks. It is important to list some of the simple tasks to be used for this investigation that include:

- driving along a road,
- parking,
- braking and stopping,
- pulling out into traffic

Vice versa there are also complex tasks to test that are those that are more psychophysically demanding and thus require greater concentration and skills.

In this sense it is possible to outline some cases to be used in the specific test programs and protocols as proposed in the following list:

- left turns,
- negotiating roundabouts,
- driving in parallel lanes,
- facing unexpected events and
- facing dangerous conditions

Neurophysiologic measurements evaluate variations of biological activities due to modification of external (environment) and internal (cognition, motivations, emotions, etc.) factors. The integration of biomedical devices and simulation allows to quantify the risks and improvements in road safety respect the human factors as well as to provide a framework to evaluate alternative design elements for vehicles, infrastructures and support systems, even considering innovative intelligent solutions devoted to enhance human machine interactions. Based on results obtained in the simulation phase it is possible to quantify the impact of the diseases and factors and identify that ones to be targeted for further investigation by measurements on the simulators; in this way specific protocols for evaluating related driving capabilities are developed and verified. The definition of these parameters and protocols is critical for further steps, because it allows to assess objectively their capabilities and risks and to define thresholds beyond which it is necessary to prevent people from driving. Experimentation on different simulation solutions allows to extend the applicability of proposed protocol all around EU. For instance, according to the study performed by Cox et al. (2010) using Full Scope Simulators (e.g. motion platform, fully immersive CAVE, real cockpit, very advanced biomedical devices etc.), the driving performance significantly improved when elderly drivers with traumatic brain injury undertook Virtual Reality Driving Simulation Training.

Meanwhile, it is possible to develop also innovative compact equipment based on Lean Simulation. Solutions in other application areas (Longo et al., 2017) or for healthy drivers (Medenica et al., 2011) have been already proposed also using Virtual and Augmented Reality approaches, however additional researches are needed for elderly drivers or drivers with diseases as discussed in this study. This new generation of Lean Simulators, combined with new biometrics, could be used to evaluate the possibility to apply the protocols on these compact, affordable and immediate available solutions that could be distributed capillary over the EU Institutions. The results carried out by the Lean Simulation could be consequentially compared with the ones obtained on the Full Scope Simulator, which would allow to evaluate the specific experimental errors and confidence band in assessing driving ability and predicting fitness to drive for impaired drivers. In this way, it is verified and certified the reliability and sensitivity of the Lean Simulation based equipment in assessing the capabilities of both individuals with neurodegenerative disease and elderly population with subtle cognitive and movement impairment. The Lean Simulation is designed to be an easy-to-use system, ready for deployment on test sites, namely driving schools, medical centers and public Institutions. The experimentations over different technological solutions (Full Scope Simulators and Lean Simulators) contribute to verification and validation of the protocols, the models, the methodologies as well as to measurement of the experimental errors (Bruzzone & Saetta 2002). These results are expected to increase the understanding of neurodegenerative diseases respect transport safety and promote the adoption of new rules and regulations in conscious and scientific way. Based on analysis of the experimental data it is possible to define clinical and behavioral markers, which are necessary to help physicians into clinically and scientifically differentiate dangerous or not dangerous drivers. The results obtained by biomedical devices and behavior intelligent classifiers during simulation coupled with clinical test for visual perception and attention, visuospatial ability, learning and memory, executive functions, language comprehension, affectivity, daily sleepiness and motor impairment, allows to define the clinical markers that could predict unfitness to drive. Results contribute to development of new regulations and procedures to address these problems; the resulting new medical protocols and measurement instruments allows applying innovative solutions to different factors devoted to prevent accidents, mitigate these conditions and overcome potential limitations in man-machine interactions. It is evident that the new protocols supported by modeling and simulation represent a major advantage to understand reaction capabilities, diversity in perception of danger, capability to apply properly driving rules and to adopt safe mobility behavior by large part of aging population. Therefore, this approach represents also a solution to quantify the influence of critical issues such as fatigue, stress and other kind of conditions and/or diseases. It is expected also to define criteria for identify a "tolerance zone" and to define appropriate cut-off parameters for drivers affected by mild degenerative diseases that still have acceptable performance respect road safety. In addition, a common procedure of driving license check as well as new regulations are desirable outcome.

4. AMBITION AND EXPECTED IMPACTS

The final goal of the study is to develop a new solution able to easily check driving capabilities of people with clinical signs considered at high risk. This solution based on a Lean Simulator which incorporates modern concepts and technologies (immersive technologies and biomedical devices) and to be used, at low cost, for extensive assessment of driving ability. The development of a new tool able to check for driving ability that is sensitive to cognitive and movement disabilities allows to introduce the concept of objectivity in driving assessment. This measure ensures a greater confidence in Institutions responsible for car license renewal and promote enhanced safety culture

and respect of the rules of the road. Today EU statistics count over 22'000 Fatalities/year for road drivers and an estimated of over 155bEuro/year of costs including Human Costs, Production Losses, Medical and Administrative Costs on Minor & Severe Injuries as well as on Fatal Accidents; this corresponds to costs over passing 28bEuro/year for elderly driving and it is expected to further grow due to the population aging despite current trends. The main ambition of the study it is to reduce up 20% the total fatalities due to road accident caused by aged impaired drivers; this corresponds for future years, based on forecasts, to over 700 lives /year. In addition, this result will correspond to decrease up to 20% the existing costs of Road Accidents caused by aged impaired drivers providing big savings that could be estimated around 1bEuro/Year based on current forecasts for 2020. The ultimate aim is to draw up a standard test protocol for the certification of fitness to drive.

5. CONCLUSIONS

The proposed study aims to develop a methodology and a simulation based approach devoted to improve road traffic safety by evaluating ability to drive of elderly persons and of people with neurodegenerative diseases. This could even lead to allow people with minor affections to drive safely and under continuous control. Obviously this paper presents just a proposal, while author are working on developments; therefore it is evident that the target is to reduce significantly car accidents and consequentially injures and costs.

ACKNOWLEDGMENTS

The authors thank all the partners of the proposal "SAFE-nEURO" for their valuable contributions in shaping of these ideas and concepts.

REFERENCES

Adler, G., & Kuskowski, M. (2003). Driving cessation in older men with dementia. Alzheimer Disease & Associated Disorders, 17(2), 68-71.

Bruzzone, A., Fadda, P., Fancello, G., Massei, M., Bocca, E., Tremori, A., ... & D'Errico, G. (2011). Logistics node simulator as an enabler for supply chain development: innovative portainer simulator as the assessment tool for human factors in port cranes. Simulation, 87(10), 857-874.

Bruzzone, A., Fadda, P., Fancello, G., D'Errico, G., Bocca, E., & Massei, M. (2009a). A vibration effect as fatigue source in a port crane simulator for training and research: Spectra validation process. Proc. of HMS, Vol. 1, pp. 77-86

Bruzzone, A., Fadda, P., Fancello, G., Tremori, A., Bocca, E., & D'Errico, G. (2009b). Measuring human factors in port activities by using simulation. Proc. SpringSim, San Diego, April

Bruzzone, A., & Saetta, S. (2002). LESNEX: Lean simulation network of excellence. In HMS2002 and MAS2002,Bergeggi, SV, Italy, October 3-5

Charlton, J., Koppel, S., Odell, M., Devlin, A., Langford, J., O'Hare, M., ... Scully, M. (2010). Influence of chronic illness on crash involvement of motor vehicle drivers: 2nd edition (No. 300). Victoria, Australia: MUARC (Monash University Accident Research Centre).

Cox, D. J., Davis, M., Singh, H., Barbour, B., Nidiffer, F. D., Trudel, T., Mourant R, Moncrief R. (2010). Driving rehabilitation for military personnel recovering from traumatic brain injury using virtual reality driving simulation: a feasibility study. Military Medicine, 175(6), 411–416.

Dobbs, B. (2005). Medical Conditions and Driving: A Review of the Scientific Literature (1960-2000), Technical Report for the National Highway and Traffic Safety Administration and the Association for the Advancement of Automotive Medicine Project No. DOT HS 809 690, Washington, D.C.

Duchek, J. M., Carr, D. B., Hunt, L., Roe, C. M., Xiong, C., Shah, K., & Morris, J. C. (2003). Longitudinal driving performance in early-stage dementia of the Alzheimer type. Journal of the American Geriatrics Society, 51(10), 1342-1347

Fancello, G., Bruzzone, A.G., Carta, M. G., Bocca, E., Tremori, A., & Fadda, P. (2010a). Truck simulator an instrument for research and training. Trends in Driving Simulation Design and Experiments, 243.

Fancello G., Carta M.G., Fadda P. (2010b) "Information relaying systems and driver perception: experimental analysis of variable message signs using eye tracker" – 12th WCTR World Conference on Transport Research, July 11-15, 2010 – Lisbon, Portugal

Fancello, G., Stamatiadis, N., Pani-Wilkinson, E., & Fadda, P. (2008). Are older drivers different in the US and Italy?. WIT Transactions on The Built Environment, 101, 679-690.

Frittelli, C., Borghetti, D., Iudice, G., Bonanni, E., Maestri, M., Tognoni, G., Pasquali, L. & Iudice, A. (2009). Effects of Alzheimer's disease and mild cognitive impairment on driving ability: a controlled clinical study by simulated driving test. Int. Journal of Geriatric Psychiatry, 24, 232-238.

European Commission (2017) Annual Accident Report. European Commission, Directorate General for Transport, June 2017.

Longo F., Nicoletti L., Padovano A., 2017. Smart operators in industry 4.0: A human-centered approach to enhance operators' capabilities and competencies within the new smart factory context. Computers and Industrial Engineering, vol. 113, pp. 144-159.

Medenica Z., Kun A.L., Paek T., Palinko O., 2011. Augmented reality vs. street views: A driving simulator study comparing two emerging navigation aids. Mobile HCI 2011 - 13th International Conference on Human-Computer Interaction with Mobile Devices and Services, pp. 265.

Meindorfner, C., Körner, Y., Möller, J.C., Stiasny-Kolster, K., Oertel, W.H. & Krüger, H. (2005), Driving in Parkinson's disease: Mobility, accidents, and sudden onset of sleep at the wheel. Mov. Disord., 20: 832-842

Polders, E., Brijs, T., Vlahogianni, E., Papadimitriou, E., Yannis, G., Leopold, F., Durso, C., Diamandouros K., (2013) ElderSafe - Risks and countermeasures for road traffic of the elderly in Europe, Final report, N° MOVE/C4/2014-244

Vaa, T. (2003). Impairment, Diseases, Age and Their Relative Risks of Accident Involvement: Results from Meta-Analysis. (No. TØI Report 690). Oslo, Norway: Institute of Transport Economics.

Wadley, V. G., Okonkwo, O., Crowe, M., Vance, D. E., Elgin, J. M., Ball, K. K., & Owsley, C. (2009). Mild cognitive impairment and everyday function: an investigation of driving performance. Journal of geriatric Psychiatry and Neurology, 22(2), 87-94

Author's index